EXAMINING THE ROLE OF REDOX BIOLOGY IN A POPULATION OF NEONATAL CARDIAC PRECURSOR CELLS MARKED BY THE TYPE III RECEPTOR TYROSINE KINASE, C-KIT

A Dissertation

Presented to the Faculty of the Graduate School

of Cornell University

in Partial Fulfillment of the Requirements for the Degree of

Doctor of Philosophy

by

Alyson Spealman Nadworny

May 2012

EXAMINING THE ROLE OF REDOX BIOLOGY IN A POPULATION OF NEONATAL CARDIAC PRECURSOR CELLS MARKED BY THE TYPE III RECEPTOR TYROSINE KINASE, C-KIT

Alyson Spealman Nadworny, Ph.D.

Cornell University 2012

Owing in large part to the low regenerative capacity of the heart, cardiovascular disease (CVD) remains a leading cause of morbidity and mortality worldwide. Compelling evidence suggests the presence of resident cardiac precursor cells (CPCs) in the neonatal and, to a lesser extent, in the adult myocardium. These CPCs are identified based on specific marker expression including c-kit, a type III receptor tyrosine kinase.

Here we report the isolation and characterization of neonatal c-kit^{+} CPCs from a bacterial artificial chromosome (BAC) transgenic mouse in which enhanced green fluorescent protein (EGFP) is driven by the *kit* locus. We demonstrate that c-kit expression identifies CPCs capable of expanding and differentiating into all three cardiac lineages. In addition, we establish that this mesodermally derived cell population comprises a mixture of precursors and more mature cells in the early stages of lineage commitment.

Progressing from the identification of CPCs, cell-based therapy has emerged as a strategy for cardiac repair. However, the pathological environment of the infarcted heart, attributed in part to the production of reactive oxygen species (ROS), impedes transplanted cell survival. In spite of well-known pathological roles, ROS also participate in normal cell development and recent research indicates that redox state is a critical regulator of precursor cell function.

Because the NADPH oxidases (Nox) are a major source of ROS in the heart, a significant amount of research has been conducted to elucidate roles for these enzymes in cardiomyogenesis and heart failure. However, little research has been directed at the function of Nox enzymes in

CPCs. As a successful cell-based therapy requires both the survival of transplanted cells and their differentiation into cardiomyocytes, understanding the mechanisms of ROS signaling in CPCs is critical.

Therefore, utilizing genetic tools to manipulate the Nox enzymes of neonatal c-kit^{+} CPCs, I demonstrate that specific cardiac Nox homologues are critical modulators of c-kit^{+} cell precursor and differentiation status. I speculate that these and other redox genes identified by messenger RNA (mRNA) arrays will provide novel targets for improving the regenerative capacity of c-kit^{+} CPCs, which can later be integrated into cell-based therapies for myocardial infarction (MI).

BIOGRAPHICAL SKETCH

Alyson Spealman Nadworny was born in Rockville, Maryland in 1984. In the early 1990's, her family relocated to Northern Virginia where she was enrolled in the Fairfax County Public school system. Nadworny participated in a wide range of extracurricular activities including playing the clarinet for both the symphonic and marching bands. In 2002, Nadworny graduated Valedictorian of her high school class and was accepted into the College of William and Mary. Her undergraduate studies focused on the hippocampal regulation of memory and elder care. In 2006, she graduated *summa cum laude* from the College of William and Mary with a dual degree in Neuroscience and Sociology and was inducted into the prestigious *Phi Beta Kappa* honor society.

Directly following her college graduation, Nadworny joined the field of Pharmacology in the Department of Biomedical Sciences at Cornell University in Ithaca, New York. Upon completion of her laboratory rotations, she joined the laboratory of Dr. Michael Kotlikoff and began developing her thesis project with a clear focus on cardiac precursor cell biology. In 2008, Nadworny was accepted into the Cornell University Graduate Linkage Program under the guidance of Drs. Robin Davisson and Michael Kotlikoff. At this time, Nadworny extended the focus of her thesis project to encompass redox biology and completed the remainder of her studies in the Department of Cell and Developmental Biology at Weill Cornell Medical College in New York, New York.

Nadworny's graduate career is marked by several honors including receipt of the *Caroline tum Suden* professional opportunity award in February 2009 and the *Stanley Stahl* research fellow award in November 2010 in conjunction with her American Heart Association Predoctoral Fellowship. During her time at Cornell, Nadworny participated in numerous

outreach programs aimed to bridge the research gap between Cornell's two campuses and was featured in a short video for the *Paint the Town Red* online series. As a woman researcher in cardiac biology, Nadworny also promoted heart health to the community and was named an American Heart Association *Rock Star of Science* at the February 2011 *Go Red for Women* campaign held in New York City.

Following completion of her Ph.D., Nadworny plans to relocate to Chicago, Illinois where her husband, Matthew Nadworny, resides. She is interested in pursuing a research career in cancer stem cell biology.

ACKNOWLEDGMENTS

I would like to express my deepest gratitude to my mentors Drs. Robin Davisson and Michael Kotlikoff for their unwavering support and willingness to jointly oversee my doctoral studies. Their guidance and leadership throughout the years truly has been inspirational. I also would like to thank my special committee members, Drs. Holger Sondermann, Heidi Stulhmann, and Tudorita Tumbar for their encouragement, enthusiasm, and insightful conversations.

Over the course of my Ph.D. work, I received mentorship and guidance in many forms. I feel incredibly blessed for the lasting friendships that developed from these relationships, especially those with Dr. Yvonne Tallini, Jane Lee, and Lorraine Capogrossi. I also would like to thank Janna Lamey for her heartfelt advice and eagerness to assist me in enrolling in the Cornell University Graduate Linkage Program. I often wonder where I would be today without her steadfast support of my move to NYC in August 2008.

Finally, I would like to thank my family members, especially my parents, Teddy and Wayne Spealman, my sister, Jenna Spealman, my aunt, Shirley Appelhans, and my husband, Matthew Nadworny, for their love and compassion. I would like to dedicate this thesis to my father, Wayne Spealman, who always knew that I would become a doctor and never let go of the dream.

TABLE OF CONTENTS

LIST OF FIGURES

LIST OF TABLES

LIST OF ABBREVIATIONS

ANP	Atrial Natriuretic Peptide
AP	Activator Protein
BAC	Bacterial Artificial Chromosome
bFGF	Basic Fibroblast Growth Factor
BM	Bone Marrow
BMP	Bone Morphogenetic Protein
CHD	Coronary Heart Disease
CM	Cardiomyocyte
CM-PC	Cardiomyocyte Precursor Cell
CPC	Cardiac Precursor Cell
cTnT	Cardiac Troponin T
CVD	Cardiovascular Disease
DHE	Dihydroethidium
dpc	Days Post Coitus
DPI	Diphenylene Iodonium
Duox	Dual Oxidase
EB	Embryoid Body
EC	Endothelial Cell
ED	Embryonic Day
EGF	Epidermal Growth Factor
EGFP	Enhanced Green Fluorescent Protein
E-PC	Endothelial Precursor Cell

EPC	Endothelial Progenitor Cell
ERK	Extracellular Signal Regulated Kinase
ESC	Embryonic Stem Cell
FACS	Fluorescence Activated Cell Sorting
FAD	Flavin Adenine Dinucleotide
FBS	Fetal Bovine Serum
FITC	Fluorescein Isothiocyanate
Flk	Fetal Liver Kinase
GDI	GDP-Dissociation Inhibitor
Gpx	Glutathione Peroxidase
H_2O_2	Hydrogen Peroxide
HIF	Hypoxia Inducible Factor
HSC	Hematopoietic Stem Cell
IGF	Insulin-Like Growth Factor
IL	Interleukin
iPSC	Induced Pluripotent Stem Cell
Isl	Islet
JNK	c-Jun N-Terminal Kinase
KDR	Kinase Insert Domain Receptor
LIF	Leukemia Inhibitory Factor
LV	Left Ventricular
MAPK	Mitogen Activated Protein Kinase
MGI	Mouse Genome Informatics

MI	Myocardial Infarction
MMP	Matrix Metalloproteinases
mRNA	Messenger Ribonucleic Acid
MSC	Mesenchymal Stem Cell
NADPH	Nicotinamide Adenine Dinucleotide Phosphate
NF	Nuclear Factor
Nox	NADPH Oxidase
NSC	Neural Stem Cell
PBS	Phosphate Buffered Saline
PCI	Percutaneous Coronary Intervention
PCNA	Proliferating Cell Nuclear Antigen
PDGF	Platelet-Derived Growth Factor
PE	Phycoerythrin
PECAM	Platelet Endothelial Cell Adhesion Molecule
pHH3	Phospho-Histone H3
phox	Phagocytic Oxidase
PI	Propidium Iodide
PI3K	Phosphatidylinositol 3 Kinase
PK	Protein Kinase
PN	Postnatal
PPAR	Peroxisome Proliferator Activated Receptor
Prdx	Peroxiredoxin
PTP	Protein Tyrosine Phosphatase

qPCR	Real-Time Quantitative PCR
Ref	Redox Effector Protein
ROS	Reactive Oxygen Species
RT	Room Temperature
Sca	Stem Cell Antigen
SCF	Stem Cell Factor
sEGFP	High EGFP Expressing Subset of Total EGFP Population
SHP	SH2 Domain-Containing Phosphatase
SMA	Smooth Muscle Actin
SMC	Smooth Muscle Cell
SM-PC	Smooth Muscle Precursor Cell
Sod	Superoxide Dismutase
SP	Side Population
TBS	Tris Buffered Saline
tEGFP	Total EGFP Population
TGF	Transforming Growth Factor
TNF	Tumor Necrosis Factor
VEGF	Vascular Endothelial Growth Factor
VSMC	Vascular Smooth Muscle Cell
vWF	Von Willebrand Factor
WT	Wildtype

CHAPTER ONE: INTRODUCTION

1.1 Cardiovascular Disease (CVD)

1.1.1 Prevalence in the United States

The term cardiovascular disease (CVD) encompasses a large group of cardiac afflictions including, but not limited to, coronary heart disease (CHD), stroke, high blood pressure, congenital defects, and heart failure. Risk factors for non-congenital CVD include high total cholesterol, hypertension, cigarette use, physical inactivity, obesity, and diabetes. According to the most recent Heart Disease and Stroke Statistics released by the American Heart Association [1], CVD was responsible for approximately one-third of all deaths in the United States in the year 2006. This accounted for more deaths than cancer, chronic lower respiratory disease, and accidents, combined. Interestingly, over half of these deaths were attributed to CHD, a category which comprises both chest pain and myocardial infarction (MI), more commonly known as a heart attack. In addition to these jarring statistics, the report predicted that close to 800,000 Americans would experience a new coronary event in the year 2010, causing roughly one death every minute.

Unfortunately, within the first five years after a MI, approximately 33% of men and 43% of women ≥40 years of age will die and many others will be diagnosed with heart failure [1]. Because heart transplantation continues to provide the only cure for heart disease, doctors perform procedures aimed to ameliorate symptoms such as percutaneous coronary intervention (PCI), bypass surgeries, and defibrillator/pacemaker implantations with the hope that they can improve the quality of life for their patients. It is this lack of a true cure for heart disease along with extensive treatment and inpatient/outpatient care that lead to combined costs associated with CHD staggering at well over $150 billion per year. Due to the severe shortage of hearts

available for organ donation and subsequent transplantation, basic research in the CHD field has turned its focus to cell populations which retain lineage plasticity and the potential for cardiac commitment. Discovering these cell types and determining their usefulness in cardiac regeneration have been topics of great interest over the last decade and serve as the foundation for this dissertation. However, it took years of research to disprove paradigms regarding the proliferative capacity of the mature heart that were established close to 100 years ago.

1.1.2 Paradigm Shift from a Terminally Differentiated Heart to a Self-Renewing Organ

Dating back to the mid-1800's and the early-1900's, the adult human heart was viewed as an organ capable of expansion through both hyperplasia (increase in the number of cells) and hypertrophy (increase in the size of cells) of existing myocytes. In the early- to mid-1900's, however, this dogma was challenged by several groups including Karsner who, in 1925, claimed that the heart grew in size via hypertrophy alone and that there was no direct evidence (i.e. signs of mitotic myocytes) supporting the ability of the heart to experience hyperplasia of existing fibers [2]. By the mid-1900's, a majority of researchers in the field refuted the idea of myocyte proliferation [3] with only a minority, specifically Linzbach in the late 1940's, propagating a theory of myocyte proliferation limited to the pathologically hypertrophied heart [4]. Although faced with some opposition, it was generally accepted throughout the remainder of the 20th century that the heart was a terminally differentiated organ and it is this paradigm that shaped basic and clinical research for several decades to come.

In 1998, however, Kajstura, et al. [5] utilized confocal microscopy to conclusively demonstrate a very low but detectable mitotic index in non-diseased human hearts of 14 myocytes per million with a ten-fold increase in mitotic index found in samples from patients with heart failure. That

same year, together with Anversa, Kajstura published a review further supporting the notion that ventricular myocytes are *not* terminally differentiated and advancing the concept that myocyte proliferation can be enhanced by stimulation with growth factors such as insulin-like growth factor (IGF)-1 [6]. In 2001, Beltrami, et al. [7] provided additional evidence challenging the dogma that the heart was a post-mitotic organ by demonstrating the presence of Ki-67 (marker of proliferation) staining in approximately 4% of myocytes in the border zone of infarcted human hearts. Whether or not these proliferating cells represented a sub-population of myocytes capable of division, a population of extra-cardiac stem cells, or an endogenous precursor cell population, however, remained largely unknown.

In the early years of the 21st century, cardiac chimerism in the transplanted heart offered skeptics even more evidence of cardiac self-renewal, utilizing the presence of the Y-chromosome to distinguish between graft and host tissue [8, 9]. However, it was not until 2009, years after the discovery of endogenous cardiac precursor cells (CPCs) which will be discussed in detail in later sections, that Bergmann, et al. [10] generated the most conclusive evidence to date demonstrating cardiomyocyte renewal in humans. In this elegant series of experiments, the group utilized knowledge of the integration of carbon-14 into DNA released atmospherically during nuclear bomb testing of the Cold War to date human cardiomyocytes [10]. They reported that cardiomyocytes in the human heart are renewed at a rate of 1% per year at 25 years of age with a close to 50% reduction in renewal rate by the age of 75. While these studies established conclusively the ability of cardiomyocytes to undergo cell proliferation, they also highlighted the fact that, at these rates, only 50% of myocytes are replaced during the lifetime, a speed at which substantial cardiac regeneration after injury such as MI is improbable. Most recently, it was

demonstrated that hearts from early postnatal (PN) mice (PN1) can regenerate after surgical resection of the left ventricular apex [11]. In this study, the regenerative process was marked by cardiomyocyte proliferation with little hypertrophy or fibrosis which are two hallmarks of the adult repair response. Interestingly, the investigators reported that this capacity to restore resected myocardium diminishes completely by PN7. The mechanisms by which this competence declines during the first week post-birth remain to be elucidated and likely will uncover novel therapeutic targets for cardiac repair.

1.1.3 Myocardial Infarction (MI)

MI is an acute form of CHD which affects over 8 million Americans each year [1]. MI typically begins when a coronary artery becomes occluded by a dislodged atherosclerotic plaque. This disruption in blood flow to the heart triggers a period of ischemia marked by hypoxia and hypoglycemia which results in damage to cell membranes and massive cell death by necrosis. Following a prolonged period of ischemia and subsequent induction of reperfusion, the heart experiences a further increase in the production of reactive oxygen species (ROS), which are extremely unstable and highly reactive molecules such as superoxide and hydrogen peroxide (H_2O_2), from several sources (i.e. mitochondria, xanthine oxidases, nicotinamide adenine dinucleotide phosphate [NADPH] oxidases) along with a surge in inflammatory cytokines [12]. Together, the production of free radicals and activation of complement drive a cytokine cascade mediated by tumor necrosis factor (TNF)- α, interleukin (IL)-1β, and IL-6 that signals the recruitment of neutrophils to the damaged area [13]. Ultimately, the cytokine cascade ends by triggering apoptosis in a large portion of the damaged cells giving way to matrix metalloproteinases (MMPs) which degrade extracellular matrices and mark the beginning of left ventricular (LV) remodeling.

Although thought to be the heart's attempt at healing, LV remodeling actually causes irreversible harm to the organ and drastically reduces its pumping capacity. This damaging remodeling is marked by processes such as hypertrophy of non-damaged regions, dilatation, thinning of the myocardial wall, and stiffness due to excessive collagen deposition and fibrosis [14]. Although it is now understood that a sub-population of cells in the heart are capable of proliferation, the regenerative potential of these cells is grossly inadequate to compensate for the immense loss of cardiomyocytes that occurs following MI. Therefore, LV remodeling in conjunction with insufficient cardiac regeneration increase a patient's risk for future arrhythmias, leading to progressively worse heart disease and ultimately to heart failure.

1.1.4 Summary

With such a high prevalence of CHD in the United States together with the heart's inability to regenerate itself after injury despite the presence of proliferative-competent cells, there has been a shift in the focus of cardiovascular research in recent years. While some research in the field focuses on finding ways to stimulate existing populations of proliferating cells in the adult heart to participate in cardiac regeneration, a majority of research in the field has turned to a cell-based therapy approach whereby cells with cardiac potential are injected into the infarcted heart with the hope that they will survive, proliferate, and differentiate into fully functional cardiomyocytes.

1.2 Cardiac Cell-Based Therapy

1.2.1 Extra-Cardiac Stem Cell Sources

Cell-based therapy is currently at the forefront of cardiovascular basic and clinical research, providing promise for a treatment that can improve the function and overall health of the heart

without necessitating a heart transplantation. Some of the earliest attempts at cell-based therapy utilized skeletal myoblasts, cells that normally regenerate skeletal muscle, in cardiac regeneration. While these early studies reported functional improvement following transplantation [15], later studies failed to demonstrate differentiation of these cells to cardiomyocytes or their electrical coupling through gap junctions with the rest of the heart [16-19]. Clinical trials from skeletal myoblast engraftments revealed an increased risk for arrhythmia and, consequently, resulted in internal defibrillator implantation in several patients under study [20]. In addition to skeletal myoblasts, many other stem cell types including bone marrow (BM)-derived cells, embryonic stem cells (ESCs), and induced pluripotent stem cells (iPSCs) have been investigated for their therapeutic potential in myocardial regeneration. Each is discussed below in turn.

1.2.1.1 Bone Marrow (BM)-Derived Cells

Around the same time that skeletal myoblasts were being assessed for a role in cardiac regeneration, Orlic, et al. [21] reported that BM-derived hematopoietic stem cells (HSCs) with a $Lin^{-}c\text{-}kit^{+}$ phenotype were capable of initiating *de novo* myocardial regeneration in the infarcted murine heart. This initial finding, however, was met with opposition several years later when two independent laboratories reported that HSCs were unable to acquire a cardiac phenotype and that previous reports were likely a product of cellular fusion, not transdifferentiation [22, 23]. In a rebuttal to these findings, Anversa's group published yet another report reaffirming that BM-derived cells were capable of cardiac differentiation independent of cell fusion [24]. While this controversy is ongoing, beneficial effects after transplantation of BM-derived cells such as endothelial progenitor cells (EPCs) [25],

mesenchymal stem cells (MSCs) [26], and c-kit$^+$ cells [27] whether the result of true cardiac differentiation or strictly paracrine effects, have since been reported.

1.2.1.2 Embryonic Stem Cells (ESCs)

In recent years, ESCs derived from the inner cell mass of the early blastocyst have been the topic of much debate. In 2001, it was first reported that human ESCs can differentiate into fully functioning myocytes *in vitro* [28]. These myocytes express typical markers of cardiac differentiation including Gata4, Nkx2.5, atrial natriuretic peptide *(*ANP), and cardiac Troponin T (cTnT). This finding sparked great interest in the potential of ESC-derived cardiomyocytes for myocardial repair. The following year, Xu, et al. [29] built upon this work by developing an enrichment strategy to isolate human ESC-derived cardiomyocytes by Percoll density gradient to a purity of approximately 70%. Protocols for cardiac enrichment have since improved, and both murine and human ESC-derived cardiomyocytes have been used to create myocardial grafts in rodents in the presence and absence of MI [30-33]. Together, these studies demonstrate long-term engraftment potential and enhanced LV cardiac function with no signs of graft rejection or tumor formation. However, despite these promising results, the use of ESCs remains highly controversial due to ethical concerns and the risk for teratoma formation in both allogeneic and syngeneic hosts.

1.2.1.3 Induced Pluripotent Stem Cells (iPSCs)

Most recently, iPSCs have risen to the forefront of cell-based therapy research, as their discovery circumvents the ethical concerns associated with ESCs. iPSCs first were generated from mouse skin fibroblasts utilizing the exogenous expression of four genes, Oct2/4, Sox2, Klf4, and c-myc [34]. Soon after, similar reprogramming was achieved in

human dermal fibroblasts [35, 36]. As with ESCs, several groups demonstrated the ability of iPSCs to differentiate into fully functioning cardiac myocytes *in vitro* [37-39]. However, when transplanted directly into the infarcted heart, undifferentiated iPSCs were found to induce teratoma formation [40, 41]. While reprogramming cardiac fibroblasts into cardiomyocyte-like cells using transcription factors Tbx5, Gata4, and Mef2c may circumvent some of these problems associated with pluripotency [42], further investigation into the safety and therapeutic potential of these stem cells is necessary before being considered a candidate population for clinical trials.

1.2.2 Identification of Cardiac Precursor Cells (CPCs)

In 2002, it was first documented that the PN heart, like other organs, contains side population (SP) cells which are capable of excluding Hoechst dye, display stem cell-like behavior, and lack markers of differentiation [43]. When isolated from mature mice, these cells represented approximately 1% of the total heart cells, but were negative for additional stem cell markers such as c-kit and Sca-1 which mark SP cells isolated from other organ systems. One year later, pioneering research from Anversa's laboratory in the newly established CPC field demonstrated that $Lin^{-}c\text{-}kit^{+}$ cells isolated from the adult rat heart are self-renewing, clonogenic, and multipotent and can be differentiated into smooth muscle, endothelial, and cardiac cells [44]. This work was supported three years later by data from Orkin's group which indicated that c-kit is a CPC marker that identifies a subpopulation of $Nkx2.5^{+}$ cells with lineage bipotential [45]. In this study, $c\text{-}kit^{+}Nkx2.5^{+}$ mouse ESCs were isolated and shown to be bipotent in that they could differentiate into smooth muscle and cardiac cells when plated as single cells *in vitro* as well as through chick xenograft assays *in vivo*. As will be presented in Chapter 2, work from our laboratory in 2009 further indicates that c-kit characterizes a cardiovascular precursor cell

population within the PN heart that can be expanded and differentiated *in vitro* into all three cell lineages that specify the heart [46]. The therapeutic potential of these cells in treating myocardial infarction in rodents also has been evaluated with moderate success [44, 47, 48].

Current evidence suggests that additional CPC populations exist and can be identified based on the expression of various cell markers including Abcg2, stem cell antigen (Sca)-1, fetal liver kinase (Flk)-1, and islet (Isl)-1. To date, it is still unknown whether or not these populations represent a single stem cell population at various stages of development or completely distinct cell populations. The origin of these precursor cells also is under scrutinizing debate. Interestingly, in the canine heart it has been reported that overlap in expression of several stem cell antigens is common, with a majority of cardiac stem cells co-expressing MDR1 (similar to Abcg2), Sca-1, and c-kit [49]. Below, each of the various cardiac stem cell markers is discussed in turn.

1.2.2.1 Abcg2/MDR1

In 2003, the same year that c-kit$^+$ precursor cells were found to have multilineage potential, Martin, et al. [50] found that the adult mouse heart also contains SP progenitor cells expressing the ATP binding cassette transporter, Abcg2, which effluxes Hoechst dye. Unlike Hierlihy's purported SP population [43], these SP cells co-expressed Sca-1 as well as low levels of c-kit, CD34 (endothelial precursor marker), and CD45 (hematopoietic precursor marker). In this study, SP cells isolated from the adult heart were shown to proliferate and differentiate along mesodermal lines. In a more recent study, it was observed that cell outgrowths from cardiac biopsies in the rat contain a

small population of progenitor cells marked by both Abcg2 and c-kit which, when introduced into the infarcted heart, initiate repair and induce functional benefits [51].

1.2.2.2 Sca-1

Along with the identification of c-kit as a potential marker of adult CPCs by Anversa's laboratory, Oh, et al. [52] isolated cardiogenic Sca-1^+ cells from the mouse myocardium and found that they home to the infarcted myocardium after intravenous injection and differentiate into myocytes via both fusion and non-fusion events. A year later, Matsuura, et al. [53] also identified that Sca-1 marks a population of adult mouse cardiac cells capable of differentiating into beating cardiomyocytes *in vitro* when treated with oxytocin. The Sca-1^+ precursor cell population has since been used therapeutically in mice following MI with some success [54, 55]. Most recently, Nkx.2.5^+Sca-1^+ embryonic epicardial progenitor cells were shown to play a key role in *de novo* cardiomyocyte generation within the thymosin β4 primed heart after infarct, providing clues into the mechanisms by which resident CPCs can be mobilized post-ischemic injury [56]. However, the human homologue for Sca-1 has yet to be uncovered, severely limiting the therapeutic potential of this population [57] .

1.2.2.3 Flk-1

In 2006, Kattman, et al. [58] demonstrated that a Flk-1^+ population derived from embryoid bodies (EBs) displays multilineage potential and that these multipotent cells also can be isolated from the head-fold-stage embryo. Several years later, Yang, et al. [59] established that human cardiovascular progenitor cells are derived from Flk-1^+ ESCs. More recently, Fatma, et al. [60] reported that activation of endogenous c-kit^+Flk-1^+ cells in the infarcted heart enhances neovascularization and leads to improved cardiac function.

1.2.2.4 Isl-1

The LIM homeobox transcription factor, Isl-1, also has been identified as a marker of cells in the PN heart capable of differentiating into functionally mature cardiomyocytes [61]. Interestingly, this population is limited in expression to the secondary heart field, contributing mainly to the right ventricle, atria, and outflow tract of the mature heart. In 2006, Moretti, et al. [62] expanded the view of Isl-1 cells by demonstrating that Isl-1^+ ESCs which later co-express Flk-1 and Nkx2.5 are capable of differentiating into smooth muscle, endothelial, and cardiac cells. Unfortunately, it also was reported that the presence of these cells rapidly declines after birth, severely limiting the population's therapeutic potential. In recent years, however, it has been shown that Isl-1^+ cells can be generated from iPSCs and differentiated into all three cardiac lineages *in vivo* without the formation tumors [39]. Even so, the stemness of this population has been called into question as its expression is linked to pre-commitment to the myocyte lineage [63] and the population lacks clonogenicity, but produces small colonies *in vitro* [64]. Therefore, the clinical applicability of Isl-1^+ cells in cardiac repair remains to be seen.

1.2.3 Summary

Taken together, these data identify populations of stem cells capable of cardiac regeneration and confirm the presence of resident CPC populations in the PN and adult myocardium that maintain an innate ability to generate all three lineages that specify the heart. Although numerous attempts at cell-based therapy have proven promising in some regards, the field has yet to identify the ideal cell type, cell number, and cell delivery method necessary for significant cardiac regeneration. In addition, reasons as to why resident precursor cells do not play a more

significant role in cardiac regeneration upon damage to the adult myocardium remain to be elucidated.

1.3 Redox Status of Stem Cells

1.3.1 Enhanced Stress Defense Mechanisms

Around the same time that resident CPCs were discovered in the adult myocardium, the mechanisms regulating stem cell self-renewal and differentiation were beginning to be elucidated. With a shared interest in regenerative biology and the recent detection of resident progenitor populations in several organ systems, stem cell biologists hypothesized that various stem cell populations might share fundamental properties and regulatory pathways. Utilizing gene expression arrays, a stem cell molecular signature was reported in 2002 by comparing the transcriptional profiles of HSCs, neural stem cells (NSCs), and ESCs [65]. Interestingly, 283 of the 4289 genes under study were shared among all three groups. A similar analysis that same year revealed 230 shared genes, painting a picture of stem cells as a population highly resistant to stress with upregulated detoxifier and DNA repair systems [66]. In 2004, this phenomenon was extended to EPCs, when it was reported that EPCs isolated from the peripheral blood exhibit increased expression of several antioxidants including catalase, glutathione peroxidase, and manganese superoxide dismutase (SOD). The authors speculated that this redox profile was necessary for progenitor cells to survive and contribute to neovascularization following ischemic injury [67]. Most recently, it was observed that iPSCs reclaim an enhanced defense system in conjunction with decreased production of ROS mediated, in part, by reduced mitochondrial biogenesis [68].

Interestingly, the protected redox state of stem cells described above was found to decline upon differentiation and lineage commitment. In the early 2000's, several reports confirmed that stem cell differentiation is accompanied by the downregulation of antioxidant and detoxifier genes as well as an increase in mitochondrial biosynthesis [69-71]. In addition, a recent report identified increased generation of mitochondrial ROS as a critical modulator in the formation of ESC-derived cardiomyocytes, without which cardiac differentiation is drastically reduced [72]. Together, these studies support the idea that a low ROS environment is a pre-requisite for multipotency and advance the theory that a redox-dependent molecular switch is necessary for stem cell differentiation.

1.3.2 Redox Regulation of Stem Cell Behavior

Further investigation into the redox state of precursor cells revealed that slight changes in redox balance greatly affect cell function, making cells more or less susceptible to signal transduction pathways regulating survival, proliferation, and differentiation. These studies proposed that redox mechanisms are critical for both stemness and differentiation with a more reduced environment conducive to cell survival and cell division and a more oxidized condition favoring differentiation and/or apoptosis [73-77]. Interestingly, in spite of their well-known pathological roles, at low levels, ROS (i.e. superoxide, H_2O_2) are involved in many physiological signaling pathways including those necessary for normal cell development and tissue-injury response. In the late 1990's, it was reported that H_2O_2, a main and highly diffusible form of ROS, is involved in the differentiation of osteoclast precursor cells into bone [78]. Shortly thereafter, a slightly more oxidized environment generated exogenously by application of a pharmacological pro-oxidant was found to drive the differentiation of oligodendrocyte precursor cells, while a more reduced environment seemed necessary for cell maintenance and self-renewal [79]. This theory soon was

extended to the BM lineages when low levels of ROS were found to be critical for the self-renewal capacity of HSCs [80] as well as HSC-derived $CD34^+$ cord blood progenitors [81], while increased ROS was shown to play a crucial role in their differentiation [82]. Although the mechanisms of action regulating these processes are still under investigation, it is thought that redox sensitive transcription factors, kinases, phosphatases, enzymes, and ion channels are all involved.

1.3.3 Summary

Taken together, these studies suggest that the redox state of a precursor cell is critical for its function, making ROS important targets in cardiac cell-based therapy as they mediate the signaling pathways necessary for successful engraftments. Over the past few years, a significant amount of research has been conducted to tease apart the function of ROS generators, specifically NADPH oxidases (Nox), in the heart and to determine their roles in developmental cardiomyogenesis. Elucidating these pathways and translating the mechanisms required for normal heart development to resident CPC function likely will advance treatments for heart disease.

1.4 Nicotinamide Adenine Dinucleotide Phosphate (NADPH) Oxidases (Nox)

1.4.1 Main Reactive Oxygen Species (ROS) Generators in Cardiac Cells

Nox enzymes are the main ROS generators in cardiac cells, critically involved in cell signaling and cardiac function [83-85]. The Nox family is composed of seven members, Nox1-5 and dual oxidases (Duox) 1-2. These enzymes generate superoxide in a highly regulated manner by catalyzing the one electron reduction of molecular oxygen using NADPH as an electron donor.

Each of the seven Nox isoforms is encoded by its own gene and shares structural similarity to the other isoforms including a cytoplasmic N-terminus, six transmembrane spanning domains, two heme binding sites at helices 3 and 5, and a C-terminal tail containing the flavin adenine dinucleotide (FAD) and NADPH binding sites (Figure 1.1) [86-88]. In addition to these shared structural characteristics, Nox5 contains a calmodulin-like domain with four calcium binding sites and the more structurally complex Duoxes demonstrate both calcium binding and a peroxidase-like domain at the N-terminus. Interestingly, only Nox1, 2, and 4 are expressed in the cardiovascular system and, therefore, will be the focus of this discussion. The other Nox isoforms have various tissue distributions with Nox3 expressed in the inner ear, Nox5 expressed in humans, but not in rodents, and the Duoxes limited in their expression to the thyroid tissue [89]. Unlike the neutrophil oxidases which release a large "respiratory burst" of superoxide to ward off pathogens [90], the cardiovascular Noxes generate lower levels of intracellular ROS which act as second messengers that are necessary for cell signaling. These cardiac Nox enzymes exhibit cell-type specific expression patterns and vary in their needs for regulatory subunits. Each of the respective cardiovascular Noxes is discussed below in detail.

1.4.1.1 Nox2

Nox2 is the prototypical Nox isoform, originally named gp91^{phox} for its role as a phagocytic oxidase in host defense and innate immunity [89]. Following its initial discovery in macrophages and neutrophils, Nox2 was found to be expressed in several cell types including those of the cardiovascular system; endothelial cells, cardiomyocytes, fibroblasts, and vascular smooth muscle cells (VSMCs) [85]. In the cell, Nox2 is predominantly localized to the plasma membrane, caveolae, and endosomes, but it also

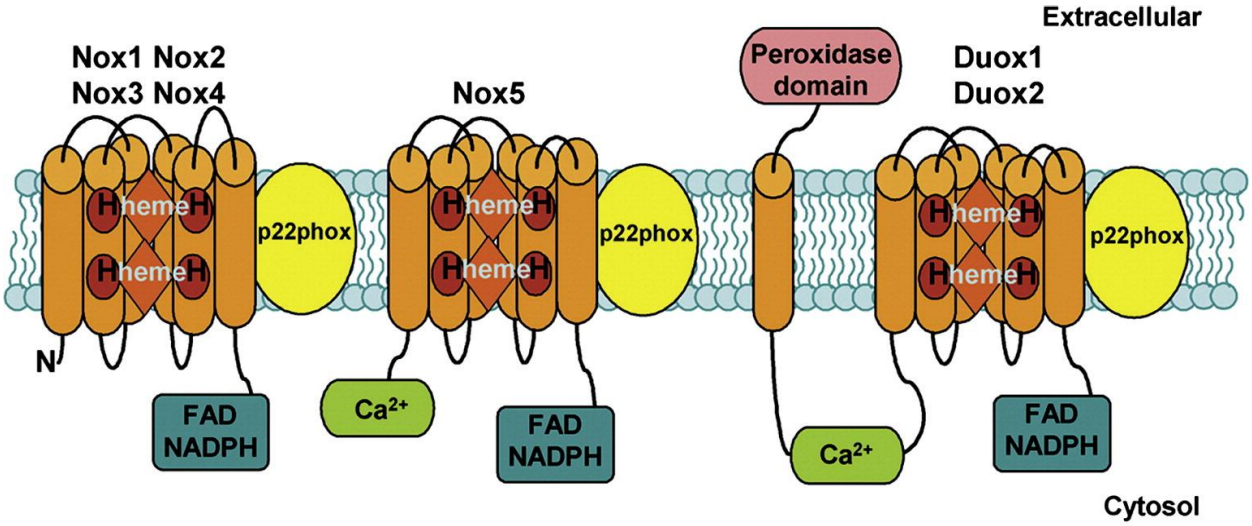

Figure 1.1. Structures of the Nox Enzymes [88]

has been found in the nucleus of apoptotic cardiomyocytes where it likely plays an important role in programmed cell death [91, 92]. The activity of Nox2 is well regulated and dependent on the presence of five additional subunits; $p22^{phox}$, $p47^{phox}$, $p67^{phox}$, $p40^{phox}$, and Rac1/2. At rest, Nox2 and $p22^{phox}$ exist as a membrane bound dimer known as cytochrome b558, while $p47^{phox}$, $p67^{phox}$, and $p40^{phox}$ are maintained as a ternary complex in the cytosol with Rac1/2 bound nearby to its inhibitory protein Rho-GDP dissociation inhibitor (GDI). Upon stimulation by various agonists which will be discussed in detail in the following sections, $p47^{phox}$ is phosphorylated by protein kinase (PK) C at several serine sites initiating a conformational change and the subsequent release of an auto-inhibitory binding domain. This activated form of $p47^{phox}$ next transports tethered $p67^{phox}$ and $p40^{phox}$ to the membrane where the three subunits attach to membrane bound cytochrome b558. In the final stages of assembly, $p67^{phox}$ binds Rac1/2 after guanine nucleotide exchange, completing the third trigger event necessary for Nox2 activity [87].

1.4.1.2 Nox1

During the 1990's, researchers discovered ROS production in several cell types other than phagocytes that seemed to be generated by a flavoprotein and not as a byproduct of cellular respiration. This finding led to the discovery of the first of the Nox homologues in 1999 [86]. Nox1, which was initially cloned from colon epithelial cells, has since been found to be expressed in VSMCs of the cardiovascular system [85] where it was recently shown to play a critical role in cell migration, proliferation, and matrix production [93]. Similar to Nox2, this Nox isoform is localized in cells to the plasma membrane, caveolae, and endosomes [92]. However, unlike Nox2, the Nox1 system has relatively few trigger events necessary for its activation. While Nox1 requires $p22^{phox}$ and homologues of

p47^{phox} (NoxO1) and p67^{phox} (NoxA1) for its activity, this isoform is already associated with p22^{phox}, NoxO1, and NoxA1 at the plasma membrane under basal conditions. Therefore, the only trigger event necessary for ROS production by Nox1 is guanine nucleotide exchange on Rac1/2 [87].

1.4.1.3 Nox4

Of the cardiac Nox isoforms, Nox4 is more distantly related to Nox2 and Nox1 [87]. This Nox enzyme is expressed at high levels in the kidney, but it is also found in all four cardiovascular cell types; endothelial cells, cardiomyocytes, fibroblasts, and VSMCs [85, 94]. Unlike Nox2 and Nox1 which are mainly localized to the plasma membrane, Nox4 is found in focal adhesions, the nucleus, endoplasmic reticulum, and mitochondria [92, 95, 96]. In cardiomyocytes, Nox4 is mainly localized to the mitochondria [96]. While Nox4 exists at the membrane in a heterodimer with p22^{phox}, it does not require p47^{phox}, p67^{phox}, p40^{phox}, or Rac1/2 for its activity. Therefore, some believe Nox4 to be a constitutively active Nox isoform [89]. However, because Nox4 is induced by the hormone insulin in a manner too fast to be explained solely by protein synthesis, unknown mechanisms likely exist to regulate its activity [87, 97]. Along these lines, purported binding partners of Nox4 have been identified recently including Poldip2 [98]. In addition, some research indicates that Nox4 produces H_2O_2 directly instead of superoxide, adding even more complexity to the mechanistic actions of this Nox isoform [99].

1.4.2 Regulation of Activity and Potential Downstream Targets

The activity of the cardiovascular Nox enzymes in the cell is very well controlled, allowing for the production of ROS in a highly regulated manner as opposed to superoxide generation as a mere byproduct of other reactions. Thus far, several agonists for Nox 1, 2, and 4 have been

identified including G-protein coupled receptor agonists such as angiotensin-II, endothelin-1, and α-adrenergic agonists [85]. In addition to these agonists, Nox activity also can be stimulated by several growth factors (e.g. vascular endothelial growth factor [VEGF], platelet derived growth factor [PDGF], bone morphogenetic protein [BMP]-4), cytokines (e.g. TNF-α, transforming growth factor [TGF]-ß), and metabolic factors (e.g. insulin, glucose) [85-87]. In fact, even broader environmental agonists of Nox activity including mechanical forces, sheer stress, and conditions of hypoxia and reoxygenation exist [85].

The ROS generated by the cardiovascular Noxes exert effects on the cell by causing reversible oxidation of reactive cysteine residues located on target molecules [77, 100]. One of the main targets of Nox-derived ROS is the family of protein tyrosine phosphatases (PTPs) such as the SH2 domain-containing phosphatases, SHP-1 and SHP-2. These enzymes dephosphorylate tyrosine residues and alter signal transduction pathways driven by a wide-array of protein kinases [77, 88]. Interestingly, some kinases (e.g. PKB, PKC, mitogen activated protein kinases [MAPKs]) and transcription factors (e.g. activator protein [AP]-1, nuclear factor [NF]-κβ, hypoxia inducible factor [HIF]-1) also are redox-sensitive, exponentially magnifying the signaling capacity of ROS in the cell. More direct effects of ROS include their ability to alter the function of enzymes such as MMPs, ion channels, and receptors [85]. Therefore, it is not surprising that physiological ROS regulation and signal transduction have become topics of great interest over the last decade.

In general, ROS signaling is implicated in a range of cell events including cell proliferation, migration, and differentiation [86, 89, 94, 101]. At toxic levels, however, ROS are known to induce programmed cell death [86]. While the Noxes are present in a variety of cell systems, the

vasculature provides a system in which roles of the specific Nox isoforms are well established. In the vasculature, Nox1 exerts its effects on VSMC migration, proliferation, and matrix formation [93] while Nox2 plays a more prominent role in endothelial cell function and neointimal formation [102-105]. Nox4 has broader implications, affecting VSMC growth and migration as well as inducing cardioprotection following injury [98, 106, 107]. Interestingly, divergent subcellular localization of the Noxes is thought to facilitate their ability to exert these specific effects and mediate distinct cellular functions [77, 108].

In the heart, the Noxes are involved in calcium signaling, contractility, and even the detrimental effects of LV remodeling following infarct [85]. In fact, Nox knock-out mice suggest a negative role for Nox2 following myocardial ischemia [109, 110] and a potential beneficial role for Nox4 during periods of chronic pressure overload [107]. Overexpression of Sod1 also was demonstrated to provide functional benefit following MI, suggesting that overall redox change is an important modulator of cardiac repair [111]. However, isoform specific roles in cardiac cell maturation and function still are being teased apart as will be discussed further in the next section.

1.4.3 Redox Regulation of Cardiac Differentiation

Redox regulation of cardiac differentiation has been well studied in ESCs where a structured model of cardiogenesis exists and results in spontaneously beating cardiomyocytes within EBs after 7 to 8 days of culture. By faithfully recapitulating the time course of embryogenesis, this system provides a good *in vitro* model for studying the effects of redox balance and ROS generation on the regulation of cardiomyocyte growth and differentiation. Using this system in murine cells, Sauer, et al. [112, 113] first reported a vital role for ROS in cardiomyogenesis. Utilizing electrical field [112] and cardiotrophin-1 [113] stimulation of ROS generation, the group

demonstrated a clear link between ROS activation and subsequent mesodermal development and cardiac differentiation by ESCs. Similar cardiogenic outcomes were obtained by applying low doses of H_2O_2 to the cell culture [114]. Interestingly, long-term exposure to higher doses of ROS was cytotoxic, suggesting a dose dependent mechanism of action. The theory of ROS as critical modulators of ESC-derived cardiomyogenesis has since been confirmed during stimulation with several other agonists including peroxisome proliferator activated receptor (PPAR)-α [115] as well as in cardiac differentiation by human ESCs [116].

In search of the mechanisms by which ROS exert their effects on cardiomyocyte generation, several known targets of ROS were evaluated for their participation in the processes of cardiac commitment and differentiation of ESCs (Figure 1.2) [117]. Of the kinases, phosphatidylinositol 3-kinase (PI3K) was identified as a key activator of Nox and the subsequent activation of extracellular signal regulated kinase (ERK) 1/2 and transcription factor NF-κβ by Nox-derived ROS [112-114]. Several years later, the ROS dependency of cardiac differentiation further was tied to the Nox enzymes when Puceat, et al. [117, 118] demonstrated a stage-dependent function of Rac, a critical Nox subunit, on cardiac proliferation and differentiation. Because these studies relied heavily on the general Nox inhibitor, diphenylene iodonium (DPI), it remained unclear which of the Nox isoforms were required for cardiac differentiation in ESCs. Therefore, several groups went on to investigate the transcript expression of the cardiac Nox isoforms during ESC differentiation. While transient expression of Nox1, Nox2, and Nox4 mRNA was observed throughout the differentiation of EBs, it was found that mechanical strain or treatment with exogenous ROS induced expression of Nox1 and Nox4, specifically, together with cardiac transcription factors Gata4, Nkx2.5, and Mef2c [119, 120]. These studies also demonstrated a clear

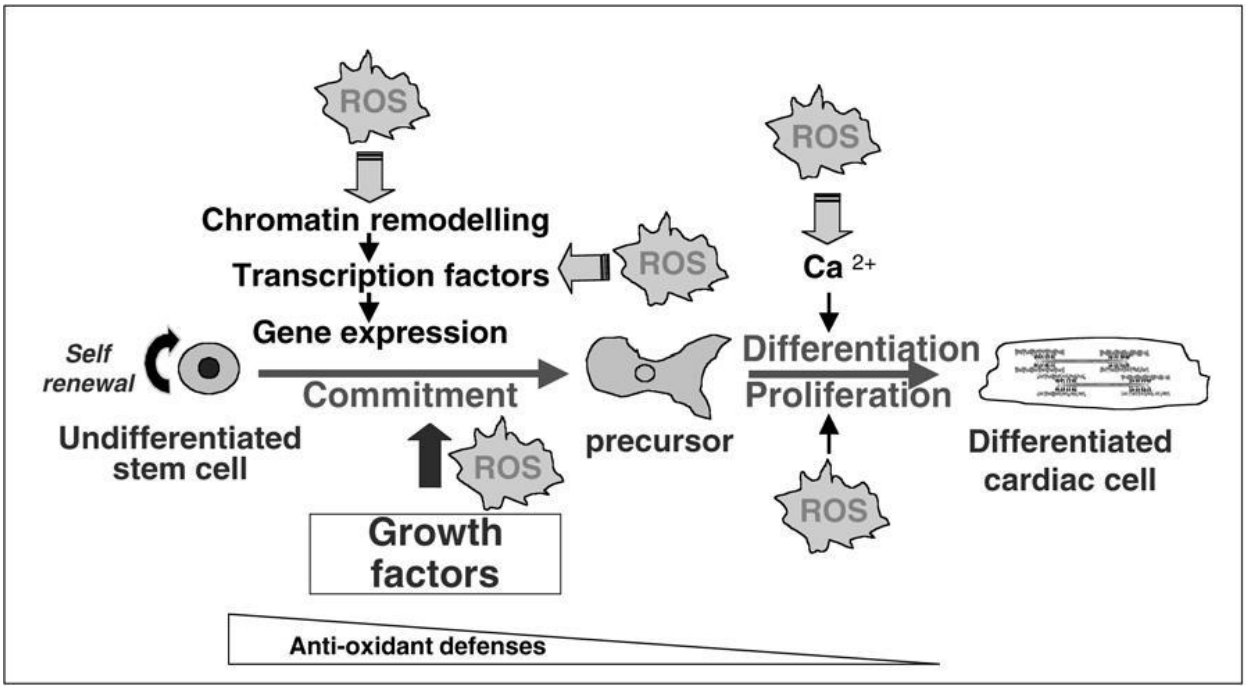

Figure 1.2. Targets of ROS during Cardiac Differentiation by ESCs [117]

redox link to MAPK signaling pathways. Around the same time, similar results implicating the MAPKs and redox sensitive transcription factors in cardiac differentiation were obtained from studies using a mouse embryonic carcinoma cell model [121, 122]. In 2006, Li, et al. [123] proposed a more specific model of cardiac differentiation, suggesting Nox4 to be the most prominent Nox isoform in cardiac differentiation. This model established Nox4-derived ROS as a driver of p38 phosphorylation and the subsequent translocation of cardiac transcription factor Mef2c to the nucleus. Most recently, Nox2 was shown to be upregulated along with Nox4 during ascorbic acid induction of cardiac differentiation, suggesting non-redundant roles for the two most abundant cardiac Nox isoforms in cardiomyogenesis [124].

1.4.4 Summary

Because it is clear that Nox-derived ROS play important physiological and pathological roles in the cardiovascular system, understanding the mechanistic actions of Nox proteins in resident CPCs is critical to enhance current strategies for cell-based therapy. With genetic modification of therapeutic cell populations becoming a popular approach for graft enhancement [125-127], altering expression levels and/or timing of Nox activity may afford essential control over CPC survival and differentiation in the infarct region.

1.5 Statement of Problem and Approach

While it was recently demonstrated that redox effector protein (Ref)-1 plays an important role in maintaining the redox balance of cardiac stem cells isolated from the adult rat heart [128], very little research has been directed at redox regulation of resident CPCs, specifically those marked by the receptor tyrosine kinase, c-kit. Because questions regarding the basic mechanisms that drive

CPC self-renewal and differentiation remain largely unanswered, I believe that further understanding redox mechanisms, particularly the functions of the cardiac Nox enzymes, and how they relate to c-kit^{+} cell function will reveal novel targets for therapeutic action. Therefore, to test the ***central hypothesis*** that c-kit^{+} CPCs exhibit a unique redox-related molecular signature that confers precursor status, and that this status influences the capacity for cardiac lineage commitment, first our laboratory generated a bacterial artificial chromosome (BAC) transgenic mouse in which enhanced green fluorescent protein (EGFP) is a fluorescent indicator of c-kit promoter activity to isolate and characterize the differentiation potential of neonatal cardiac c-kit^{+} cells (Chapter 2). The findings presented in this chapter were generated through the close collaboration among four key investigators, Dr. Yvonne Tallini, Dr. Kai Su Greene, Dr. Michael Craven, and myself. It is important to note that the BAC transgenic construct was generated by Dr. Kai Su Greene. Dr. Kai Su Greene also worked with Dr. Yvonne Tallini to perform the initial characterization of transgenic founder lines which was nearly complete prior to my arrival in the laboratory. I contributed to the *in vivo* and *in vitro* characterization of the lineage status and potential of neonatal cardiac c-kit^{+} cells and Dr. Michael Craven performed the patch clamp experiments necessary to determine the electrical physiology of our purported precursor cell population. Utilizing c-kit^{+} cells isolated from the hearts of neonatal c-kit^{BAC}-EGFP transgenic mice along with redox and molecular biology techniques, next I investigated the redox status of c-kit^{+} CPCs and examined the effects of reduced Nox expression on CPC stemness and differentiation *in vitro* (Chapter 3).

The findings presented in Chapter 2 provide strong evidence for the stemness of neonatal c-kit^{+} CPCs and rationale for their use as a therapeutic population in the treatment of MI. Chapter 3

establishes a link between redox biology and c-kit^{+} CPC cell function and identifies several target molecules including pro-oxidants (Nox2 and Nox4), transcription factors (Gata6 and Gata4), and a cytokine (TGF-β1) all of which are involved in c-kit^{+} CPC lineage specification. A final summary of findings, significance of research, and future directions are presented in Chapter 4 and leave the reader anticipating additional scientific discovery, which will reveal a more precise understanding of the complexities involved in the balance between c-kit^{+} CPC status and lineage commitment.

1.6 References

1. Lloyd-Jones D, Adams RJ, Brown TM, Carnethon M, Dai S, De Simone G, Ferguson TB, Ford E, Furie K, Gillespie C, Go A, Greenlund K, Haase N, Hailpern S, Ho PM, Howard V, Kissela B, Kittner S, Lackland D, Lisabeth L, Marelli A, McDermott MM, Meigs J, Mozaffarian D, Mussolino M, Nichol G, Roger VL, Rosamond W, Sacco R, Sorlie P, Stafford R, Thom T, Wasserthiel-Smoller S, Wong ND, Wylie-Rosett J, American Heart Association Statistics Committee and Stroke Statistics Subcommittee. Executive summary: Heart disease and stroke statistics--2010 update: A report from the american heart association. *Circulation*. 2010;121:948-954.

2. Karsner HT, Saphir O, Todd TW. The state of the cardiac muscle in hypertrophy and atrophy. *Am J Pathol*. 1925;1:351-372.1.

3. Zak R. Development and proliferative capacity of cardiac muscle cells. *Circ Res*. 1974;35:suppl II:17-26.

4. LINZBACH AJ. Heart failure from the point of view of quantitative anatomy. *Am J Cardiol*. 1960;5:370-382.

5. Kajstura J, Leri A, Finato N, Di Loreto C, Beltrami CA, Anversa P. Myocyte proliferation in end-stage cardiac failure in humans. *Proc Natl Acad Sci U S A*. 1998;95:8801-8805.

6. Anversa P, Kajstura J. Ventricular myocytes are not terminally differentiated in the adult mammalian heart. *Circ Res*. 1998;83:1-14.

7. Beltrami AP, Urbanek K, Kajstura J, Yan SM, Finato N, Bussani R, Nadal-Ginard B, Silvestri F, Leri A, Beltrami CA, Anversa P. Evidence that human cardiac myocytes divide after myocardial infarction. *N Engl J Med*. 2001;344:1750-1757.

8. Quaini F, Urbanek K, Beltrami AP, Finato N, Beltrami CA, Nadal-Ginard B, Kajstura J, Leri A, Anversa P. Chimerism of the transplanted heart. *N Engl J Med*. 2002;346:5-15.

9. Thiele J, Varus E, Wickenhauser C, Kvasnicka HM, Lorenzen J, Gramley F, Metz KA, Rivero F, Beelen DW. Mixed chimerism of cardiomyocytes and vessels after allogeneic bone marrow and stem-cell transplantation in comparison with cardiac allografts. *Transplantation*. 2004;77:1902-1905.

10. Bergmann O, Bhardwaj RD, Bernard S, Zdunek S, Barnabe-Heider F, Walsh S, Zupicich J, Alkass K, Buchholz BA, Druid H, Jovinge S, Frisen J. Evidence for cardiomyocyte renewal in humans. *Science*. 2009;324:98-102.

11. Porrello ER, Mahmoud AI, Simpson E, Hill JA, Richardson JA, Olson EN, Sadek HA. Transient regenerative potential of the neonatal mouse heart. *Science*. 2011;331:1078-1080.

12. Kutala VK, Khan M, Angelos MG, Kuppusamy P. Role of oxygen in postischemic myocardial injury. *Antioxid Redox Signal*. 2007;9:1193-1206.

13. Frangogiannis NG, Smith CW, Entman ML. The inflammatory response in myocardial infarction. *Cardiovasc Res*. 2002;53:31-47.

14. Hori M, Nishida K. Oxidative stress and left ventricular remodelling after myocardial infarction. *Cardiovasc Res*. 2009;81:457-464.

15. Menasche P, Hagege AA, Scorsin M, Pouzet B, Desnos M, Duboc D, Schwartz K, Vilquin JT, Marolleau JP. Myoblast transplantation for heart failure. *Lancet*. 2001;357:279-280.

16. Reinecke H, Poppa V, Murry CE. Skeletal muscle stem cells do not transdifferentiate into cardiomyocytes after cardiac grafting. *J Mol Cell Cardiol*. 2002;34:241-249.

17. Leobon B, Garcin I, Menasche P, Vilquin JT, Audinat E, Charpak S. Myoblasts transplanted into rat infarcted myocardium are functionally isolated from their host. *Proc Natl Acad Sci U S A*. 2003;100:7808-7811.

18. Menasche P, Hagege AA, Desnos M. Myoblast transplantation for heart failure: Where are we heading? *Arch Mal Coeur Vaiss*. 2005;98:649-654.

19. Fouts K, Fernandes B, Mal N, Liu J, Laurita KR. Electrophysiological consequence of skeletal myoblast transplantation in normal and infarcted canine myocardium. *Heart Rhythm*. 2006;3:452-461.

20. Menasche P, Hagege AA, Vilquin JT, Desnos M, Abergel E, Pouzet B, Bel A, Sarateanu S, Scorsin M, Schwartz K, Bruneval P, Benbunan M, Marolleau JP, Duboc D. Autologous skeletal myoblast transplantation for severe postinfarction left ventricular dysfunction. *J Am Coll Cardiol*. 2003;41:1078-1083.

21. Orlic D, Kajstura J, Chimenti S, Jakoniuk I, Anderson SM, Li B, Pickel J, McKay R, Nadal-Ginard B, Bodine DM, Leri A, Anversa P. Bone marrow cells regenerate infarcted myocardium. *Nature*. 2001;410:701-705.

22. Nygren JM, Jovinge S, Breitbach M, Sawen P, Roll W, Hescheler J, Taneera J, Fleischmann BK, Jacobsen SE. Bone marrow-derived hematopoietic cells generate cardiomyocytes at a low frequency through cell fusion, but not transdifferentiation. *Nat Med*. 2004;10:494-501.

23. Murry CE, Soonpaa MH, Reinecke H, Nakajima H, Nakajima HO, Rubart M, Pasumarthi KB, Virag JI, Bartelmez SH, Poppa V, Bradford G, Dowell JD, Williams DA, Field LJ. Haematopoietic stem cells do not transdifferentiate into cardiac myocytes in myocardial infarcts. *Nature*. 2004;428:664-668.

24. Kajstura J, Rota M, Whang B, Cascapera S, Hosoda T, Bearzi C, Nurzynska D, Kasahara H, Zias E, Bonafe M, Nadal-Ginard B, Torella D, Nascimbene A, Quaini F, Urbanek K, Leri A, Anversa P. Bone marrow cells differentiate in cardiac cell lineages after infarction independently of cell fusion. *Circ Res*. 2005;96:127-137.

25. Iwasaki H, Kawamoto A, Ishikawa M, Oyamada A, Nakamori S, Nishimura H, Sadamoto K, Horii M, Matsumoto T, Murasawa S, Shibata T, Suehiro S, Asahara T. Dose-dependent contribution of CD34-positive cell transplantation to concurrent vasculogenesis and cardiomyogenesis for functional regenerative recovery after myocardial infarction. *Circulation*. 2006;113:1311-1325.

26. Hatzistergos KE, Quevedo H, Oskouei BN, Hu Q, Feigenbaum GS, Margitich IS, Mazhari R, Boyle AJ, Zambrano JP, Rodriguez JE, Dulce R, Pattany PM, Valdes D, Revilla C, Heldman AW, McNiece I, Hare JM. Bone marrow mesenchymal stem cells stimulate cardiac stem cell proliferation and differentiation. *Circ Res*. 2010;107:913-922.

27. Loffredo FS, Steinhauser ML, Gannon J, Lee RT. Bone marrow-derived cell therapy stimulates endogenous cardiomyocyte progenitors and promotes cardiac repair. *Cell Stem Cell*. 2011;8:389-398.

28. Kehat I, Kenyagin-Karsenti D, Snir M, Segev H, Amit M, Gepstein A, Livne E, Binah O, Itskovitz-Eldor J, Gepstein L. Human embryonic stem cells can differentiate into myocytes with structural and functional properties of cardiomyocytes. *J Clin Invest*. 2001;108:407-414.

29. Xu C, Police S, Rao N, Carpenter MK. Characterization and enrichment of cardiomyocytes derived from human embryonic stem cells. *Circ Res*. 2002;91:501-508.

30. Hodgson DM, Behfar A, Zingman LV, Kane GC, Perez-Terzic C, Alekseev AE, Puceat M, Terzic A. Stable benefit of embryonic stem cell therapy in myocardial infarction. *Am J Physiol Heart Circ Physiol*. 2004;287:H471-9.

31. Laflamme MA, Gold J, Xu C, Hassanipour M, Rosler E, Police S, Muskheli V, Murry CE. Formation of human myocardium in the rat heart from human embryonic stem cells. *Am J Pathol*. 2005;167:663-671.

32. Kolossov E, Bostani T, Roell W, Breitbach M, Pillekamp F, Nygren JM, Sasse P, Rubenchik O, Fries JW, Wenzel D, Geisen C, Xia Y, Lu Z, Duan Y, Kettenhofen R, Jovinge S, Bloch W, Bohlen H, Welz A, Hescheler J, Jacobsen SE, Fleischmann BK. Engraftment of engineered ES cell-derived cardiomyocytes but not BM cells restores contractile function to the infarcted myocardium. *J Exp Med*. 2006;203:2315-2327.

33. Laflamme MA, Chen KY, Naumova AV, Muskheli V, Fugate JA, Dupras SK, Reinecke H, Xu C, Hassanipour M, Police S, O'Sullivan C, Collins L, Chen Y, Minami E, Gill EA, Ueno S, Yuan C, Gold J, Murry CE. Cardiomyocytes derived from human embryonic stem cells in pro-survival factors enhance function of infarcted rat hearts. *Nat Biotechnol*. 2007;25:1015-1024.

34. Takahashi K, Yamanaka S. Induction of pluripotent stem cells from mouse embryonic and adult fibroblast cultures by defined factors. *Cell*. 2006;126:663-676.

35. Takahashi K, Tanabe K, Ohnuki M, Narita M, Ichisaka T, Tomoda K, Yamanaka S. Induction of pluripotent stem cells from adult human fibroblasts by defined factors. *Cell*. 2007;131:861-872.

36. Yu J, Vodyanik MA, Smuga-Otto K, Antosiewicz-Bourget J, Frane JL, Tian S, Nie J, Jonsdottir GA, Ruotti V, Stewart R, Slukvin II, Thomson JA. Induced pluripotent stem cell lines derived from human somatic cells. *Science*. 2007;318:1917-1920.

37. Mauritz C, Schwanke K, Reppel M, Neef S, Katsirntaki K, Maier LS, Nguemo F, Menke S, Haustein M, Hescheler J, Hasenfuss G, Martin U. Generation of functional murine cardiac myocytes from induced pluripotent stem cells. *Circulation*. 2008;118:507-517.

38. Narazaki G, Uosaki H, Teranishi M, Okita K, Kim B, Matsuoka S, Yamanaka S, Yamashita JK. Directed and systematic differentiation of cardiovascular cells from mouse induced pluripotent stem cells. *Circulation*. 2008;118:498-506.

39. Moretti A, Bellin M, Jung CB, Thies TM, Takashima Y, Bernshausen A, Schiemann M, Fischer S, Moosmang S, Smith AG, Lam JT, Laugwitz KL. Mouse and human induced

pluripotent stem cells as a source for multipotent Isl1+ cardiovascular progenitors. *FASEB J*. 2010;24:700-711.

40. Zhang Y, Wang D, Chen M, Yang B, Zhang F, Cao K. Intramyocardial transplantation of undifferentiated rat induced pluripotent stem cells causes tumorigenesis in the heart. *PLoS One*. 2011;6:e19012.

41. Ahmed RP, Ashraf M, Buccini S, Shujia J, Haider HK. Cardiac tumorigenic potential of induced pluripotent stem cells in an immunocompetent host with myocardial infarction. *Regen Med*. 2011;6:171-178.

42. Ieda M, Fu JD, Delgado-Olguin P, Vedantham V, Hayashi Y, Bruneau BG, Srivastava D. Direct reprogramming of fibroblasts into functional cardiomyocytes by defined factors. *Cell*. 2010;142:375-386.

43. Hierlihy AM, Seale P, Lobe CG, Rudnicki MA, Megeney LA. The post-natal heart contains a myocardial stem cell population. *FEBS Lett*. 2002;530:239-243.

44. Beltrami AP, Barlucchi L, Torella D, Baker M, Limana F, Chimenti S, Kasahara H, Rota M, Musso E, Urbanek K, Leri A, Kajstura J, Nadal-Ginard B, Anversa P. Adult cardiac stem cells are multipotent and support myocardial regeneration. *Cell,*. 2003;114:763-776.

45. Wu SM, Fujiwara Y, Cibulsky SM, Clapham DE, Lien C, Schultheiss TM, Orkin SH. Developmental origin of a bipotential myocardial and smooth muscle cell precursor in the mammalian heart. *Cell,*. 2006;127:1137-1150.

46. Tallini YN, Greene KS, Craven M, Spealman A, Breitbach M, Smith J, Fisher PJ, Steffey M, Hesse M, Doran RM, Woods A, Singh B, Yen A, Fleischmann BK, Kotlikoff MI. C-kit expression identifies cardiovascular precursors in the neonatal heart. *Proc Natl Acad Sci U S A*. 2009;106:1808-1813.

47. Yang CF, Chou KY, Weng ZC, Hung SC, Lai ST, Hsu CP, Wang JS. Cardiac myocyte progenitors from adult hearts for myocardial regenerative therapy. *J Chin Med Assoc*. 2008;71:79-85.

48. Li Q, Guo Y, Ou Q, Chen N, Wu WJ, Yuan F, O'Brien E, Wang T, Luo L, Hunt GN, Zhu X, Bolli R. Intracoronary administration of cardiac stem cells in mice: A new, improved technique for cell therapy in murine models. *Basic Res Cardiol*. 2011.

49. Linke A, Muller P, Nurzynska D, Casarsa C, Torella D, Nascimbene A, Castaldo C, Cascapera S, Bohm M, Quaini F, Urbanek K, Leri A, Hintze TH, Kajstura J, Anversa P. Stem cells in the dog heart are self-renewing, clonogenic, and multipotent and regenerate infarcted myocardium, improving cardiac function. *Proc Natl Acad Sci U S A*. 2005;102:8966-8971.

50. Martin CM, Meeson AP, Robertson SM, Hawke TJ, Richardson JA, Bates S, Goetsch SC, Gallardo TD, Garry DJ. Persistent expression of the ATP-binding cassette transporter, Abcg2, identifies cardiac SP cells in the developing and adult heart. *Developmental Biology,*. 2004;265:262-275.

51. Davis DR, Kizana E, Terrovitis J, Barth AS, Zhang Y, Smith RR, Miake J, Marban E. Isolation and expansion of functionally-competent cardiac progenitor cells directly from heart biopsies. *J Mol Cell Cardiol*. 2010;49:312-321.

52. Oh H, Bradfute SB, Gallardo TD, Nakamura T, Gaussin V, Mishina Y, Pocius J, Michael LH, Behringer RR, Garry DJ, Entman ML, Schneider MD. Cardiac progenitor cells from adult myocardium: Homing, differentiation, and fusion after infarction. *Proc Natl Acad Sci U S A*. 2003;100:12313-12318.

53. Matsuura K, Nagai T, Nishigaki N, Oyama T, Nishi J, Wada H, Sano M, Toko H, Akazawa H, Sato T, Nakaya H, Kasanuki H, Komuro I. Adult cardiac sca-1-positive cells differentiate into beating cardiomyocytes. *J Biol Chem*. 2004;279:11384-11391.

54. Wang X, Hu Q, Nakamura Y, Lee J, Zhang G, From AH, Zhang J. The role of the sca-1+/CD31- cardiac progenitor cell population in postinfarction left ventricular remodeling. *Stem Cells*. 2006;24:1779-1788.

55. Matsuura K, Honda A, Nagai T, Fukushima N, Iwanaga K, Tokunaga M, Shimizu T, Okano T, Kasanuki H, Hagiwara N, Komuro I. Transplantation of cardiac progenitor cells ameliorates cardiac dysfunction after myocardial infarction in mice. *J Clin Invest*. 2009;119:2204-2217.

56. Smart N, Bollini S, Dube KN, Vieira JM, Zhou B, Davidson S, Yellon D, Riegler J, Price AN, Lythgoe MF, Pu WT, Riley PR. De novo cardiomyocytes from within the activated adult heart after injury. *Nature*. 2011;474:640-644.

57. Rosenblatt-Velin N, Ogay S, Felley A, Stanford WL, Pedrazzini T. Cardiac dysfunction and impaired compensatory response to pressure overload in mice deficient in stem cell antigen-1. *FASEB J*. 2011.

58. Kattman SJ, Huber TL, Keller GM. Multipotent flk-1+ cardiovascular progenitor cells give rise to the cardiomyocyte, endothelial, and vascular smooth muscle lineages. *Dev Cell*. 2006;11:723-732.

59. Yang L, Soonpaa MH, Adler ED, Roepke TK, Kattman SJ, Kennedy M, Henckaerts E, Bonham K, Abbott GW, Linden RM, Field LJ, Keller GM. Human cardiovascular progenitor cells develop from a KDR+ embryonic-stem-cell-derived population. *Nature*. 2008;453:524-528.

60. Fatma S, Selby DE, Singla RD, Singla DK. Factors released from embryonic stem cells stimulate c-kit-FLK-1(+ve) progenitor cells and enhance neovascularization. *Antioxid Redox Signal*. 2010;13:1857-1865.

61. Laugwitz KL, Moretti A, Lam J, Gruber P, Chen Y, Woodard S, Lin LZ, Cai CL, Lu MM, Reth M, Platoshyn O, Yuan JX, Evans S, Chien KR. Postnatal isl1+ cardioblasts enter fully differentiated cardiomyocyte lineages. *Nature*. 2005;433:647-653.

62. Moretti A, Caron L, Nakano A, Lam JT, Bernshausen A, Chen Y, Qyang Y, Bu L, Sasaki M, Martin-Puig S, Sun Y, Evans SM, Laugwitz KL, Chien KR. Multipotent embryonic isl1+ progenitor cells lead to cardiac, smooth muscle, and endothelial cell diversification. *Cell*. 2006;127:1151-1165.

63. Dodou E, Verzi MP, Anderson JP, Xu SM, Black BL. Mef2c is a direct transcriptional target of ISL1 and GATA factors in the anterior heart field during mouse embryonic development. *Development*. 2004;131:3931-3942.

64. Bu L, Jiang X, Martin-Puig S, Caron L, Zhu S, Shao Y, Roberts DJ, Huang PL, Domian IJ, Chien KR. Human ISL1 heart progenitors generate diverse multipotent cardiovascular cell lineages. *Nature*. 2009;460:113-117.

65. Ivanova NB, Dimos JT, Schaniel C, Hackney JA, Moore KA, Lemischka IR. A stem cell molecular signature. *Science*. 2002;298:601-604.

66. Ramalho-Santos M, Yoon S, Matsuzaki Y, Mulligan RC, Melton DA. "Stemness": Transcriptional profiling of embryonic and adult stem cells. *Science*. 2002;298:597-600.

67. Dernbach E, Urbich C, Brandes RP, Hofmann WK, Zeiher AM, Dimmeler S. Antioxidative stress-associated genes in circulating progenitor cells: Evidence for enhanced resistance against oxidative stress. *Blood*. 2004;104:3591-3597.

68. Armstrong L, Tilgner K, Saretzki G, Atkinson SP, Stojkovic M, Moreno R, Przyborski S, Lako M. Human induced pluripotent stem cell lines show stress defense mechanisms and mitochondrial regulation similar to those of human embryonic stem cells. *Stem Cells*. 2010;28:661-673.

69. Saretzki G, Armstrong L, Leake A, Lako M, von Zglinicki T. Stress defense in murine embryonic stem cells is superior to that of various differentiated murine cells. *Stem Cells*. 2004;22:962-971.

70. Cho YM, Kwon S, Pak YK, Seol HW, Choi YM, Park do J, Park KS, Lee HK. Dynamic changes in mitochondrial biogenesis and antioxidant enzymes during the spontaneous

differentiation of human embryonic stem cells. *Biochem Biophys Res Commun*. 2006;348:1472-1478.

71. Saretzki G, Walter T, Atkinson S, Passos JF, Bareth B, Keith WN, Stewart R, Hoare S, Stojkovic M, Armstrong L, von Zglinicki T, Lako M. Downregulation of multiple stress defense mechanisms during differentiation of human embryonic stem cells. *Stem Cells*. 2008;26:455-464.

72. Crespo FL, Sobrado VR, Gomez L, Cervera AM, McCreath KJ. Mitochondrial reactive oxygen species mediate cardiomyocyte formation from embryonic stem cells in high glucose. *Stem Cells*. 2010;28:1132-1142.

73. Noble M, Mayer-Proschel M, Proschel C. Redox regulation of precursor cell function: Insights and paradoxes. *Antioxid Redox Signal*. 2005;7:1456-1467.

74. Haneline LS. Redox regulation of stem and progenitor cells. *Antioxid Redox Signal*. 2008;10:1849-1852.

75. Ogasawara MA, Zhang H. Redox regulation and its emerging roles in stem cells and stem-like cancer cells. *Antioxid Redox Signal*. 2008.

76. Pervaiz S, Taneja R, Ghaffari S. Oxidative stress regulation of stem and progenitor cells. *Antioxid Redox Signal*. 2009.

77. Ushio-Fukai M, Urao N. Novel role of NADPH oxidase in angiogenesis and stem/progenitor cell function. *Antioxid Redox Signal*. 2009;11:2517-2533.

78. Steinbeck MJ, Kim JK, Trudeau MJ, Hauschka PV, Karnovsky MJ. Involvement of hydrogen peroxide in the differentiation of clonal HD-11EM cells into osteoclast-like cells. *J Cell Physiol*. 1998;176:574-587.

79. Smith J, Ladi E, Mayer-Proschel M, Noble M. Redox state is a central modulator of the balance between self-renewal and differentiation in a dividing glial precursor cell. *Proc Natl Acad Sci U S A*. 2000;97:10032-10037.

80. Jang YY, Sharkis SJ. A low level of reactive oxygen species selects for primitive hematopoietic stem cells that may reside in the low-oxygenic niche. *Blood*. 2007;110:3056-3063.

81. Fan J, Cai H, Tan WS. Role of the plasma membrane ROS-generating NADPH oxidase in CD34+ progenitor cells preservation by hypoxia. *J Biotechnol*. 2007;130:455-462.

82. Owusu-Ansah E, Banerjee U. Reactive oxygen species prime drosophila haematopoietic progenitors for differentiation. *Nature*. 2009;461:537-541.

83. Griendling KK, Sorescu D, Ushio-Fukai M. NAD(P)H oxidase: Role in cardiovascular biology and disease. *Circ Res*. 2000;86:494-501.

84. Griendling KK. Novel NAD(P)H oxidases in the cardiovascular system. *Heart*. 2004;90:491-493.

85. Akki A, Zhang M, Murdoch C, Brewer A, Shah AM. NADPH oxidase signaling and cardiac myocyte function. *J Mol Cell Cardiol*. 2009;47:15-22.

86. Lambeth JD. NOX enzymes and the biology of reactive oxygen. *Nat Rev Immunol*. 2004;4:181-189.

87. Lambeth JD, Kawahara T, Diebold B. Regulation of nox and duox enzymatic activity and expression. *Free Radic Biol Med*. 2007;43:319-331.

88. Chan EC, Jiang F, Peshavariya HM, Dusting GJ. Regulation of cell proliferation by NADPH oxidase-mediated signaling: Potential roles in tissue repair, regenerative medicine and tissue engineering. *Pharmacol Ther*. 2009;122:97-108.

89. Touyz RM, Briones AM, Sedeek M, Burger D, Montezano AC. NOX isoforms and reactive oxygen species in vascular health. *Mol Interv*. 2011;11:27-35.

90. Babior BM, Lambeth JD, Nauseef W. The neutrophil NADPH oxidase. *Arch Biochem Biophys*. 2002;397:342-344.

91. Meischl C, Krijnen PA, Sipkens JA, Cillessen SA, Munoz IG, Okroj M, Ramska M, Muller A, Visser CA, Musters RJ, Simonides WS, Hack CE, Roos D, Niessen HW. Ischemia induces nuclear NOX2 expression in cardiomyocytes and subsequently activates apoptosis. *Apoptosis*. 2006;11:913-921.

92. Manea A. NADPH oxidase-derived reactive oxygen species: Involvement in vascular physiology and pathology. *Cell Tissue Res*. 2010;342:325-339.

93. Lee MY, San Martin A, Mehta PK, Dikalova AE, Garrido AM, Datla SR, Lyons E, Krause KH, Banfi B, Lambeth JD, Lassegue B, Griendling KK. Mechanisms of vascular smooth muscle

NADPH oxidase 1 (Nox1) contribution to injury-induced neointimal formation. *Arterioscler Thromb Vasc Biol*. 2009;29:480-487.

94. Maejima Y, Kuroda J, Matsushima S, Ago T, Sadoshima J. Regulation of myocardial growth and death by NADPH oxidase. *J Mol Cell Cardiol*. 2011;50:408-416.

95. Chen K, Kirber MT, Xiao H, Yang Y, Keaney JF,Jr. Regulation of ROS signal transduction by NADPH oxidase 4 localization. *J Cell Biol*. 2008;181:1129-1139.

96. Ago T, Kuroda J, Pain J, Fu C, Li H, Sadoshima J. Upregulation of Nox4 by hypertrophic stimuli promotes apoptosis and mitochondrial dysfunction in cardiac myocytes. *Circ Res*. 2010;106:1253-1264.

97. Mahadev K, Motoshima H, Wu X, Ruddy JM, Arnold RS, Cheng G, Lambeth JD, Goldstein BJ. The NAD(P)H oxidase homolog Nox4 modulates insulin-stimulated generation of H2O2 and plays an integral role in insulin signal transduction. *Mol Cell Biol*. 2004;24:1844-1854.

98. Lyle AN, Deshpande NN, Taniyama Y, Seidel-Rogol B, Pounkova L, Du P, Papaharalambus C, Lassegue B, Griendling KK. Poldip2, a novel regulator of Nox4 and cytoskeletal integrity in vascular smooth muscle cells. *Circ Res*. 2009;105:249-259.

99. Wu RF, Ma Z, Liu Z, Terada LS. Nox4-derived H2O2 mediates endoplasmic reticulum signaling through local ras activation. *Mol Cell Biol*. 2010;30:3553-3568.

100. Rivera J, Sobey CG, Walduck AK, Drummond GR. Nox isoforms in vascular pathophysiology: Insights from transgenic and knockout mouse models. *Redox Rep*. 2010;15:50-63.

101. Rocic P, Lucchesi PA. NAD(P)H oxidases and TGF-beta-induced cardiac fibroblast differentiation: Nox-4 gets smad. *Circ Res*. 2005;97:850-852.

102. Violi F, Sanguigni V, Carnevale R, Plebani A, Rossi P, Finocchi A, Pignata C, De Mattia D, Martire B, Pietrogrande MC, Martino S, Gambineri E, Soresina AR, Pignatelli P, Martino F, Basili S, Loffredo L. Hereditary deficiency of gp91(phox) is associated with enhanced arterial dilatation: Results of a multicenter study. *Circulation*. 2009;120:1616-1622.

103. Loukogeorgakis SP, van den Berg MJ, Sofat R, Nitsch D, Charakida M, Haiyee B, de Groot E, MacAllister RJ, Kuijpers TW, Deanfield JE. Role of NADPH oxidase in endothelial ischemia/reperfusion injury in humans. *Circulation*. 2010;121:2310-2316.

104. Chen Z, Keaney JF,Jr, Schulz E, Levison B, Shan L, Sakuma M, Zhang X, Shi C, Hazen SL, Simon DI. Decreased neointimal formation in Nox2-deficient mice reveals a direct role for NADPH oxidase in the response to arterial injury. *Proc Natl Acad Sci U S A*. 2004;101:13014-13019.

105. Urao N, Inomata H, Razvi M, Kim HW, Wary K, McKinney R, Fukai T, Ushio-Fukai M. Role of nox2-based NADPH oxidase in bone marrow and progenitor cell function involved in neovascularization induced by hindlimb ischemia. *Circ Res*. 2008;103:212-220.

106. Ismail S, Sturrock A, Wu P, Cahill B, Norman K, Huecksteadt T, Sanders K, Kennedy T, Hoidal J. NOX4 mediates hypoxia-induced proliferation of human pulmonary artery smooth muscle cells: The role of autocrine production of transforming growth factor-{beta}1 and insulin-like growth factor binding protein-3. *Am J Physiol Lung Cell Mol Physiol*. 2009;296:L489-99.

107. Zhang M, Brewer AC, Schroder K, Santos CX, Grieve DJ, Wang M, Anilkumar N, Yu B, Dong X, Walker SJ, Brandes RP, Shah AM. NADPH oxidase-4 mediates protection against chronic load-induced stress in mouse hearts by enhancing angiogenesis. *Proc Natl Acad Sci U S A.* 2010;107:18121-18126.

108. Anilkumar N, Weber R, Zhang M, Brewer A, Shah AM. Nox4 and nox2 NADPH oxidases mediate distinct cellular redox signaling responses to agonist stimulation. *Arterioscler Thromb Vasc Biol*. 2008;28:1347-1354.

109. Looi YH, Grieve DJ, Siva A, Walker SJ, Anilkumar N, Cave AC, Marber M, Monaghan MJ, Shah AM. Involvement of Nox2 NADPH oxidase in adverse cardiac remodeling after myocardial infarction. *Hypertension*. 2008;51:319-325.

110. Doerries C, Grote K, Hilfiker-Kleiner D, Luchtefeld M, Schaefer A, Holland SM, Sorrentino S, Manes C, Schieffer B, Drexler H, Landmesser U. Critical role of the NAD(P)H oxidase subunit p47phox for left ventricular remodeling/dysfunction and survival after myocardial infarction. *Circ Res*. 2007;100:894-903.

111. Wang P, Chen H, Qin H, Sankarapandi S, Becher MW, Wong PC, Zweier JL. Overexpression of human copper, zinc-superoxide dismutase (SOD1) prevents postischemic injury. *Proc Natl Acad Sci U S A*. 1998;95:4556-4560.

112. Sauer H, Rahimi G, Hescheler J, Wartenberg M. Effects of electrical fields on cardiomyocyte differentiation of embryonic stem cells. *J Cell Biochem*. 1999;75:710-723.

113. Sauer H, Neukirchen W, Rahimi G, Grunheck F, Hescheler J, Wartenberg M. Involvement of reactive oxygen species in cardiotrophin-1-induced proliferation of cardiomyocytes differentiated from murine embryonic stem cells. *Exp Cell Res*. 2004;294:313-324.

114. Sauer H, Rahimi G, Hescheler J, Wartenberg M. Role of reactive oxygen species and phosphatidylinositol 3-kinase in cardiomyocyte differentiation of embryonic stem cells. *FEBS Lett*. 2000;476:218-223.

115. Sharifpanah F, Wartenberg M, Hannig M, Piper HM, Sauer H. Peroxisome proliferator-activated receptor alpha agonists enhance cardiomyogenesis of mouse ES cells by utilization of a reactive oxygen species-dependent mechanism. *Stem Cells*. 2008;26:64-71.

116. Serena E, Figallo E, Tandon N, Cannizzaro C, Gerecht S, Elvassore N, Vunjak-Novakovic G. Electrical stimulation of human embryonic stem cells: Cardiac differentiation and the generation of reactive oxygen species. *Exp Cell Res*. 2009.

117. Puceat M. Role of rac-GTPase and reactive oxygen species in cardiac differentiation of stem cells. *Antioxid Redox Signal*. 2005;7:1435-1439.

118. Puceat M, Travo P, Quinn MT, Fort P. A dual role of the GTPase rac in cardiac differentiation of stem cells. *Mol Biol Cell*. 2003;14:2781-2792.

119. Schmelter M, Ateghang B, Helmig S, Wartenberg M, Sauer H. Embryonic stem cells utilize reactive oxygen species as transducers of mechanical strain-induced cardiovascular differentiation. *FASEB J*. 2006;20:1182-1184.

120. Buggisch M, Ateghang B, Ruhe C, Strobel C, Lange S, Wartenberg M, Sauer H. Stimulation of ES-cell-derived cardiomyogenesis and neonatal cardiac cell proliferation by reactive oxygen species and NADPH oxidase. *J Cell Sci*. 2007;120:885-894.

121. Davidson SM, Morange M. Hsp25 and the p38 MAPK pathway are involved in differentiation of cardiomyocytes. *Dev Biol*. 2000;218:146-160.

122. Eriksson M, Leppa S. Mitogen-activated protein kinases and activator protein 1 are required for proliferation and cardiomyocyte differentiation of P19 embryonal carcinoma cells. *J Biol Chem*. 2002;277:15992-16001.

123. Li J, Stouffs M, Serrander L, Banfi B, Bettiol E, Charnay Y, Steger K, Krause KH, Jaconi ME. The NADPH oxidase NOX4 drives cardiac differentiation: Role in regulating cardiac transcription factors and MAP kinase activation. *Mol Biol Cell*. 2006;17:3978-3988.

124. Bartsch C, Bekhite MM, Wolheim A, Richter M, Ruhe C, Wissuwa B, Marciniak A, Muller J, Heller R, Figulla HR, Sauer H, Wartenberg M. NADPH oxidase and eNOS control cardiomyogenesis in mouse embryonic stem cells on ascorbic acid treatment. *Free Radic Biol Med*. 2011.

125. Mangi AA, Noiseux N, Kong D, He H, Rezvani M, Ingwall JS, Dzau VJ. Mesenchymal stem cells modified with akt prevent remodeling and restore performance of infarcted hearts. *Nat Med*. 2003;9:1195-1201.

126. Fischer KM, Cottage CT, Wu W, Din S, Gude NA, Avitabile D, Quijada P, Collins BL, Fransioli J, Sussman MA. Enhancement of myocardial regeneration through genetic engineering of cardiac progenitor cells expressing pim-1 kinase. *Circulation*. 2009;120:2077-2087.

127. Xiang FL, Lu X, Hammoud L, Zhu P, Chidiac P, Robbins J, Feng Q. Cardiomyocyte-specific overexpression of human stem cell factor improves cardiac function and survival after myocardial infarction in mice. *Circulation*. 2009;120:1065-74, 9 p following 1074.

128. Gurusamy N, Mukherjee S, Lekli I, Bearzi C, Bardelli S, Das DK. Inhibition of ref-1 stimulates the production of reactive oxygen species and induces differentiation in adult cardiac stem cells. *Antioxid Redox Signal*. 2009;11:589-600.

CHAPTER TWO: C-KIT EXPRESSION IDENTIFIES CARDIOVASCULAR PRECURSORS IN THE NEONATAL HEART*

*Largely reprinted from Tallini YN, Greene KS, Craven M, **Spealman A**, Breitbach M, Smith J, Fisher PJ, Steffey M, Hesse M, Doran RM, Woods A, Singh B, Yen A, Fleischmann BK, Kotlikoff MI. C-kit expression identifies cardiovascular precursors in the neonatal heart. *Proc Natl Acad Sci U S A.* 2009;106:1808-1813 [1] with modification. Author contributions are as follows: Y.N.T., K.S.G., M.C., **A.S.**, M.B., J.S., P.J.F., M.S., M.H., A.Y., B.K.F., and M.I.K. designed research; Y.N.T., K.S.G., M.C., **A.S.**, M.B., J.S., P.J.F., M.S., M.H., R.M.D., A.W., and B.S. performed research; Y.N.T., K.S.G., M.C., **A.S.**, M.B., J.S., P.J.F., M.H., and R.M.D. analyzed data; and Y.N.T., M.C., M.H., B.K.F., and M.I.K. wrote the paper (modifications from original print were written by **A.S.**).

ABSTRACT

Directed differentiation of embryonic stem cells (ESCs) indicates that mesodermal lineages in the mammalian heart (smooth muscle, cardiac, and endothelial) develop from a common, multipotent cardiovascular precursor. To isolate and characterize the lineage potential of a resident pool of cardiac precursor cells (CPCs), we developed bacterial artificial chromosome (BAC) transgenic mice in which enhanced green fluorescent protein (EGFP) is placed under control of the c-kit locus (c-kit^{BAC}-EGFP mice). Discrete c-kit-EGFP^{+} cells were observed at different stages of differentiation in embryonic hearts, increasing in number to a maximum at about postnatal (PN) 2; thereafter c-kit-EGFP^{+} cells declined and were rarely observed in the adult heart. C-kit-EGFP $^{+}$ cells purified from PN0-5 hearts were nestin-positive and expanded in culture; 67% of cells were fluorescent after 9 days. Purified cells differentiated into smooth muscle, cardiac, and endothelial cells, and differentiation could be directed by specific growth factors. CPC-derived cardiomyocytes displayed rhythmic beating and action potentials characteristic of multiple cardiac cell types, similar to ESC-derived cardiomyocytes. Single cell dilution studies confirmed the potential of individual CPCs to form all three cardiovascular lineages. In adult hearts, cryoablation resulted in c-kit-EGFP^{+} expression, peaking 7 days post-cryolesion. Expression occurred in smooth muscle and endothelial cells in the revascularizing infarct, and in terminally differentiated cardiomyocytes in the border zone surrounding the infarct. Similar co-localization of exogenously transplanted c-kit-EGFP^{+}/LacZ^{+} cells within the injured vasculature also was observed. Thus c-kit expression marks CPCs in the neonatal heart that are capable of directed differentiation *in vitro*; however, c-kit expression in cardiomyocytes in the adult heart following injury does not identify cardiac myogenesis.

INTRODUCTION

The process of early heart cell specification from pluripotent CPCs recently has been advanced by reports that a common cardiovascular precursor can give rise to smooth muscle cells, cardiomyocytes, and endothelial cells through directed differentiation of ESCs *in vitro*, and when these cells are implanted into adult hearts [2-7]. Several markers have been reported to identify CPCs, including the kinase insert domain protein receptor KDR (also known as Flk-1) [2, 3, 8], the stem cell factor (SCF) receptor c-kit [5, 6, 9], the LIM-homeobox transcription factor islet-1 (Isl-1) [10-12], and the cardiac transcription factor Nkx2.5 [5, 13]. *In vitro* directed differentiation of ESCs suggests that mammalian heart development involves mesoderm specification to a multipotent precursor stage. However such cells have not been isolated from the heart and shown to undergo multipotent differentiation *in vitro*, and Nkx2.5-expressing cells isolated from embryonic day (ED) 7.5 and ED 8.5 mouse embryos could not be induced to expand and differentiate [5].

Used extensively as a marker to identify adult hematopoietic stem cells (HSCs), c-kit is expressed during various stages of cell lineage commitment in germ, mast, stellate, epithelial, endothelial, and smooth muscle cells [14-16]. Wu, et al. [5] isolated c-kit$^+$ cells from ED9.5 and ED10.5 embryos and demonstrated that these cells express smooth muscle and cardiac genes *in vitro* and differentiate to smooth and cardiac myocytes in xenotransplants. Here we report the isolation and characterization of neonatal c-kit$^+$ cells from a transgenic mouse in which EGFP expression is placed under control of the *kit* locus within a BAC. C-kit-EGFP$^+$ cells from PN c-kit^{BAC}-EGFP mouse hearts expand in culture and differentiate *in vitro* into smooth muscle, cardiac, and endothelial cells. The study of isolated CPCs is likely to provide important

information with respect to the genetic status, mechanism of differentiation and commitment, and biological potential of these cells.

MATERIALS AND METHODS

BAC Targeting and Founder Genotyping

Two fragments, 564 and 541 base-pairs in length located 5' and 3', respectively, to the c-kit ATG start codon in Exon 1, were designed and inserted into the pBS-EGFP-pA-FRT-Neo/Kan-FRT vector by Dr. Kai Su Greene. This targeting construct was then released by XhoI/SacII digestion and electroporated into EL250- RP24-330G11 cells. Chloramphenicol (12.5 µg/ml) and kanamycin (25 µg/ml) resistant clones were genotyped by amplification and sequenced to identify homologous recombinants. The neomycin cassette was removed by L(+)-arabinose (0.1%) recombinase induction, leaving only one FRT site. C-kit^{BAC}-EGFP-PA-FRT DNA was cesium chloride purified and injected into the pronuclei of zygotes by standard methods. A similar targeting strategy was utilized to generate transgenic mice with EGFP expression under the control of the Connexin 45 (gap junction protein) and Acta2 (smooth muscle specific protein) gene loci (**A.S.** rotation project). The generation of these two lines is ongoing.

Genotyping of c-kit^{BAC}-EGFP mice was performed using primer pairs BefArm1/EGFPR1 (BefArm1:GCAGGTGGAGAAACTGAGCATG; EGFPR1: CCAGGATGTTGCCGTCCTCCT) yielding a 1095 base-pair product. Cycling parameters were: 2 minutes at 94ºC; (30 seconds at 94ºC, 30 seconds at 57ºC, 1 minute 10 seconds at 68ºC) x40; 10 minutes at 68ºC; hold at 4ºC. Newborns (PN0-5) also were screened for EGFP expression using a KL2500 cold light source (Schott Fostec) and safety glasses covered with Wratten filter #12 (Kodak). For transplant studies, c-kit^{BAC}-EGFP homozygote mice were crossed with a commercially available Rosa26-LacZ reporter line in which LacZ is knocked into the ubiquitous Rosa locus. All procedures

were approved by Cornell Institutional Animal Care and Use Committee and adhered to the standards published in Guide for the Care and Use of Laboratory Animals.

Embryos and Adult Hearts

Whole embryos [14.5 and 18.5 days post coitus (dpc)] and excised PN2 or 6-16 week old adult hearts were fixed with 4% PFA or Stefanini solution, preserved with 20% sucrose, frozen, and cut into 8-10 µm sections. Cryosections were prepared and examined for EGFP expression or immunostained using primary antibodies directed against α–actinin (Sigma-Aldrich), α-smooth muscle actin (SMA) (Sigma-Aldrich), CD45 (Lab Vision), GFP, Flk-1, or platelet endothelial cell adhesion molecule (PECAM)1/CD31 (all from BD Pharmingen). All primary antibodies were visualized by appropriate secondary Cy3- or Cy5-conjugated donkey antibodies (Jackson ImmunoResearch Laboratories). Nuclei were stained with Hoechst 33258 (Sigma). Heart sections were imaged using a ProgRes C10+ (Jenoptik) camera connected to a Leica MZ16F stereo-fluorescence microscope or an AxioCamMRm camera connected to a Zeiss Axiovert 200 microscope.

Cell Morphometry

To calculate the total number of cells per neonatal heart, 7-13 sections from each heart (n=6) were imaged with a 20X objective and the total number of Hoechst stained nuclei was determined automatically using AxioVision AutMess Software (Zeiss). The number of $EGFP^+$ cells was determined by manually counting the nuclei of green cells. Cell numbers were extrapolated to the total amount of heart sections, correcting for overlap based on the average nuclear size.

Fluorescence Activated Cell Sorting (FACS) and Culturing Parameters

Following dissociation, cells were resuspended in proliferation media (see below) containing 20% fetal bovine serum (FBS) and maintained in an incubator at 95% O_2/5% CO_2 and 37 ºC until ready for FACS. Cell suspensions from neonatal c-kit^{BAC}-EGFP mice cardiac isolations were analyzed and sorted by flow cytometry on a Becton Dickinson Biosciences FACS Aria. EGFP was excited by a 488 nm laser and emission was collected in a fluorescein isothiocyanate (FITC) channel using a 502 longpass dichroic mirror and a 530/30 bandpass filter. A parent population of cells that represented only whole cells gated to exclude debris by forward and side scatter first was determined. Autofluorescent cells were then identified as cells with a high phycoerythrin (PE) 585/42 to 530/30 signal ratio and excluded by gating. The total EGFP$^+$ heart cell population (tEGFP) was identified as those cells with signal exceeding the Gaussian distribution of heart cells obtained from transgene negative littermates. A high EGFP expressing subgroup (sEGFP) was identified as those cells having a signal >5-fold above control, a population that comprised on average the brightest 5% of cells. Cells were sorted at 65 psi through a 70 µm nozzle oscillating at 87 Hz, into proliferation media (see below). Cell viability was evaluated by propidium iodide (PI) exclusion and averaged 92% pre-FACS and 78% post-FACS.

Cells were plated on Lab Tek 8-well chambered cover glass slides (BD Biosciences) pretreated with 0.1% gelatin (Chemicon International), plated at a density of 80,000-160,000/cm^2 or 8,000-20,000/cm^2, and cultured for 2-3 days in proliferation media, containing F12K media (Gibco), 5% FBS (Chemicon International), 10 ng/mL basic fibroblast growth factor (bFGF; Sigma-Aldrich), 10 ng/mL leukemia inhibitory factor (LIF; Chemicon International), and 1%

penicillin/streptomycin (Gibco). Thereafter, cells were switched to basic media containing DMEM/Ham's F12 (1:1) (Gibco), B27 Supplement (Gibco), 10 ng/mL bFGF, 20 ng/mL epidermal growth factor (EGF; Sigma-Aldrich), 10 ng/mL LIF, and 1% penicillin/streptomycin until the day of the experiment [6, 10, 17]. To induce smooth muscle differentiation 5 ng/ml of transforming growth factor-β1 (TGF-β1; R&D Systems) was added to the basic media that in some experiments lacked LIF [18]; to promote endothelial cell differentiation the basic media was altered by removal of B27, EGF, and LIF and supplemented with 10 ng/ml vascular endothelial growth factor (VEGF; PeproTech Inc.), 5 U/ml of heparin sodium (Baxter Healthcare Corporation), and 5% FBS [19].

For single cell expansion experiments, cells were diluted in proliferation media (see above) to yield one cell/well and plated on 96-well cell culture plates (Corning) that were pretreated with 0.1% gelatin. Three days post-plating, individual wells with EGFP fluorescent single cells were identified using a Nikon Eclipse TE300 inverted microscope (GFP excitation 470/20; GFP emission 510/20) and maintained in proliferation media for three weeks.

Electrophysiology

After 2-3 days in proliferation media, approximately 20% of the cells began to spontaneously contract and relax. Glass slides or 35 mm Nunc culture dishes containing sEGFP cells were then placed in a specially designed, sealed chamber, and mounted on a Nikon Eclipse TE300 microscope for patch clamping by Dr. Michael Craven. Current recordings were made using the Amphotericin B (300 μg/ml) perforated patch clamp method [20]. Patch pipettes were pulled from filamented borosilicate capillary glass (TW 150 F4, World Precision Instruments) to a tip

diameter of 1-1.5 µm and a resistance of 3-5 MΩ using a P-87 Flaming/Brown micropipette puller (Sutter Instrument Co.). Patch pipettes were tip-filled by briefly dipping them into pipette solution (in mM: 133 KCl, 1 $MgCl_2$, 3 EGTA, 1 $CaCl_2$, 10 Hepes) and then back-filled with the Amphotericin B containing pipette solution. After gigaseal formation, experiments were initiated once access resistance fell to 10-20 MΩ.

Voltage and current clamp protocols were applied with an Axopatch 200B patch clamp amplifier (Axon Instruments) interfaced to a computer by a Digidata 1200 series AD/DA converter (Axon Instruments). During experiments, cells were continually superfused with Hank's solution (in mM: 140 NaCl, 3 KCl, 2 $CaCl_2$, 2 $MgCl_2$, 10 Hepes, 10 glucose) using a solution heater and controller (SHM-6, TC344 Warner Instruments Corp.). The solution switching dead space time was approximately 5 seconds. All experiments were performed at 37 ^{o}C. Patch clamp data was analyzed offline using Clampex 8.2 (Axon Instruments) and Prism 4 (Graphpad Software Inc.).

Immunocytochemistry

Individual Markers Co-Labeled with GFP

Cells cultured on 8-well cover glass slides or in 96-well plates, along with positive control tissue slides, were fixed in 4% PFA for 20 minutes at 25 ºC, rinsed 3 times with 0.01 M phosphate buffered saline (PBS), and stored at 4 ºC until immunostaining was performed. Cells and control tissues were permeabilized for 5 minutes (2 minutes for PCNA [proliferating cell nuclear antigen] and CD31) with 0.01 M PBS 0.05% Triton-X (0.2% for PCNA), and blocked for 1 hour with normal mouse IgG (M.O.M. labeling kit, Vector Laboratories) followed by 10% normal donkey serum for 15 minutes at room temperature (RT). Primary antibodies were combined in

tris buffered saline (TBS)/M.O.M. buffer; antibodies and dilutions were: mouse anti-α-SMA (1:20, Dako, M0851), mouse anti-PCNA (1:5, Dako, MO879), rat anti-nestin (1:5, Chemicon, MAB353), mouse anti-Troponin T (cTnT) (1:200, Neomarkers, Ab-1 13-11), mouse anti-Isl-1 (1:50, Developmental Studies Hybridoma Bank), or rat anti-PECAM1/CD31 (1:5, BD Pharmingen, #550274) combined with rabbit anti-GFP (1:5, Chemicon). The combined antibodies were applied for 25 minutes at 37 ^{o}C and 40 minutes at RT (Note: CD31 co-labels were incubated 30 minutes at 37 ^{o}C with CD31 antibody before adding combined antibodies). To detect GFP, all samples were washed and incubated with FITC donkey anti-rabbit IgG H&L (1:80, Jackson ImmunoResearch Laboratories) diluted in TBS at RT for 20 minutes and protected from light. They were then washed and incubated with Texas Red donkey anti-mouse IgG H&L (1:80, Jackson ImmunoResearch Laboratories) diluted in TBS M.O.M. buffer for 15 minutes to detect α-SMA, PCNA, nestin, or cTnT, while CD31 co-labels were incubated with biotinylated donkey anti-rat (1:50, Jackson ImmunoResearch Laboratories) followed by Streptavidin Texas Red (1:200, Vector) diluted in TBS for 20 minutes at RT. Stained cells and sections were mounted with Vectashield DAPI (Vector).

α-SMA or cTnT Co-Labeled with CD31

For co-labeling mouse anti-α-SMA or cTnT with rat anti-CD31, the mouse antibodies were detected with AMCA donkey anti-mouse IgG H&L (1:40, Jackson ImmunoResearch Laboratories) diluted in M.O.M. buffer for 15 minutes at RT and protected from light. CD31 was detected with biotin/Streptavidin Texas Red as in the previous protocol, and DAPI counterstaining was omitted.

CD117 Co-Labeled with GFP

Co-labeling with rabbit anti-GFP (1:5) and goat anti-CD117 (1:30, R&D Systems) followed a similar protocol except that cells were incubated for 10 minutes with TBS 0.2% Triton-X to permeabilize, M.O.M. blocking was omitted, and cells were blocked with 10% normal donkey serum with 10% nonfat dry milk. Antibodies were diluted in TBS 0.05% Triton-X and incubated 1.5 hours at 37 ^{o}C. CD117 was detected with biotinylated donkey goat (1:100, Jackson ImmunoResearch Laboratories) and Streptavidin Texas Red (1:200).

α-SMA Co-Labeled with cTnT

For co-labeling with mouse anti-α-SMA and mouse anti-cTnT cells were washed in 0.01 M PBS and permeabilized for 5 minutes with 0.01 M PBS 0.05% Triton-X. On Day 1, cells were blocked with normal mouse IgG M.O.M. labeling kit for 1 hour, per instructions, followed by 10% donkey serum/2X casein for 15 minutes at RT, and M.O.M. buffer for an additional 5 minutes. Mouse anti-cTnT primary antibody was diluted 1:150 in PBS/M.O.M. buffer and applied for 25 minutes at 37 ^{o}C and 40 minutes at RT. Texas Red conjugated donkey anti-mouse IgG H&L min X secondary antibody (1:80, Jackson ImmunoResearch Laboratories) diluted in M.O.M. buffer was incubated on the slides for 20 minutes at RT and protected from light. The fluorescent slides were washed and stored overnight in distilled water. On Day 2 the cells were blocked 15 minutes with 10% goat serum, again blocked with normal mouse IgG, rinsed and incubated with goat mouse fragments (1:50, Jackson ImmunoResearch Laboratories) for 30 minutes at 37 ^{o}C and washed. Mouse anti-α-SMA antibody was applied at 1:20 in M.O.M. buffer as above. After several rinses, slides were incubated with AMCA blue conjugated donkey

anti-mouse IgG H&L min X (1:40, Jackson ImmunoResearch Laboratories) for 20 minutes in the dark. Cells were washed several times with PBS and mounted with Vectashield (Vector).

Controls and Imaging

Normal mouse IgG (Santa Cruz Biotechnology), rat IgG, or goat IgG (Vector) combined with normal rabbit IgG (Vector), at final dilutions (μg/ml) equivalent to corresponding primary antibodies served as negative controls. Mouse tissue including embryo and adult stomach and esophagus were fixed and stained along with cultured cells to validate primary antibodies in appropriate cell types. Images were obtained by confocal microscopy (Zeiss 510 Meta Scanning Confocal Microscope), a Kodak DCS 460C camera coupled to an Olympus Provis microscope, or a Retiga 2000R camera coupled to a Leica DMI 6000B microscope.

Cryoablation and Cell Transplant

Adult, 8-12 week old, male c-kit^{BAC}-EGFP mice underwent cryoablation surgery by Dr. Michele Steffey [21, 22]. Mice were anesthetized with 2-3% isoflurane and intubated by suspending them on a specially designed platform at a 45 º angle and using a 2 cm PE-90 catheter attached to the base of a needle for insertion into the trachea [23]. Immediately following intubation, mice were placed on a warming pad and connected to a ventilator set at 100-120 breaths/minute with a tidal volume between .2 and .5 ml. Mice were kept anesthetized using approximately 1% isoflurane. After hair removal and sterilization of the surgical area, a thoracotomy was performed and a retractor was used to expose the apex of the heart. Next, a liquid nitrogen cooled 3 mm copper probe was placed against the left ventricle for 10-20 seconds 2-3 times and a chest drain was inserted in the pleural space. The chest wall, muscle layer, and skin were closed with Ethicon 6-

0 suture and the pneumothorax was drained prior to removal of the chest drain. Mice were extubated and allowed to recover on a warm surface. They were administered ketoprofen (5 mg/kg) and ceftazidime (25 mg/kg) for 2 days post-operatively. Mice were euthanized for experiments at specific time points.

For transplant studies, c-kit-EGFP^{+}/LacZ^{+} cells were isolated from c-kit^{BAC}-EGFP/Rosa26-LacZ neonatal mouse hearts as described above on the day of surgery. 150,000-200,000 sorted c-kit-EGFP^{+}/LacZ^{+} cells were separated into sterile 1.5 ml centrifuge tubes and pelleted. Cells were then resuspended in 10 µl sterile saline/trypan blue for two 5 µl injections into the peri-infarct region of C57Bl/6 adult mice. Injections were performed using a 29G needle connected with polyethylene tubing to a 10 µl Hamilton syringe and the injections were visually verified by trypan blue [21]. Control animals were injected as above with vehicle (sterile saline/trypan blue) alone.

Data Analysis

Data were analyzed with SigmaPlot/SigmaStat/Graphpad Prism 4 software using one-way Analysis of Variance with Tukey's post-hoc comparisons or a Student's *t*-test. Summary values are mean ± SEM. Differences were accepted as statistically significant with $p<0.05$.

RESULTS

Generation of C-kit^{BAC}-EGFP Mice

To facilitate the study of heart precursors known to express c-kit [5, 6, 9], Dr. Kai Su Greene inserted the EGFP coding sequence in frame at the start codon of c-kit (1st exon) [24] within a 186 kb BAC by recombineering methods (Figure 2.1A) [25]. A founder line was identified by a 1.1 kb PCR amplicon that included c-kit and EGFP DNA (Figures 2.1A-B). Neonatal c-kit^{BAC}-EGFP pups displayed intense skin fluorescence consistent with the expression of c-kit in melanocytes (Figure 2.1C) [16], and were easily distinguished from non-transgenic wildtype (WT) littermates using a hand held fluorescent light source and filtered goggles (see Materials and Methods). In adult mice strong c-kit-EGFP fluorescence was observed in a variety of organs in a pattern consistent with endogenous c-kit expression (Figure 2.1D); expression was observed in interstitial cells of the intestines and stomach, muscle layer of the uterus, and testis. C-kit-EGFP fluorescence was detected by immunohistochemistry in Leydig cells and outer layer spermatogonium in the testis, in basket and stellate cells in the molecular layer of the cerebellum, and within the hippocampus (Figure 2.1E), consistent with the cell-type specific expression of c-kit in these tissues [26, 27]. As expected from a genetic strategy in which the endogenous locus was not altered, c-kit^{BAC}-EGFP mice display no apparent phenotype and transmit the transgene in a Mendelian ratio; the line is registered with the Mouse Genome Informatics (MGI) as Tg(RP24-330G11-EGFP)1Mik, number 3760303.

Spatial and Temporal Expression of EGFP in the Heart

The expression pattern of c-kit-EGFP fluorescence was analyzed in heart sections from embryonic [14.5 and 18.5 dpc], PN2-3, and adult c-kit^{BAC}-EGFP mice. Fluorescent cells were

Figure 2.1. Generation and Evaluation of C-kit^{BAC}-EGFP Mice.

A) BAC targeting strategy placing EGFP in frame at the c-kit initiation codon; Neo cassette was removed before DNA injection. Arrows indicate PCR genotyping primers. B) 1.1 kb PCR product in founder (Lane 1); water and WT controls shown in Lanes 2 and 3; 1kb DNA ladder in Lane 4. C) Bright field (left) and fluorescent (right) images of PN0 c-kit^{BAC}-EGFP pups. D) C-kit-EGFP expression in adult tissues shows predicted pattern of expression. E) Immunolocalization of c-kit-EGFP in Leydig and outer region of spermatogonium (arrow) in adult testis, stellate and basket cells in the molecular layer of the cerebellum, and selective hippocampal neurons. Scale bars: C, 1 mm; D, testis 1 mm, others 100 µm; E, testis 25 µm, brain 50 µm. ***A.S.** contributed to c-kit^{BAC}-EGFP mouse husbandry, genotyping by fluorescence, cryosectioning, and microscopy. **A.S.** also was involved in the design of two additional BAC transgenics (Connexin 45 and Acta2) not described here.

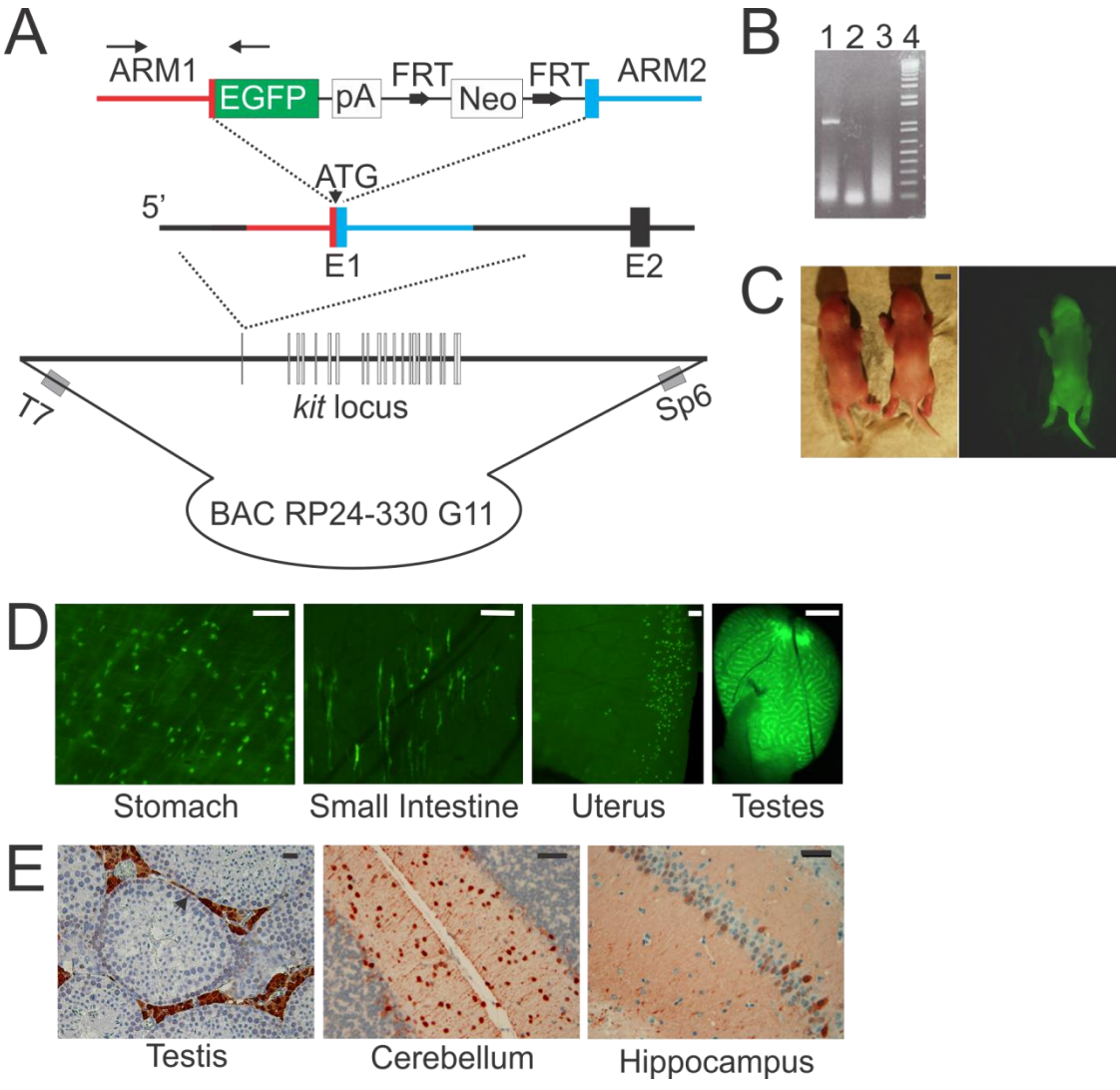
A
ARM1
EGFP
pA
FRT
Neo
FRT
ARM2
ATG
5'
E1
E2
T7
kit locus
Sp6
BAC RP24-330 G11
B
1 2 3 4
C
D
Stomach
Small Intestine
Uterus
Testes
E
Testis
Cerebellum
Hippocampus

observed in the atrial and ventricular walls of 14.5 dpc mice (Figure 2.2A, top) and by 18.5 dpc discrete areas of c-kit-EGFP$^+$ cells could be detected within the thickening chamber walls (data not shown). The total number of c-kit- EGFP$^+$ cells increased as the heart expanded in size, reaching a maximum shortly after birth (PN2-3; Figure 2.2A, middle). Thereafter, the number declined rapidly and c-kit-EGFP$^+$ cells only occasionally were observed as mononuclear cells within the vascular compartment, or rarely as striated myocytes within the cardiac interstitium, in adult mice (Figure 2.2A, bottom). In the PN heart, c-kit-EGFP$^+$ cells were observed in the atrioventricular region (Figure 2.2C), in the atrial and ventricular walls (Figure 2.2A), and the epicardial border, where intensely staining cells often were observed. C-kit co-expression was examined by dual immunolabeling of heart sections (Figure 2.2B) and by immunodetection of c-kit in cells sorted by EGFP fluorescence. The coincidence of anti-EGFP and anti-CD117 staining was >90% within clusters (Figure 2.2B), but isolated cells often only stained with one of the two antibodies (approximately 45% coincidence). The latter result may be due to differences in protein half-life, technical issues related particularly to the CD117 antibody, or incomplete transcriptional fidelity of the c-kit transgene.

We examined the lineage and developmental status of c-kit-EGFP$^+$ cells within the postnatal (PN2-3) heart by immunostaining in tissue sections that retained EGFP fluorescence. In the atrioventricular region, concentrated clusters of c-kit-EGFP fluorescent cells were observed at various stages of cardiovascular development (Figure 2.2C). Some cells co-stained with α-actinin and displayed early cardiac morphology whereas smaller, elongated α-actinin negative cells that co-stained with Flk-1, the VEGF receptor 2, which marks ESC-derived CPCs [2, 3, 8] also were observed (Figure 2.2D). The latter group included clusters of cells co-expressing the

Figure 2.2. EGFP Expression in C-kit^{BAC}-EGFP Mouse Hearts.

A) C-kit-EGFP expression in the heart wall of 14.5 dpc embryo (fluorescence) and PN3 (immunostaining) neonates. In the adult heart only rare immunostained cells were observed. Control - no 1^{o} antibody. B) EGFP/c-kit expression concordance. Anti-EGFP (green); Anti-CD117 (red). Note lack of co-expression (top) and co-localization within a niche (bottom). C) Native c-kit-EGFP expression in the atrioventricular region of a PN2 heart. D) Some cells co-expressed Flk-1 and c-kit-EGFP. E) Some c-kit-EGFP^{+} cells co-expressed PECAM1, indicating endothelial commitment. Very bright c-kit-EGFP expressing cells commonly were observed in the epicardium; these cells co-expressed the hematopoietic lineage marker, CD45. F) c-kit-EGFP^{+} cells in the atrioventricular region showing a gradient of EGFP expression, from less differentiated bright cells (arrows), to less fluorescent striated cells. Abbreviations: A, atrium; AV, atrioventricular region; and V, ventricle. Hoechst staining is shown in blue for B, D, E and F. Scale bars: A, 14.5 dpc 50 µm, others, 25 µm; B, 10µm; C, 50 µm ; D, 25 µm, blow-up, 10 µm; E left 25 µm, middle 20 µm, blow-up 5 µm; and F, 25 µm. *__A.S.__ contributed to tissue harvest, cryosectioning, and microscopy.

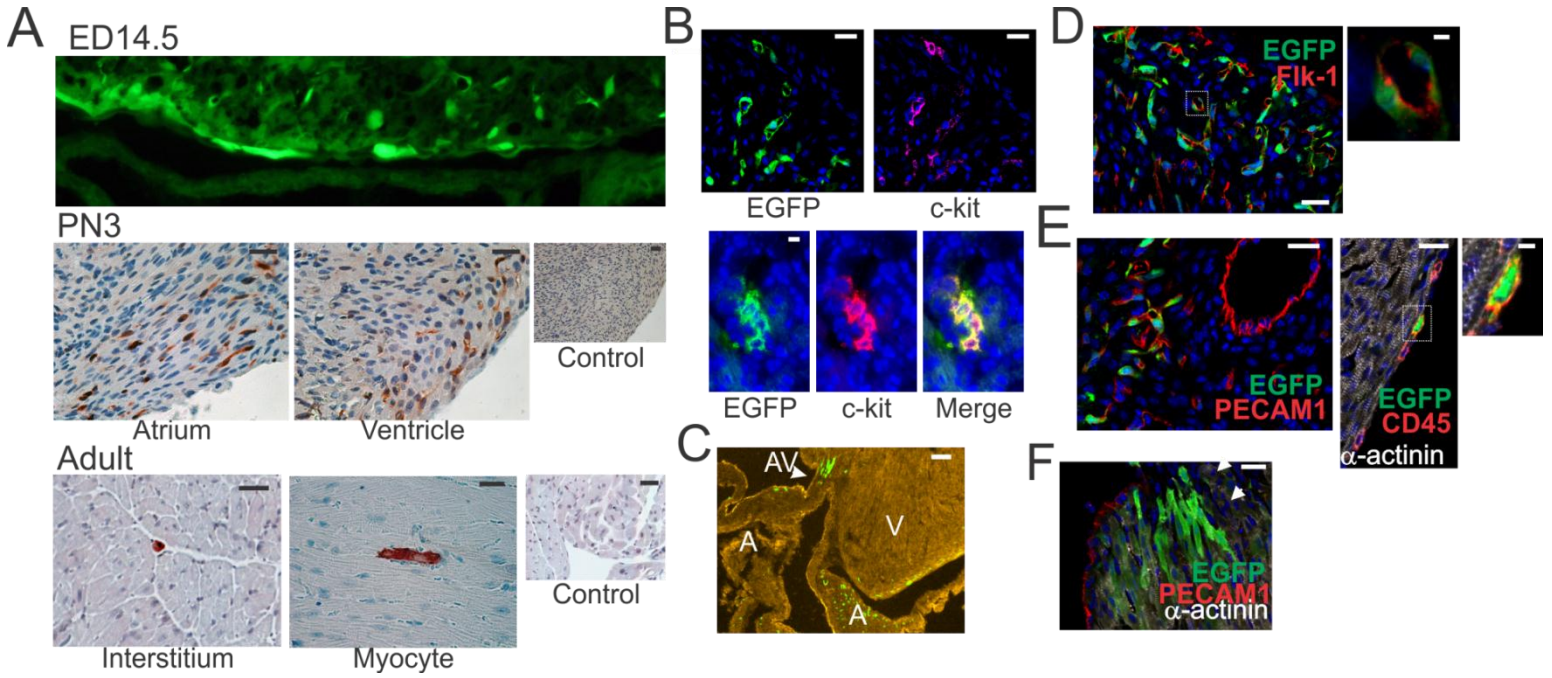
A
ED14.5
PN3
Atrium
Ventricle
Control
Adult
Interstitium
Myocyte
Control
B
EGFP
c-kit
EGFP
c-kit
Merge
C
AV
A
V
A
D
EGFP
Flk-1
E
EGFP
PECAM1
EGFP
CD45
α-actinin
F
EGFP
PECAM1
α-actinin

endothelial lineage marker PECAM1 (Figure 2.2E, left). Intensely fluorescent cells also were observed at the epicardial border, which were CD45 positive, indicating hematopoietic lineage (Figure 2.2E, middle and right). In some clusters a gradation from less differentiated and more intensely fluorescent, to more striated and weakly fluorescent cells, was observed (Figure 2.2F). Quantitative morphometry indicated that the more intense staining epicardial cells represented 0.101±0.004% of all heart cells (3,373±330/heart), whereas non–epicardial c-kit-EGFP^{+} cells characterized 0.46±0.14% of all cells (16,044±6,343/heart). Thus, we estimate that c-kit-EGFP^{+} cells constitute less than 1% (0.56±0.16; n=6) of all cells in the neonatal mouse heart. Taken together, these results indicate that the c-kit-EGFP^{+} cell population includes CPCs in several stages of development and lineage commitment.

Expansion and Differentiation of Neonatal C-kit^{+} Cells In Vitro

To isolate c-kit-EGFP^{+} expressing cells and determine their potential to differentiate into multiple cell lineages we optimized a dissociation protocol adapted from Worthington's Neonatal Cardiomyocyte Isolation System and sorted cells from pooled PN0-5 c-kit^{BAC}-EGFP hearts. C-kit-EGFP^{+} cells could be distinguished by FACS from background fluorescence of non-transgenic cells, although there was some overlap at the low end of EGFP expression, as shown by the comparison of fluorescence histograms of heart cells from c-kit^{BAC}-EGFP and WT littermates (Figure 2.3A). Using a gate that captured cells 5-fold brighter than the mean fluorescence intensity, sEGFP cells could be obtained that included only c-kit-EGFP^{+} cells (Figure 2.3A). In some experiments the tEGFP was obtained and c-kit-EGFP^{+} cells distinguished from non-expressing EGFP cells by epifluorescent microscopic examination, whereas in others the sEGFP fraction was used. The total number of sEGFP cells/heart averaged

Figure 2.3. Isolation and Expansion of FACS Cardiac C-kit-EGFP^{+} Cells.

A) Representative FACS from PN c-kit^{BAC}-EGFP and WT littermate hearts. WT and EGFP histograms are normalized to the same peak maximum. tEGFP population overlaps with brightly autofluorescent WT cells; sEGFP identifies a pure c-kit-EGFP^{+} population of cells that are 5 times brighter than background fluorescence. B) Morphometry and FACS estimate of total number of c-kit-EGFP^{+} cells in neonatal hearts. C) C-kit-EGFP expression and PCNA (red) staining indicates cycling in sEGFP cells cultured for 9 days in basic media. Arrow indicates punctuate PCNA staining. D) C-kit-EGFP expressing cells at 24 hours (left) and 9 days (middle) post-FACS. Note differences in cell size and shape. At right, tEGFP cells plated on feeders expand rapidly (3 days) in a network pattern. E) Merged brightfield and fluorescent image taken after 1 day in culture of tEGFP cells in a cluster. F) Images taken from the same field of view 9 days (left) and 16 days (right) post-sEGFP plating in basic media showing expansion of cells. A small population of cells at both 9 and 16 days are no longer fluorescent. G) Distribution of committed cells 24 hours post-FACS (tEGFP cells). Note lack of endothelial cells (PECAM1) and roughly equal distribution of smooth muscle (α-SMA) and cardiac cells (cTnT). Nestin staining suggests a sub-set of undifferentiated cells. Number of experiments indicated in bars. H) Co-staining 9-16 days post-FACS (sEGFP cells). I) c-kit (green) cell expressing both α-SMA (blue) and cTnT (red) markers. J) Nestin (red) and c-kit (green) co-staining in cells cultured for 9 days. DAPI staining (blue) in H and I. Scale bars: C, 20 μm; D, E, F, H, and J, 50 μm; and I, 10 μm. *__A.S.__ contributed to optimization of neonatal cardiomyocyte dissociation protocol and media conditions, preparation of cells for FACS, maintenance of cells in culture, preparation of cells for immunostaining, microscopy for cell imaging and quantification, and data analysis.

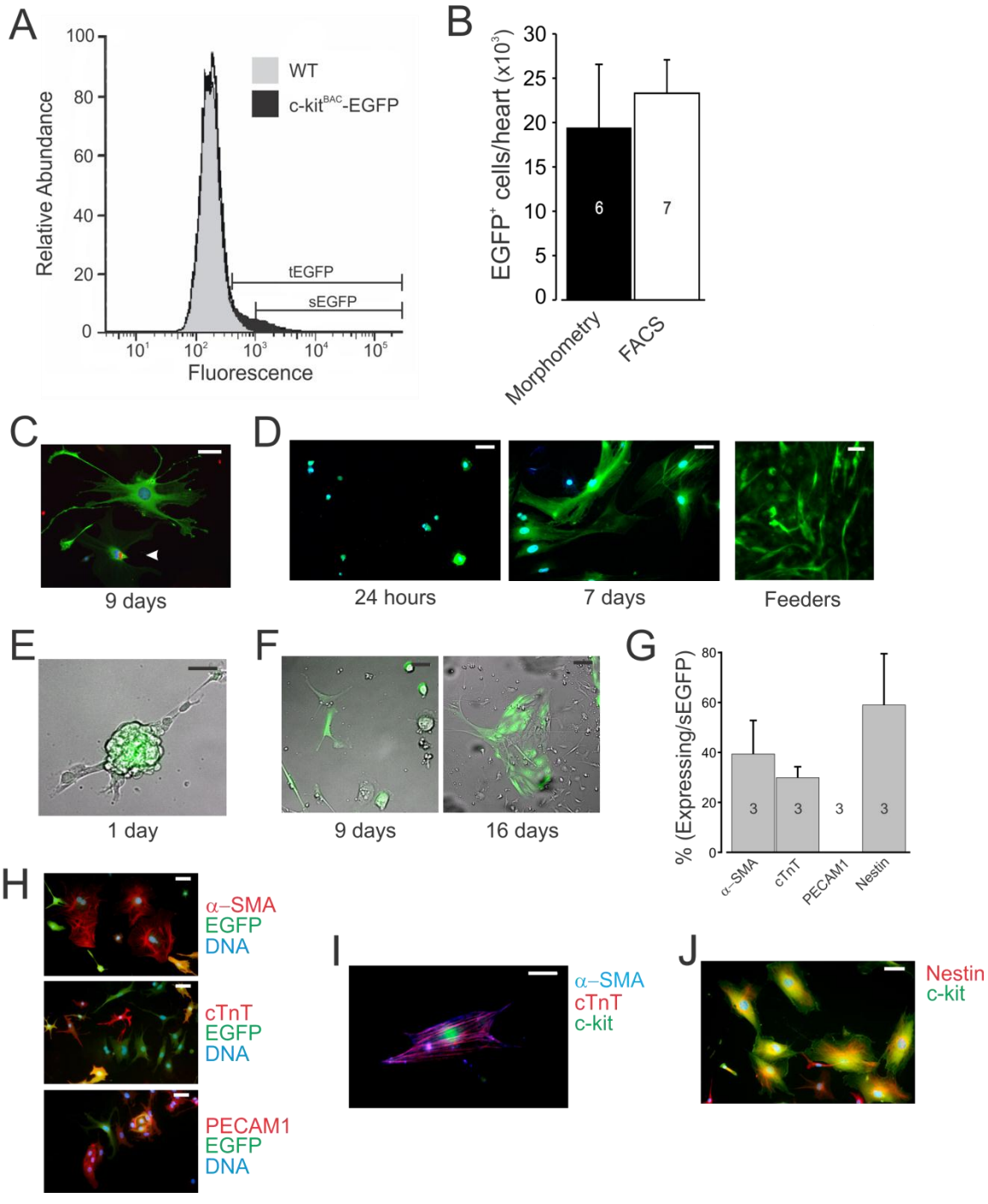
A
Relative Abundance
Fluorescence
WT
c-kit^BAC-EGFP
tEGFP
sEGFP
B
EGFP+ cells/heart (x10^3)
6
7
Morphometry
FACS
C
9 days
D
24 hours
7 days
Feeders
E
1 day
F
9 days
16 days
G
% (Expressing/sEGFP)
3
3
3
3
α–SMA
cTnT
PECAM1
Nestin
H
α–SMA
EGFP
DNA
cTnT
EGFP
DNA
PECAM1
EGFP
DNA
I
α–SMA
cTnT
c-kit
J
Nestin
c-kit

23,300±3773 (n=7) from FACS analysis, a finding similar to that obtained by counting cells in individual heart slices (19,418±7138; n=6) (Figure 2.3B).

tEGFP and sEGFP cell fractions plated on gelatin coated chambered slides rapidly expanded in an optimized proliferation media, with individual fluorescent cells undergoing cell cycling as indicated by anti-PCNA staining (Figure 2.3C) and the formation of clusters of fluorescent cells from isolated cell populations. Approximately 1 week post-differentiation, a significant difference in binucleated cell count between the tEGFP (1.09 ± .25%, n=6) and sEGFP (9.4 ± .88%, n=6) cell fractions was observed, suggesting an innate difference in cell division and cardiac commitment between the two populations. Therefore, the sEGFP population was utilized for a majority of our studies except where cell number was too low to obtain significant results. 24 hours after plating, sEGFP cell fractions were 100% fluorescent, consisting of small, brightly fluorescent cells containing little cytoplasm, flat cells with a large amount of cytoplasm, or spindle-shaped cells; following several days in culture, cells markedly increased in size, often forming long processes or extensions that contacted neighboring cells (Figure 2.3D, left and middle). Cells also expanded rapidly when plated on irradiated feeder cells (Figure 2.3D, right). The expanding cell population gradually lost expression of EGFP, by 9-16 days after plating of sEGFP cells 67±4% (n=3) expressed EGFP and many of these cells co-expressed nestin. Cells expanded as clusters with a central clump of c-kit-EGFP^{+} cells (Figure 2.3E) or as flattened cell aggregates (Figure 2.3F).

Cells analyzed 24 hours post-plating lacked expression of HSC markers CD45 and CD34, indicating that the prominent epicardial cells did not survive disaggregation. Surprisingly, the

endothelial marker PECAM1 barely was detected at 24 hours (0.003±0.003%), although cells did induce expression after several days in culture. Another endothelial marker, Von Willebrand Factor (vWF) also was undetectable at 24 hours post-plating. While cells were negative for microfilament marker, sarcomeric actin, approximately 1/3 of the cells did express smooth or cardiac muscle specific proteins at 24 hours (39±13% and 30±4%, respectively, Figure 2.3G). Not surprisingly, the cells were negative for early skeletal muscle transcription factor, myogenin, suggesting specific commitment to the heart musculature. 9-16 days post-FACS several sEGFP cells displayed smooth muscle, cardiac muscle, and endothelial markers (Figure 2.3H). On rare occasion α-SMA, cTnT, and c-kit protein were observed in the same cell demonstrating their bipotential capacity (Figure 2.3I). No co-expression of Isl-1 and c-kit-EGFP was observed, consistent with separate developmental populations (data no shown) [10, 11]. We also did not see evidence of Sca-1, another purported CPC marker, in the cells at the 24 hour timepoint. However, over 80% of the cells were nestin-positive at 24 hours with greater than 50% of the cells retaining nestin expression 9 days after initial plating, further suggesting their precursor status (Figures 2.3G and 2.3J) [28, 29].

Cardiac Differentiation of C-kit-EGFP$^+$ Cells

Several days after plating in media containing bFGF, many c-kit-EGFP$^+$ cells began to spontaneously contract. As cells expanded in culture, contractions spread over clusters of c-kit-EGFP expressing and non-expressing cells. Contractions also were observed in single, non-striated c-kit-EGFP expressing cells after several days in culture (Figure 2.4A), likely indicating ongoing myogenesis and the development of a muscle phenotype in culture.

Figure 2.4. Cardiac Phenotype of Spontaneously Beating C-kit-EGFP$^+$ Cells.

A) Representative contractile c-kit-EGFP expressing cell at left in a single frame from a time series. Line through image indicates area used for sequential scans of fluorescence shown at right. Left edge of linescan shows rhythmic contraction of the top left cell extension at roughly 2 Hz. B) Action potentials ranged from nodal-like (top), to more atrial (middle), or ventricular (bottom), morphologies. Note prominent diastolic depolarization phases. Networked c-kit-EGFP$^+$ cells fired rhythmical burst-like activity, interrupted by periods of quiescence accompanied by prominent membrane hyperpolarization. C) Tetrodotoxin (10 µM, n=5) or D) Nifedipine (1 µM, n=5), reversibly abolished action potentials. Scale bar: A, 25 µm. *__A.S.__ contributed to preparation of cells for FACS, maintenance of cells in culture, and preparation of cells for patch clamp analysis by Dr. Michael Craven.

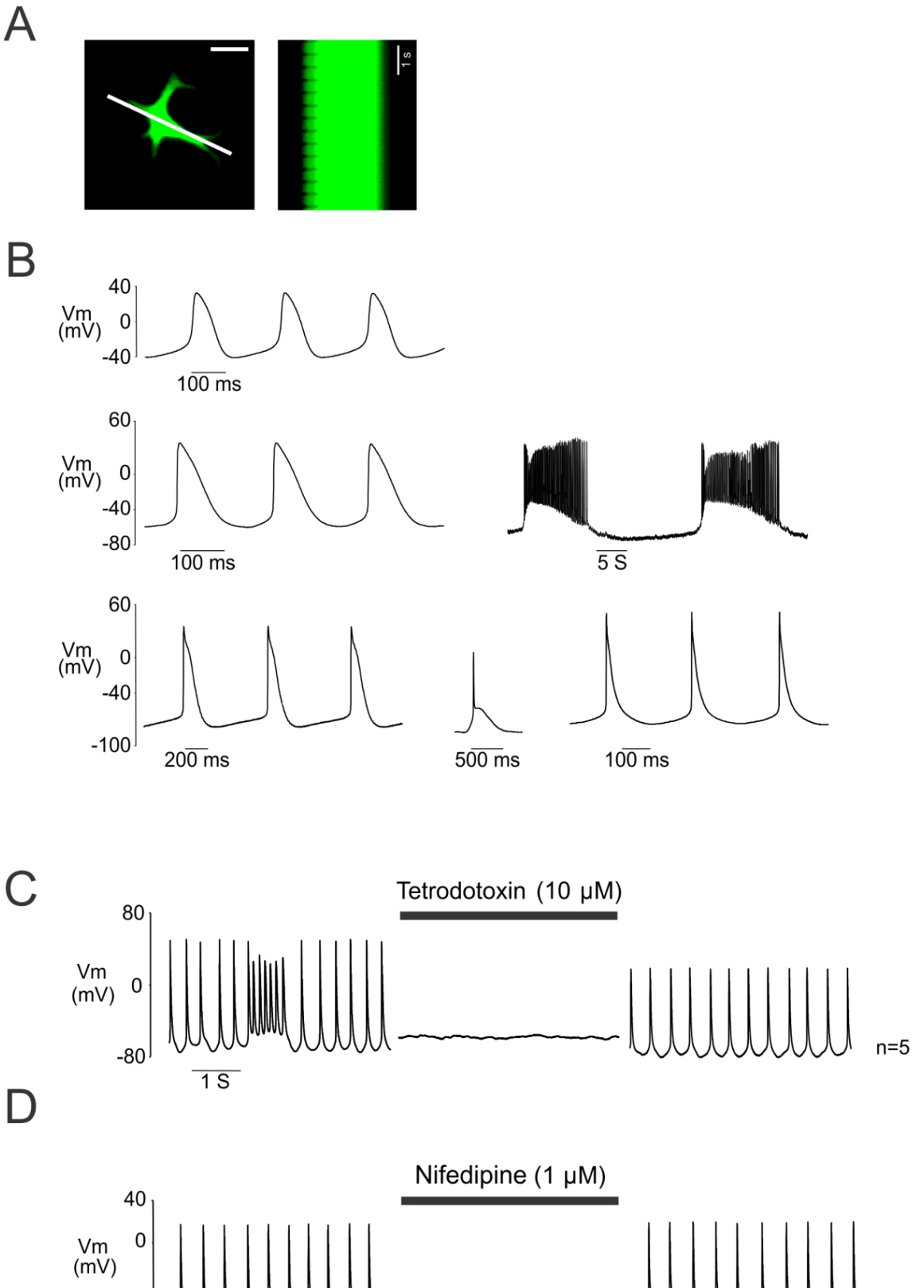
A
1 s
B
40
Vm
(mV)
0
-40
100 ms
60
Vm
(mV)
0
-40
-80
100 ms
5 S
60
Vm
(mV)
0
-40
-100
200 ms
500 ms
100 ms
C
Tetrodotoxin (10 μM)
80
Vm
(mV)
0
-80
1 S
n=5
D
Nifedipine (1 μM)
40
Vm
(mV)
0
-80
1 S
n=5

To determine the electrical phenotype of neonatal c-kit-EGFP$^+$ cells, sorted sEGFP cells were cultured for 5-7 days and spontaneously contracting cells were examined using patch clamp methods by Dr. Michael Craven. Current clamp recordings revealed spontaneous, rhythmic action potentials with characteristics similar to those previously reported from embryonic, and ESC-derived cardiac myocytes [30-32]. The range of action potential morphologies included nodal, atrial, and ventricular characteristics (Figure 2.4B). Spontaneously depolarizing phase 0 (pacemaker) currents and stable resting potential were observed, as well as a range of depolarization patterns that included atrial or ventricular-like plateau phases and nodal type transient depolarizations. Phasic electrical activity included both stable depolarization rates and more complex, repeated burst-type activity, as observed in embryoid body (EB) differentiated myocytes [33]. The latter pattern was observed mainly in networked c-kit-EGFP$^+$ cells, and only occasionally in single c-kit-EGFP$^+$ cells.

The ion channel dependence of the action potentials was investigated using known blockers of cardiac fast sodium channels (tetrodotoxin, 10 μM) and L-type calcium channels (nifedipine, 1 μM). Tetrodotoxin abolished action potentials in a reversible manner (Figure 2.4C), indicating the cardiac nature of these currents, as vascular smooth muscle cells (VSMCs) do not express voltage-dependent sodium channels and action potentials are tetrodotoxin-insensitive; nifedipine also inhibited the action potentials, indicating the importance of L-type Ca^{2+} channels (Figure 2.4D). Taken together, these data support the cardiac phenotype of spontaneously contracting c-kit-EGFP$^+$-derived cells.

Lineage Potential of C-kit$^+$-EGFP Precursor Cells

To determine whether individual c-kit-EGFP$^+$ cells are multipotent, we sorted sEGFP cells and cultured them for 9-16 days under conditions designed to promote cardiovascular lineage differentiation. Wells were stained for cardiac (cTnT), smooth muscle (α-SMA), or endothelial (PECAM1) markers and the fraction of positive cells was counted in all wells. Cardiac differentiation was markedly favored in media containing bFGF, with approximately 15% of cells expressing the cardiac muscle specific marker cTnT, compared to less than 3% in media containing TGF-β1or VEGF (Figure 2.5A). Addition of VEGF to the media enhanced the expansion of endothelial and smooth muscle cells, and the latter effect was more potent than that observed in TGF-β1 media. TGF-β1, which has been reported to promote smooth muscle differentiation [3, 5, 34], slightly increased the average fraction of α-SMA positive cells, but was not significant, although there was a significant decrease in cardiac myogenesis. Several other cardiogenic factors including 5-azacytidine, cardiogenol-C, cardiotrophin-1, and 2-mercaptoethanol were evaluated for their roles in cardiac lineage commitment with little change (data not shown). Taken together, these results demonstrate that c-kit-EGFP$^+$ cells from neonatal hearts can be manipulated *in vitro* to selectively expand the three cardiovascular lineages.

As the above results could reflect the induced expansion of pre-committed cells or selective differentiation of multipotent precursors, we performed limiting dilution studies to determine the fate of individual clonal populations. A proliferation media containing bFGF and LIF was used for these studies, as c-kit-EGFP$^+$ cells did not survive in standard ESC media. Cells were plated to yield one cell/well and cultured for 21 days; approximately 15% of the individual cells counted on day 3 survived and expanded during the culture period (Figure 2.5B). Separate immunostaining of the expanded populations revealed individual committed cardiac (cTnT),

Figure 2.5. C-kit-EGFP$^+$ Neonatal Heart Cells are Cardiovascular Precursors.

A) Modification of commitment outcomes by addition of specific growth factors. Number of experiments indicated in bars. B) Clonal expansion showing a single c-kit-EGFP$^+$ cell at 24 hours (left) and the clone after 20 days (right). C) Immunostaining of clones from a single c-kit-EGFP$^+$ cell after 21 days. Individual cells showing commitment to all three heart lineages. D) Co-immunostaining of clonal populations demonstrate commitment to cardiac (left) or smooth muscle (right) and endothelium in the same clone. DAPI staining (blue) in C. Scale bars: B, C and D, 50 μm. *__A.S.__ contributed to preparation of cells for FACS, maintenance of cells in culture, design of media conditions to alter lineage commitment, optimization of serial dilutions, tracking of clonal populations by microscopy, preparation of cells for immunostaining, microscopy for cell imaging and quantification, and data analysis.

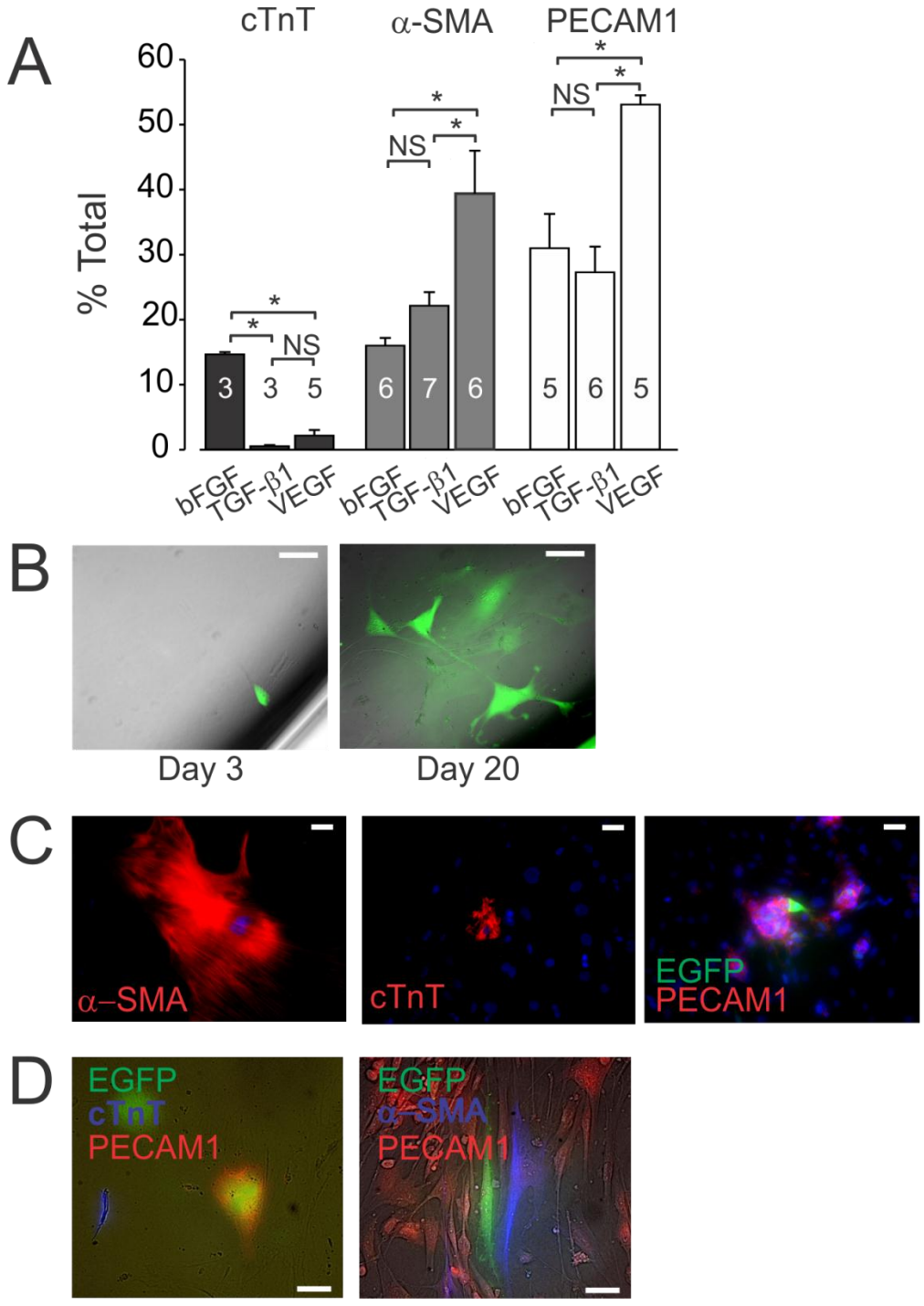
A
cTnT
α-SMA
PECAM1
% Total
60
50
40
30
20
10
0
*
*
NS
3
3
5
6
7
6
5
6
5
bFGF
TGF-β1
VEGF
B
Day 3
Day 20
C
α–SMA
cTnT
EGFP
PECAM1
D
EGFP
cTnT
PECAM1
EGFP
α–SMA
PECAM1

smooth muscle (α-SMA), and endothelial (PECAM1) cells amongst cells that did not express these markers (Figure 2.5C). The above result, in which cells of all three lineages were detected was repeated in 19 separate dilution experiments. Moreover, co-staining for α-SMA and PECAM1 or cTnT and PECAM1 clearly demonstrated smooth muscle and endothelial or cardiac and endothelial lineages arising in clonal expansions (Figure 2.5D). *In vitro* expansion of single clones to all 3 cardiovascular lineages indicates that c-kit-EGFP^{+} cells from neonatal hearts include a population of undifferentiated cells similar to ESC-derived CPCs [3, 5, 11].

Re-expression and Engraftment of C-kit-EGFP^{+} Following Injury

To analyze c-kit expression following myocardial injury, surgeon Dr. Michele Steffey induced cryolesions in the left ventricle of adult c-kit^{BAC}-EGFP mice [22] and we analyzed c-kit-EGFP expression in and around the infarct region which was identified by Sirius red staining of newly formed collagen. 7 days after cryolesion there was a marked expression of fluorescent cells in the infarct and within the border zone, with fluorescent cells often associated with vessels within the infarcts, and modestly fluorescent striated cardiomyocytes surrounding the border zone (Figure 2.6A). In sham operated mice rare c-kit-EGFP^{+} cells were equally distributed throughout the myocardium. C-kit-EGFP expression increased by day 3 after the lesion, peaked at 7 days, and declined at 21 days post-injury, whereas in sham operated hearts no temporal pattern of c-kit-EGFP^{+} expression was observed.

C-kit-EGFP^{+} cells within the infarct were found preferentially in the vicinity of, and contributing to, blood vessels (Figure 2.6B, left and blow up). Luminal c-kit-EGFP expressing cells in vessels were PECAM1 positive (Figure 2.6B, right), whereas the outer cells surrounding larger

Figure 2.6. Re-Expression of C-kit-EGFP Following Injury in the Adult Heart.

A) Left, Stefanini-fixed heart 7 days post-surgery. Note the large number of c-kit-EGFP^{+} cells at the border zone and within the infarcted (darker) area. Right, rare fluorescent cells in sham heart. B) C-kit-EGFP cells within infarct. Left image, fluorescence wide-field image of adult c-kit^{BAC}-EGFP heart 14 days post-cryoablation. Note fluorescent cells lining vessel. Right, c-kit-EGFP^{+} endothelial cells lining an artery 7 days post-injury are identified by PECAM1 staining; surrounding smooth muscle cells also express c-kit-EGFP. C) C-kit-EGFP^{+} cardiomyocytes at border zone. Left, fluorescent and non-fluorescent striated cardiomyocytes. Middle and right, clusters of c-kit-EGFP^{+} myocytes at border zone 7 days post-infarct. D) Lack of pHH3 in c-kit-EGFP^{+} cardiac myocytes. Left, c-kit-EGFP^{+} and EGFP^{-} myocytes at border zone. Right, single pHH3^{+} non-myocyte within infarct. Scale bars: A, left, 360 µm, right, 280 µm; B) left, 250µm, blow-up 100 µm, right, 10 µm; C, 22 µm; D, left, 14 µm, right, 16 µm. ***A.S.** contributed to surgical assistance to Dr. Michele Steffey, post-operative care, tissue harvest, cryosectioning, imaging by microscopy, and data analysis.

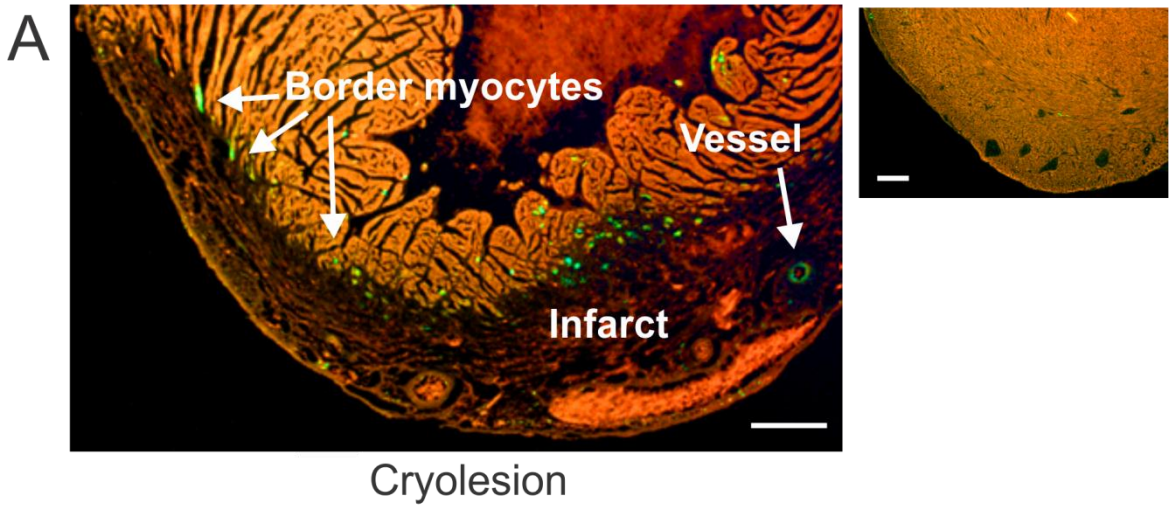
A
Border myocytes
Vessel
Infarct
Cryolesion
B
PECAM1EGFP DNA
EGFP DNA
C
EGFP DNA
EGFP DNA
EGFP DNA
D
pHH3
α-actinin
EGFP
DNA

vessels stained for α-SMA (data not shown), thus contributing to the endothelium and smooth muscle layer of vessels, respectively. Single endothelial cells formed lumens, consistent with early angiogenesis. Fluorescent cells integrated within vessels still were observed 21 days after the lesion. The bulk of the c-kit-EGFP$^+$ cells within the infarct at day 7 were vimentin positive (data not shown).

By contrast, the pattern of c-kit-EGFP expression in the border zone of the cryoinfarct was markedly different, with modest, but distinct, c-kit-EGFP expression in striated cardiomyocytes (Figure 2.6C) and more robust expression in elongated fibroblasts. EGFP expression in border zone cardiomyocytes was confirmed by immunostaining (data not shown). C-kit-EGFP$^+$ cardiomyocytes did not express phospho-histone H3 (pHH3), a marker of cell proliferation, and the number of these cells peaked at day 7 and declined to the level of sham control by day 21 (Figure 2.6D). Neither mitotic figures nor immature cardiomyocytes were observed post-cryoablation. cTnT positive cells never were observed within the infarct, indicating a lack of cardiac myogenesis associated with c-kit expression. pHH3$^+$ fibroblasts and leukocytes were observed within the infarct and at the border zone, only about 1% of pHH3$^+$ cells were also c-kit$^+$. Thus c-kit expression is observed in cells associated with the early revascularization and fibrosis of the infarcted heart, declining within a few weeks after injury, but is also seen in differentiated myocytes. The latter expression is not associated with myocyte proliferation, suggesting caution with respect to the interpretation of the role of c-kit$^+$ myocytes in heart repair. When c-kit-EGFP$^+$/LacZ$^+$ cells were transplanted into the peri-infarct region of wildtype mice, exogenously delivered c-kit-EGFP$^+$/LacZ$^+$ cells could be identified even after terminal differentiation in and around the ablated myocardium. In preliminary studies, we observed

$LacZ^+$ cells in the tunica media region of blood vessels, further supporting a role for c-kit^+ cells in vascular repair and angiogenesis (data not shown). We did not observe any LacZ staining in control animals, ruling out endogenous expression of β-galactosidase in the cardiac region of interest. These studies are on-going in the laboratory.

DISCUSSION

The stem cell surface antigen, c-kit, is at the center of an array of cell lineage determinants. Recent evidence suggests that within the developing heart a resident population of CPCs exist, with the capacity to differentiate into multiple cardiovascular cell lineages [5]. C-kit expression appears to characterize a developmental stage of one subset of these cardiovascular precursor cells [2], however studies in mouse [5] and human [3, 4] ESC-derived precursors suggest that a c-kit negative stage precedes commitment. To examine the role of c-kit expression in CPCs, and to facilitate their isolation and analysis, we created BAC transgenic mice in which EGFP is placed under the transcriptional control of the c-kit locus, as this genetic strategy can achieve very high expression levels and outstanding transcriptional fidelity [35, 36].

Previously, minimal promoter or knock-in strategies have been used to mark c-kit expression [37], but few studies have examined expression in the developing heart. Bernex and colleagues [37] and Wouters, et al. [38] knocked reporters into the c-kit locus, but did not examine cardiac expression, and the dominant nature of the c-kit locus significantly complicates this strategy. Fransioli, et al. [39] reported the development of a transgenic line in which GFP was driven by a minimal c-kit promoter construct; similar to our observations, they reported that individual c-kit expressing cells were observed in the developing heart and that the concordance of anti-CD117 and anti-GFP staining was strong but not complete. Moreover, EGFP labeled cells increased until shortly after birth and declined thereafter [39, 40].

We now show that embryonic and postnatal c-kit$^+$ cells are in a mixed developmental state within the developing heart (Figure 2.2), as predicted for a population of cells transitioning from

precursor to committed status. Neonatal c-kit^{+} cells are characterized by the co-expression of nestin (Figure 2.3), a marker of a variety of cells with multilineage potential [28, 29], and some of these cells also express cardiac, endothelial, or smooth muscle commitment markers (Figure 2.3).

C-kit^{+} cells isolated by FACS expanded, while differentiating in culture on feeder cells and gelatin coated plates (Figure 2.3). When plated as a mixed (c-kit^{+} and c-kit^{-} cells) population, c-kit^{+} cells often formed extended networks next to more compact, contracting cells. EGFP expressing cells also began to contract in culture and when purified to complete homogeneity by FACS individual fluorescent cells were shown to contract, further demonstrating the mixed differentiation status of c-kit-EGFP^{+} cells. EGFP expression declined gradually in cultured cells, particularly in mixed cultures, indicating the ongoing differentiation of cells in the presence of growth factors such as bFGF.

Many of these cells displayed clear cardiac-like action potentials that were sensitive to tetrodotoxin and had a marked plateau phase. However, some cells also displayed more nodal-like activity without a prominent plateau phase (Figure 2.4). The presence of cells with mixed electrical activity is also a characteristic of ESC-derived cardiomyocytes and the presence of multiple ion currents in the same cells appears to be a characteristic of cardiac development [30, 32, 41]. The plateau phase morphology of some action potentials and their inhibition by tetrodotoxin establishes the definitive cardiac phenotype of these cells. VSMCs do not display a characteristic action potential feature, it is possible that rhythmically active cells without a plateau phase represent this lineage, or alternatively that differentiating smooth muscle cells, unlike committed cardiac cells, do not display spontaneous rhythmicity.

Following initial plating, a fraction of c-kit$^+$ cells stained for either cTnT or α-SMA, but despite the identification of PECAM1 staining fluorescent cells in the neonatal heart (Figure 2.2), adherent cells were not PECAM1 positive after 1 day in culture (Figure 2.3G), whereas after several days in culture PECAM1 was readily detected (Figure 2.3H). This may reflect a failure of endothelial-committed cells to attach or partial digestion of the PECAM1/CD31 epitope during enzymatic cell dissociation.

Our initial attempts to culture single purified c-kit$^+$ cells isolated by FACS resulted in cell death in ESC media. Switching to a media containing bFGF, a growth factor associated with mesodermal cell survival, promotion of cell proliferation, and angiogenesis [5, 42], produced viable cells that expanded and generated differentiated mesenchymal cells in culture. Wu, et al. [5] also tried to culture Nkx2.5$^+$ cells isolated from 7.5-8.5 dpc embryonic hearts by FACS in similar ESC media without success. The addition of bFGF, which is associated with mesodermal cell survival, or other growth factors, appears to be necessary for the propagation of c-kit$^+$ cells in culture.

To establish the lineage potential of neonatal c-kit$^+$ cells, we manipulated growth factors in the culture media and examined the proportion of cell displaying evidence of smooth muscle, cardiac, or endothelial commitment. The number of cells expressing cTnT markedly was increased by inclusion of bFGF in the culture media, whereas VEGF shifted the differentiation profile toward vascular cells, significantly increasing the number of cells expressing α-SMA and PECAM1 (Figure 2.5A). Substitution of the growth factor TGF-β1, a known smooth muscle

mitogen, did not significantly increase smooth muscle or endothelial differentiation, although it did markedly decrease cardiac commitment (Figure 2.5A).

As c-kit-EGFP$^+$ cells display various stages of differentiation in the neonatal heart (Figure 2.2), the above results could suggest either the presence of multipotent cardiovascular precursors within the purified cell population, or the selective survival and expansion of pre-committed populations under appropriate *in vitro* conditions. To determine whether c-kit-EGFP$^+$ cells include uncommitted precursors, we undertook a clonal analysis by plating cells at limiting dilutions that yielded individual cells within multi-well plates. The absence of attachment factors and conditioning substances resulted in relatively low viability of dilute clones; however individual surviving cells were observed to expand into clonal colonies and were probed for lineage commitment 21-25 days after plating. Evidence of commitment to all three cardiovascular lineages was observed in these clonal populations, although the great majority of cells did not express any lineage-specific markers (Figure 2.5C). The presence of uncommitted cells within these colonies suggests that the results are not simply explained by expansion of a previously committed cell, definitive evidence of multilineage potential was obtained by co-staining of these clonal populations (Figure 2.5D). Differentiation of individual cells to both muscle (smooth and cardiac) and endothelium was observed, definitively establishing the multilineage potential of neonatal c-kit-EGFP$^+$ cells. These results are similar to those reported by Moretti, et al. [11], who clonally amplified Isl-1$^+$ cells from ED8-8.5 heart cell cultures, and showed that a rare number of these cells differentiated into smooth muscle cells, cardiac myocytes, and endothelium. These Isl-1$^+$ and/or Nkx2.5$^+$ cells, isolated from hearts at a

markedly earlier stage of development, do not express c-kit [10], and our results confirm a lack of Isl-1 staining in c-kit-EGFP$^+$ cells.

Recent work from Li, et al. [40] demonstrated that pressure overload results in augmented expression of c-kit in cardiomyocytes. Such expression could reflect cardiomyogenesis from c-kit$^+$ cells, or could be the result of c-kit re-expression in myocytes subsequent to exposure to inflammatory products and mesenchymal stem cell (MSC)-derived cytokines. We show that c-kit expression in the adult, injured heart is associated with fibrous and vascular infarct repair, but not myogenesis. C-kit expression is detectable within 3 days post-injury, peaks at 7 days, and declines within a 4 week period to near baseline. C-kit-EGFP$^+$ expression in cardiomyocytes only was observed in striated, terminally differentiated cells. The lack of c-kit-EGFP$^+$ myocytes within the infarct zone, absence of immature (non-striated) cTnT-positive myocytes, and lack of mitotic figures or pHH3 staining in c-kit-EGFP$^+$ myocytes indicates that cryoinjury does not provoke cardiomyogenesis through activation of c-kit. Rather, that c-kit re-expression occurs in differentiated cardiomyocytes at regions surrounding cardiac injury, activated by local conditions such as hypoxia or inflammatory cytokines, as these cells are not seen at remote regions. Thus, rather than unequivocally identifying adult cardiac precursors, c-kit re-expression in adult cardiac myocytes appears to play a role in the transcriptional activation of fetal/neonatal genes that are induced during cardiac stress [40, 43, 44].

In summary, we describe the purification of a population of cells that includes mesodermally-derived, CPCs, as well as cells in early stages of cardiovascular development. Our results indicate that true CPCs persist through embryonic development and that the PN heart contains a

significant number of these cells, which decline rapidly in the first weeks after birth. Isolated CPCs differentiate into rhythmically contracting cell networks, and individual cells display complex electrical activity similar to that observed following the directed differentiation of ESCs [30, 32]. C-kit-EGFP$^+$ cells can be expanded efficiently *in vitro*, although the multipotency of expanded and passaged c-kit-EGFP$^+$ cells remains to be demonstrated. Finally, c-kit-EGFP$^+$ cells are observed transiently in damaged heart tissue, but do not identify prominent re-activation of resident CPCs in the adult heart. Neonatal c-kit-EGFP$^+$ cells may prove useful for determination of the genetic basis of CPC status and provide a model for the directed differentiation of pluripotent cells for cardiac cell-based therapy.

REFERENCES

1. Tallini YN, Greene KS, Craven M, Spealman A, Breitbach M, Smith J, Fisher PJ, Steffey M, Hesse M, Doran RM, Woods A, Singh B, Yen A, Fleischmann BK, Kotlikoff MI. C-kit expression identifies cardiovascular precursors in the neonatal heart. *Proc Natl Acad Sci U S A*. 2009;106:1808-1813.

2. Kattman SJ, Huber TL, Keller GM. Multipotent flk-1+ cardiovascular progenitor cells give rise to the cardiomyocyte, endothelial, and vascular smooth muscle lineages. *Dev Cell*. 2006;11:723-732.

3. Yang L, Soonpaa MH, Adler ED, Roepke TK, Kattman SJ, Kennedy M, Henckaerts E, Bonham K, Abbott GW, Linden RM, Field LJ, Keller GM. Human cardiovascular progenitor cells develop from a KDR+ embryonic-stem-cell-derived population. *Nature*. 2008;453:524-528.

4. Laflamme MA, Chen KY, Naumova AV, Muskheli V, Fugate JA, Dupras SK, Reinecke H, Xu C, Hassanipour M, Police S, O'Sullivan C, Collins L, Chen Y, Minami E, Gill EA, Ueno S, Yuan C, Gold J, Murry CE. Cardiomyocytes derived from human embryonic stem cells in pro-survival factors enhance function of infarcted rat hearts. *Nat Biotechnol*. 2007;25:1015-1024.

5. Wu SM, Fujiwara Y, Cibulsky SM, Clapham DE, Lien C, Schultheiss TM, Orkin SH. Developmental origin of a bipotential myocardial and smooth muscle cell precursor in the mammalian heart. *Cell,*. 2006;127:1137-1150.

6. Beltrami AP, Barlucchi L, Torella D, Baker M, Limana F, Chimenti S, Kasahara H, Rota M, Musso E, Urbanek K, Leri A, Kajstura J, Nadal-Ginard B, Anversa P. Adult cardiac stem cells are multipotent and support myocardial regeneration. *Cell,*. 2003;114:763-776.

7. Li Q, Guo Y, Ou Q, Chen N, Wu WJ, Yuan F, O'Brien E, Wang T, Luo L, Hunt GN, Zhu X, Bolli R. Intracoronary administration of cardiac stem cells in mice: A new, improved technique for cell therapy in murine models. *Basic Res Cardiol*. 2011.

8. Fatma S, Selby DE, Singla RD, Singla DK. Factors released from embryonic stem cells stimulate c-kit-FLK-1(+ve) progenitor cells and enhance neovascularization. *Antioxid Redox Signal*. 2010;13:1857-1865.

9. Urbanek K, Cesselli D, Rota M, Nascimbene A, De Angelis A, Hosoda T, Bearzi C, Boni A, Bolli R, Kajstura J, Anversa P, Leri A. Stem cell niches in the adult mouse heart. *Proc Natl Acad Sci U S A*. 2006;103:9226-9231.

10. Laugwitz KL, Moretti A, Lam J, Gruber P, Chen Y, Woodard S, Lin LZ, Cai CL, Lu MM, Reth M, Platoshyn O, Yuan JX, Evans S, Chien KR. Postnatal isl1+ cardioblasts enter fully differentiated cardiomyocyte lineages. *Nature*. 2005;433:647-653.

11. Moretti A, Caron L, Nakano A, Lam JT, Bernshausen A, Chen Y, Qyang Y, Bu L, Sasaki M, Martin-Puig S, Sun Y, Evans SM, Laugwitz KL, Chien KR. Multipotent embryonic isl1+ progenitor cells lead to cardiac, smooth muscle, and endothelial cell diversification. *Cell*. 2006;127:1151-1165.

12. Moretti A, Bellin M, Jung CB, Thies TM, Takashima Y, Bernshausen A, Schiemann M, Fischer S, Moosmang S, Smith AG, Lam JT, Laugwitz KL. Mouse and human induced pluripotent stem cells as a source for multipotent Isl1+ cardiovascular progenitors. *FASEB J*. 2010;24:700-711.

13. Smart N, Bollini S, Dube KN, Vieira JM, Zhou B, Davidson S, Yellon D, Riegler J, Price AN, Lythgoe MF, Pu WT, Riley PR. De novo cardiomyocytes from within the activated adult heart after injury. *Nature*. 2011;474:640-644.

14. Reber L, Da Silva CA, Frossard N. Stem cell factor and its receptor c-kit as targets for inflammatory diseases. *Eur J Pharmacol*. 2006;533:327-340.

15. Yasuda H, Galli SJ, Geissler EN. Cloning and functional analysis of the mouse c-kit promoter. *Biochem Biophys Res Commun*. 1993;191:893-901.

16. Alexeev V, Yoon K. Distinctive role of the cKit receptor tyrosine kinase signaling in mammalian melanocytes. *J Invest Dermatol*. 2006;126:1102-1110.

17. Tropepe V, Sibilia M, Ciruna BG, Rossant J, Wagner EF, van der Kooy D. Distinct neural stem cells proliferate in response to EGF and FGF in the developing mouse telencephalon. *Dev Biol*. 1999;208:166-188.

18. Sinha S, Hoofnagle MH, Kingston PA, McCanna ME, Owens GK. Transforming growth factor-beta1 signaling contributes to development of smooth muscle cells from embryonic stem cells. *Am J Physiol Cell Physiol*. 2004;287:C1560-8.

19. Yamamoto H, Kato H, Uruma M, Nitta M, Takamoto S. Identification of two distinct populations of endothelial progenitor cells differing in size and antigen expression from human umbilical cord blood. *Ann Hematol*. 2008;87:87-95.

20. Rae J, Cooper K, Gates P, Watsky M. Low access resistance perforated patch recordings using amphotericin B. *J Neurosci Methods*. 1991;37:15-26.

21. Roell W, Fan Y, Xia Y, Stoecker E, Sasse P, Kolossov E, Bloch W, Metzner H, Schmitz C, Addicks K, Hescheler J, Welz A, Fleischmann BK. Cellular cardiomyoplasty in a transgenic mouse model. *Transplantation*. 2002;73:462-465.

22. Roell W, Lewalter T, Sasse P, Tallini YN, Choi BR, Breitbach M, Doran R, Becher UM, Hwang SM, Bostani T, von Maltzahn J, Hofmann A, Reining S, Eiberger B, Gabris B, Pfeifer A, Welz A, Willecke K, Salama G, Schrickel JW, Kotlikoff MI, Fleischmann BK. Engraftment of connexin 43-expressing cells prevents post-infarct arrhythmia. *Nature*. 2007;450:819-824.

23. Brown RH, Walters DM, Greenberg RS, Mitzner W. A method of endotracheal intubation and pulmonary functional assessment for repeated studies in mice. *J Appl Physiol*. 1999;87:2362-2365.

24. Andre C, Hampe A, Lachaume P, Martin E, Wang XP, Manus V, Hu WX, Galibert F. Sequence analysis of two genomic regions containing the KIT and the FMS receptor tyrosine kinase genes. *Genomics*. 1997;39:216-226.

25. Gokkel E, Grossman Z, Ramot B, Yarden Y, Rechavi G, Givol D. Structural organization of the murine c-kit proto-oncogene. *Oncogene*. 1992;7:1423-1429.

26. Rishniw M, Fisher PW, Doran RM, Meadows E, Klein WH, Kotlikoff MI. Smooth muscle persists in the muscularis externa of developing and adult mouse esophagus. *J Muscle Res Cell Motil*. 2007;28:153-165.

27. Manova K, Bachvarova RF, Huang EJ, Sanchez S, Pronovost SM, Velazquez E, McGuire B, Besmer P. C-kit receptor and ligand expression in postnatal development of the mouse cerebellum suggests a function for C-kit in inhibitory interneurons. *J Neurosci*. 1992;12:4663-4676.

28. Drapeau J, El-Helou V, Clement R, Bel-Hadj S, Gosselin H, Trudeau LE, Villeneuve L, Calderone A. Nestin-expressing neural stem cells identified in the scar following myocardial infarction. *J Cell Physiol*. 2005;204:51-62.

29. Scobioala S, Klocke R, Kuhlmann M, Tian W, Hasib L, Milting H, Koenig S, Stelljes M, El-Banayosy A, Tenderich G, Michel G, Breithardt G, Nikol S. Up-regulation of nestin in the infarcted myocardium potentially indicates differentiation of resident cardiac stem cells into various lineages including cardiomyocytes. *FASEB J*. 2008;22:1021-1031.

30. Kolossov E, Lu Z, Drobinskaya I, Gassanov N, Duan Y, Sauer H, Manzke O, Bloch W, Bohlen H, Hescheler J, Fleischmann BK. Identification and characterization of embryonic stem cell-derived pacemaker and atrial cardiomyocytes. *FASEB J*. 2005;19:577-579.

31. Gryshchenko O, Fischer IR, Dittrich M, Viatchenko-Karpinski S, Soest J, Bohm-Pinger MM, Igelmund P, Fleischmann BK, Hescheler J. Role of ATP-dependent K(+) channels in the electrical excitability of early embryonic stem cell-derived cardiomyocytes. *J Cell Sci*. 1999;112 (Pt 17):2903-2912.

32. Kuzmenkin A, Liang H, Xu G, Pfannkuche K, Eichhorn H, Fatima A, Luo H, Saric T, Wernig M, Jaenisch R, Hescheler J. Functional characterization of cardiomyocytes derived from murine induced pluripotent stem cells in vitro. *FASEB J*. 2009;23:4168-4180.

33. Maltsev VA, Wobus AM, Rohwedel J, Bader M, Hescheler J. Cardiomyocytes differentiated in vitro from embryonic stem cells developmentally express cardiac-specific genes and ionic currents. *Circ Res*. 1994;75:233-244.

34. Kurpinski K, Lam H, Chu J, Wang A, Kim A, Tsay E, Agrawal S, Schaffer DV, Li S. Transforming growth factor-beta and notch signaling mediate stem cell differentiation into smooth muscle cells. *Stem Cells*. 2010;28:734-742.

35. Tallini YN, Shui B, Greene KS, Deng KY, Doran R, Fisher PJ, Zipfel W, Kotlikoff MI. BAC transgenic mice express enhanced green fluorescent protein in central and peripheral cholinergic neurons. *Physiol Genomics*. 2006;27:391-397.

36. Tallini YN, Brekke JF, Shui B, Doran R, Hwang SM, Nakai J, Salama G, Segal SS, Kotlikoff MI. Propagated endothelial Ca2+ waves and arteriolar dilation in vivo: Measurements in Cx40BAC GCaMP2 transgenic mice. *Circ Res*. 2007;101:1300-1309.

37. Bernex F, De Sepulveda P, Kress C, Elbaz C, Delouis C, Panthier JJ. Spatial and temporal patterns of c-kit-expressing cells in WlacZ/+ and WlacZ/WlacZ mouse embryos. *Development*. 1996;122:3023-3033.

38. Wouters M, Smans K, Vanderwinden JM. WZsGreen/+: A new green fluorescent protein knock-in mouse model for the study of KIT-expressing cells in gut and cerebellum. *Physiol Genomics*. 2005;22:412-421.

39. Fransioli J, Bailey B, Gude NA, Cottage CT, Muraski JA, Emmanuel G, Wu W, Alvarez R, Rubio M, Ottolenghi S, Schaefer E, Sussman MA. Evolution of the c-kit-positive cell response to pathological challenge in the myocardium. *Stem Cells*. 2008;26:1315-1324.

40. Li M, Naqvi N, Yahiro E, Liu K, Powell PC, Bradley WE, Martin DI, Graham RM, Dell'Italia LJ, Husain A. C-kit is required for cardiomyocyte terminal differentiation. *Circ Res*. 2008;102:677-685.

41. DiFrancesco D. Funny channels in the control of cardiac rhythm and mode of action of selective blockers. *Pharmacol Res*. 2006;53:399-406.

42. Zhang YH, Zhang GW, Gu TX, Li-Ling J, Wen T, Zhao Y, Wang C, Fang Q, Yu L, Liu B. Exogenous basic fibroblast growth factor promotes cardiac stem cell-mediated myocardial regeneration after miniswine acute myocardial infarction. *Coron Artery Dis*. 2011;22:279-285.

43. Heineke J, Molkentin JD. Regulation of cardiac hypertrophy by intracellular signalling pathways. *Nat Rev Mol Cell Biol*. 2006;7:589-600.

44. Park JY, Li W, Zheng D, Zhai P, Zhao Y, Matsuda T, Vatner SF, Sadoshima J, Tian B. Comparative analysis of mRNA isoform expression in cardiac hypertrophy and development reveals multiple post-transcriptional regulatory modules. *PLoS One*. 2011;6:e22391.

CHAPTER THREE: NADPH OXIDASE ISOFORMS DIFFERENTIALLY INFLUENCE NEONATAL C-KIT^{+} CARDIAC PRECURSOR CELL STATUS AND DIFFERENTIATION

ABSTRACT

Heart disease is a leading cause of death in part due to the inability of the adult heart to support cardiac myogenesis following large-scale injury. Cardiac precursor cells (CPCs) are found in significant numbers in the neonatal mammalian heart; however, the mechanisms regulating CPC function are incompletely understood. Recently, redox status has emerged as critical in modulating stemness and lineage commitment in several precursor cell types, however, little is known in CPCs. NADPH oxidase (Nox)-derived reactive oxygen species (ROS) are key components of cardiac signaling and function. Therefore, I tested the hypothesis that CPCs marked by type III receptor tyrosine kinase c-kit (c-kit^{+}) exhibit a unique Nox signature that confers precursor status, and that alterations in this profile influence lineage specification. Dihydroethidium (DHE) microfluorography showed reduced basal ROS formation within early postnatal c-kit^{+} CPCs. Real-time quantitative PCR (qPCR) revealed downregulation of the ROS generator Nox2 and its subunit p67^{phox} in c-kit^{+} CPCs under basal conditions, but upregulation of Nox2 and Nox4 over the course of differentiation. Adenoviral silencing of Nox2 and Nox4 increased expression of CPC markers, c-kit and Flk-1, and blunted smooth and cardiac muscle differentiation, respectively. These changes were accompanied by altered expression of transcription factors, Gata6 and Gata4, and the cytokine, TGF-β1. In conclusion, c-kit^{+} CPCs exist in a low ROS state like other precursor cells, in part due to reduced Nox2 expression and increases in Nox2 and Nox4 are important for the differentiation of these cells into smooth and cardiac muscle, respectively. I speculate that these may be novel targets in CPCs which could prove useful in cell-based therapy of the heart.

INTRODUCTION

Owing in large part to the low regenerative capacity of the adult heart [1], coronary heart disease (CHD) remains one of the leading causes of death in the developed world. In 2007, CHD accounted for 1 out of every 6 deaths in the United States [2]. Evidence from directed differentiation of embryonic stem cells (ESCs) and in neonatal mice indicates a significant population of cardiac precursor cells (CPCs) at this developmental stage capable of generating the three lineages that specify the heart: smooth muscle, cardiac, and endothelial [3-6]. Unfortunately, the extent and capacity of adult CPCs [7] to cope with the loss of tissue following myocardial infarction or other damage is limited, suggesting that exogenous expansion and therapeutic delivery may be necessary to achieve substantial cardiac regeneration. Recently, it has been proposed that redox mechanisms play important roles both in maintaining stemness and in mediating lineage commitment of several precursor cell types [8, 9]. Collectively, these reports suggest that a more reduced environment is conducive to cell survival and cell division, while a more oxidized condition favors differentiation and/or apoptosis.

NADPH oxidase (Nox) enzymes are essential components of cardiac redox biology and generate reactive oxygen species (ROS) in a highly regulated manner [10, 11]. Unlike the neutrophil oxidases which release a large "respiratory burst" of superoxide to ward off pathogens, the Nox enzymes (Nox1, Nox2, and Nox4) generate lower levels of intracellular ROS which are necessary for cell signaling and survival [10]. Of these Nox homologues, Nox2 and Nox4 are most abundantly expressed in the myocardium [11]. While Nox2 and Nox4 knockout mice do not demonstrate defects in heart development [12, 13], likely due to compensatory mechanisms, recent evidence indicates that Nox2- and Nox4- derived ROS play critical roles in cardiovascular cell

function. Nox2 has been linked to neointimal remodeling and neovascularization after hindlimb ischemia as well as left ventricular remodeling following myocardial infarction [14-16], while Nox4 has been linked to enhanced myocardial capillary density upon pressure overload as well as increased expression of smooth muscle-specific genes during vascular formation from embryonic stem cells (ESCs) [12, 17]. The Nox enzymes also are implicated in cardiac cell differentiation. For example, Rac, a critical Nox subunit, was found to play an important role in early cardiomyogenesis by ESCs [18], while stimulation of peroxisome proliferator-activated receptor alpha (PPARα) is thought to enhance ESC-mediated cardiomyogenesis via pathways involving both ROS and Nox activity [19]. The majority of the studies implicating Nox-derived ROS in smooth muscle generation and cardiac differentiation have been performed in ESCs [17-21]. However, a recent study linking redox gene Ref-1 to the redox status of adult c-kit$^+$ cardiac stem cells and their commitment to the cardiac fate suggests that Nox regulation also might be a critical modulator of CPC function [22].

CPCs can be identified by their surface markers including Sca-1 (a member of the Ly-6 family) [23], Flk-1 (a receptor for vascular endothelial growth factor (VEGF)) [5], and c-kit (a type III receptor tyrosine kinase) [4, 6, 7]. Research from our laboratory and others demonstrates that c-kit identifies a mesodermally-derived cell population consisting of both precursors that co-express Flk-1 and cardiac cells co-expressing α-actinin in the very early stages of lineage commitment and development [4, 6]. When isolated from the early postnatal (PN) heart, c-kit$^+$ cells expand and differentiate *in vitro* into all three cardiac lineages and display morphological characteristics of nodal, atrial, and ventricular action potentials [6]. With an increased understanding of CPCs and their potential in cell-based therapies, elucidating the redox mechanisms that regulate CPC

function including the interplay between Nox-derived ROS and CPC lineage commitment is critical.

As such, the goal of this study was to test the hypothesis that c-kit$^+$ CPCs exhibit a unique Nox molecular signature that confers precursor status, and that alterations in this profile influence cardiac cell differentiation. Utilizing genetic tools to selectively manipulate the Nox enzymes of early postnatal c-kit$^+$ CPCs, my results demonstrate that Nox2 and Nox4 modulate the balance between c-kit$^+$ cell precursor and differentiation status. I found that silencing Nox2 and Nox4 blunts the differentiation of c-kit$^+$ CPCs along the smooth muscle and cardiac lineages, while simultaneously increasing the expression of early precursor cell markers and altering the expression of transcription factors and cytokines necessary for cardiac lineage specification. I speculate that these redox genes, along with others identified by mRNA PCR arrays, will provide novel targets for improving the regenerative capacity of c-kit$^+$ CPCs, which eventually may be integrated into cell-based therapies for myocardial infarction.

MATERIALS AND METHODS

Animals

Bacterial artificial chromosome (BAC) transgenic mice in which enhanced green fluorescent protein (EGFP) is a transcriptional indicator of c-kit promoter activity (c-kit^{BAC}-EGFP) and their wildtype (WT) C57BL/6 littermates (ages postnatal (PN) 0-4) were utilized for these studies [6]. C-kit^{BAC}-EGFP heterozygote and homozygote transgenic mice were obtained from in-house colonies and bred. C-kit^{BAC}-EGFP newborns (PN0-4) were screened for EGFP expression using a KL2500 cold light source (Leica) with safety glasses covered with Wratten filter #12 (Kodak). All procedures involving the use of animals were approved by the Institutional Animal Care and Use Committee at Weill Cornell Medical College in New York, NY and met the standards set forth by the NIH *Guide for the Care and Use of Laboratory Animals*, United States Department of Agriculture regulations, and the American Veterinary Medical Association Panel on Euthanasia.

Cell Isolation and Fluorescence Activated Cell Sorting (FACS)

Cardiac c-kit^{+} cells from PN0-4 heterozygote c-kit^{BAC}-EGFP pups, hereafter referred to as "freshly isolated c-kit^{+} cells," or total cardiomyocytes from age-matched WT littermates, hereafter referred to as "control cardiomyocytes," were dispersed using a modified version of Worthington's Neonatal Cardiomyocyte Isolation System and isolated by flow cytometry [6, 24]. FACS was undertaken using a Becton-Dickinson FACSVantage SE at the Flow Cytometry Facility at the Hospital for Special Surgery in New York, NY. For sorting, cells were resuspended in a DMEM medium (Gibco) without phenol red containing Stasis^{TM} Stem Cell Qualified U.S. Origin Fetal Bovine Serum (2%, Gemini Bio-Products) and sorted into an F12K

Nutrient Mixture, Kaighn's Modification medium (see Culturing Conditions Section) with 20% FBS. Cells were sorted under 13 psi sheath pressure through a 70 μm nozzle. Cells were gated into a parent population using a side scatter area vs. forward scatter area plot. This parent population was then gated to include only single cells using a side scatter width vs. side scatter area plot. Finally, $EGFP^+$ cells were identified using a 488 nm excitation laser and two bandpass filters (fluorescein isothiocyanate (FITC) 530/30 and phycoerythrin (PE) 575/26). Total $EGFP^+$ (tEGFP) cells were effectively separated from autofluorescing cells using a final plot, FITC area vs. PE area [6]. Total cardiomyocytes from age-matched WT littermates were sorted under identical conditions and served as control cells.

Culturing Conditions

Immediately after FACS, freshly isolated c-kit^+ cells were seeded onto Lab-Tek™ II 4-well chamber slides (Nunc) and cultured in a F12K Nutrient Mixture, Kaighn's Modification medium (Gibco) containing Stasis™ Stem Cell Qualified U.S. Origin Fetal Bovine Serum (5%, Gemini Bio-Products), bFGF (10 ng/ml, Invitrogen), LIF (10ng/ml, Millipore), and Pen Strep (1%, Gibco) [6]. For the Nox differentiation timecourse, freshly isolated c-kit^+ cells were cultured in the F12K medium for 3 days and then switched to a Dulbecco's Modified Eagle Medium: Nutrient Mixture F-12 (DMEM/F-12) Media (Gibco) supplemented with B27 (2%, Invitrogen), bFGF (10 ng/ml), LIF (10 ng/ml), EGF (20 ng/ml, Invitrogen), and Pen Strep (1%) [6]. Cells were incubated in a NAPCO Series 8000 DH CO2 incubator (95% air/5% CO2) at 37 ºC and media was changed every 3-4 days.

ROS Detection

ROS production was assessed using dihydroethidium (DHE) as an indicator. For *in vitro* ROS detection, c-kit^{+} cells were cultured at low density for 48 hours. At this time, cell media was aspirated and cells were rinsed twice with warmed DPBS (Gibco). Cells were then treated with 2.5 µM DHE (Invitrogen) dissolved in DMSO and diluted in DPBS for 30 minutes at 37 ºC in the dark. Following DHE application, cells were rinsed for 5 minutes and coverslipped using Aqua-Mount (Fisher Scientific). Coverslipped cells were imaged the same day using an Orca-ER B/W camera (Hamamatsu Photonics) connected to a Zeiss Axioplan 2 microscope. DHE fluorescence intensity was quantified using NIH ImageJ software and expressed relative to c-kit^{+} cells [25]. Background fluorescence was subtracted from the red and green channels. Next, the cell was identified in the green channel and traced using the elliptical function. This selection was then restored onto the corresponding red channel image and pixel number was measured. C-kit^{+} cells were identified as those with bright EGFP fluorescence compared to non-c-kit expressing cells within the same well [26]. This process was repeated for each field. In total, approximately 12 fields were analyzed (3 fields/well) for each of the 3 biological replicates.

For *in vivo* DHE microfluorography [27, 28], PN0-1 homozygote c-kit^{BAC}-EGFP pups were anesthetized using hypothermia [29] for 3 minutes and injected with DHE (10 µl I.P.; 4 mg/ml; dissolved in DMSO and diluted in sterile saline) using a 30 G needle. After a 1.5-2 hour incubation period on a warming pad, pups were euthanized and the heart tissue was harvested. Heart tissue was fixed for exactly 1 hour in 4% PFA at 4 ºC and dehydrated overnight in 20% sucrose. Hearts were embedded in OCT and cryosectioned at 8 µm. Sections were coverslipped using Vectashield mounting media for fluorescence (Vector) and imaged the same day on a LSM 5 Live confocal microscope (Zeiss). DHE fluorescence intensity was quantified as above except

3 directly neighboring c-kit$^-$ cells were used for the comparison and areas of the tissue remote to the c-kit$^+$ clusters were used to account for autofluorescence. Approximately 5-10 sections per neonatal heart were analyzed from a total of 5 biological replicates.

Real-time Quantitative PCR (qPCR)

RNA was harvested from freshly isolated c-kit$^+$ cells and control cardiomyocytes directly after FACS or cultured c-kit$^+$ cells using an optimized version of the TRIzol (Invitrogen) protocol to increase precipitation time in isopropanol. 1-2 randomly selected samples from each RNA batch were assigned RIN values by an Agilent 2100 bioanalyzer to determine RNA integrity and all samples were reverse transcribed into cDNA using a TaqMan Reverse Transcription Kit (Applied Biosystems) and the cycling parameters provided by the manufacturer. qPCR was performed using 8-20 ng of RNA template per well, PerfeCTa SYBR Green FastMix (Quanta), gene specific primers (Table 3.1), and an iQ5 Cycler (Bio-Rad) as described [30]. Cycling parameters were as follows: 10 minutes at 95 ºC; 40 x [15 seconds at 95 ºC, 1 minute at 60 ºC]. All primers (Table 3.1) were verified by standard and melt curve analyses using RNA isolated from ESCs, control cardiomyocytes, and/or PN4 wildtype hearts. Values were normalized to β-actin mRNA expression.

Adenoviral Vectors

Recombinant E1-deleted adenoviral vectors (human Ad serotype 5) encoding siRNA targeted against Nox2 (AdsiNox2), Nox4 (AdsiNox4), and EGFP (AdsiCON) have been described and characterized previously [30-33]. For all adenoviral knockdown studies, c-kit$^+$ cells were infected on Day 7 of culture (100 pfu/cell, Figures 3.1A-B) and RNA was isolated (see qPCR Section),

Table 3.1. Primers Used in this Study.

Transcript from Gene	Gene Bank Accession Number	Forward primer (5' → 3')	Reverse Primer (5' → 3')
Acta2 (α-SMA)	NM_007392	ATTGTGCTGGACTCTGGAGATGGT	TGATGTCACGGACAATCTCACGCT
B-actin	NM_007393	CATCCTCTTCCTCCCTGGAGAAGA	ACAGGATTCCATACCCAAGAAGGAAGG
C-kit	NM_021099	TCATCGAGTGTGATGGGAAA	GGTGACTTGTTTCAGGCACA
Cat	NM_009804	AGCGACCAGATGAAGCAGTG	TCCGCTCTCTGTCAAAGTGTG
Cygb	NM_030206	CCGGGCGACATGGAGATAGA	GTCCTCGCAGTTGGCATACAG
Gata4	NM_008092	GAAAACGGAAGCCCAAGAACC	TGCTGTGCCCATAGTGAGATGAC
Gata6	NM_010258	TTGCTCCGGTAACAGCAGTG	GTGGTCGCTTGTGTAGAAGGA
Gpx4	NM_008162	GTGTGCATCCCGCGATGATT	CCCCTGTACTTATCCAGGCAGA
Kdr (Flk-1)	NM_010612	TTTGGCAAATACAACCCTTCAGA	GCAGAAGATACTGTCACCACC
Klf4	NM_010637	GGTGCAGCTTGCAGCAGTAA	AAAGTCTAGGTCCAGGAGGTCGTT
Ncf2 ($p67^{phox}$)	NM_010877	AGCTTCTGCTCCTGTCCGAAGAAA	AATAAGACCTTGGTCACCCACCGT
Nox1	NM_172203	CGTGATTACCAAGGTTGTCATGCAC	GATGCCACTCCAGGAAGGAAATGGA
Nox2	NM_007807	TTCCAGTGCGTGTTGCTCGAC	GATGGCGGTGTGCAGTGCTAT
Nox4	NM_015760	GGATCACAGAAGGTCCCTAGCAG	GCGGCTACATGCACACCTGAGAA
Prdx2	NM_011563	GGCAACGCAAATCGGAAAG	TCCAGTGGGTAGAAAAAGAGGA
Prdx3	NM_007452	GGTTGCTCGTCATGCAAGTG	CCACAGTATGTCTGTCAAACAGG
Prdx6	NM_007453	CGCCAGAGTTTGCCAAGAG	TCCGTGGGTGTTTCACCATTG
Sod1	NM_011434	AACCAGTTGTGTCAGGAC	CCACCATGTTTCTTAGAGTGAGG
Sod2	NM_013671	CAGACCTGCCTTACGACTATGG	CTCGGTGGCGTTGAGATTGTT
Sod3	NM_011435	GGTTGAGAAGATAGGCGACAC	CGTGGCTGATGGTTGTACC
Tgfb1	NM_011577	GATCCTGTCCAAACTAAGGCTC	ACCTCTTTAGCATAGTAGTCCGC
Tnnt2 (cTnT)	NM_011619	CAGAGGAGGCCAACGTAGAAG	CTCCATCGGGGATCTTGGGT
Vegfa	NM_009505	CTTGTTCAGAGCGGAGAAAGC	CATCTGCAAGTACGTTCGTTT
Vwf	NM_011708	CTTCTGTACGCCTCAGCTATG	GCCGTTGTAATTCCCACACAAG

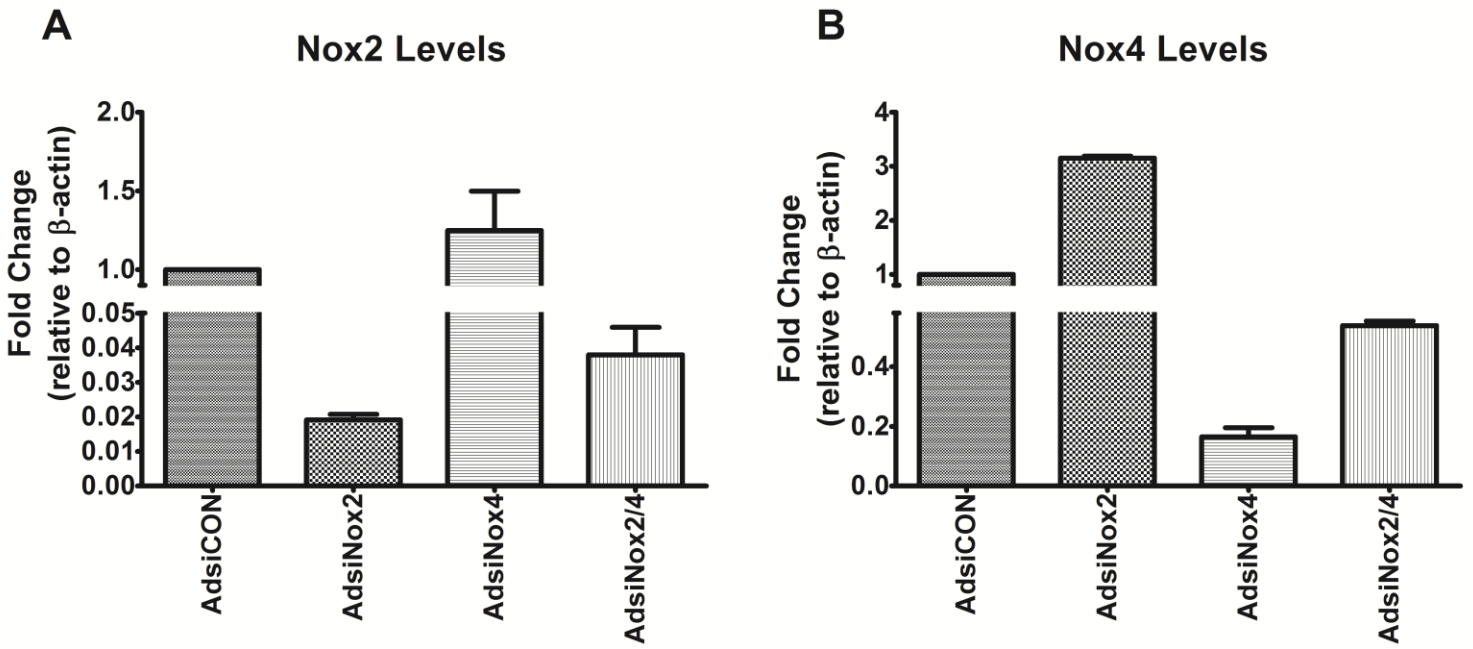

Figure 3.1. Nox2 and Nox4 Transcript Levels by qPCR (Nox knockdown verification).

(A) Nox2 and (B) Nox4 transcript levels analyzed by qPCR in c-kit^{+} cells isolated from PN0-4 heterozygote c-kit^{BAC}-EGFP pup hearts and infected with AdsiCON, AdsiNox2, AdsiNox4, or AdsiNox2/4 for 48 hours. n=3/group. Gene expression was normalized to β-actin.

protein was harvested (see Western Immunoblot Section), or cells were fixed for immunocytochemistry (see Immunocytochemistry Section) on Day 14. All adenoviral vectors were obtained from the Iowa Gene Transfer Vector Core.

Western Immunoblot

C-kit protein levels were assessed by Western immunoblot performed on c-kit^{+} cells isolated from PN0-4 heterozygote c-kit^{BAC}-EGFP pup hearts and infected with AdsiCON, AdsiNox2, AdsiNox4, or AdsiNox2/4 utilizing SDS-PAGE. Samples were incubated with polyclonal rabbit anti-c-kit antibody (sc-168, Santa Cruz Biotechnology, Inc.; 1:100 in TBS with 3% BSA and .1% Tween-20) followed by goat anti-rabbit HRP (sc-2030, Santa Cruz Biotechnology, Inc.; 1:10,000) and subjected to chemiluminescence. Band intensity was quantified by densitometry using NIH ImageJ and normalized to GAPDH loading controls.

Immunocytochemistry

C-kit^{+} cells cultured on Lab-Tek™ II 4-well chamber slides (Nunc) and treated with adenovirus (AdsiCON, AdsiNox2, and/or AdsiNox4) were fixed in 4% PFA for 25 minutes at room temperature (RT) and washed 3 times with DPBS (Gibco). Cells were stored at 4 ºC in DPBS until immunocytochemistry was performed.

For primary antibodies monoclonal mouse anti-α-SMA (1:15, Dako, M0851) [6] and monoclonal mouse anti-cTnT (1:150, Thermo Scientific, MS-295-P0) [6] the following protocol was followed. Cells were permeabilized for 15 minutes with .05% Triton-X (Fisher Scientific) in TBS (Bio-Rad) and blocked for 1.5 hours with Mouse Ig Blocking Reagent (M.O.M. Immunodetection Kit,

Vector Laboratories) followed by 10% normal donkey serum (Millipore) for 30 minutes at RT. After a quick wash with TBS, primary antibodies were diluted in M.O.M. Diluent (M.O.M. Immunodetection Kit, Vector Laboratories) and applied overnight at 4 ºC in a humidified chamber. Cells were then washed 3 times with TBS and incubated with AlexaFluor 594 donkey anti-mouse IgG (1:200, Invitrogen) diluted in M.O.M. Diluent for 1 hour at RT. After secondary incubation, cells were washed 4 times with TBS. Stained cells were then mounted with Vectashield mounting media with DAPI for fluorescence (Vector) and quantified. The percent of positive cells in each condition was determined and expressed fold AdsiCON. A "no primary antibody" control was utilized to determine specificity. Images were obtained using a Retiga 1300i camera (QImaging) connected to a Nikon Eclipse 80i microscope. Three biological samples were evaluated.

For primary antibody polyclonal rabbit anti-Ki67 (1:100, Abcam, ab15580) the following protocol was followed. Cells were permeabilized for 15 minutes with .2% Triton-X in TBS and washed 2 times for 2 minutes each with TBS. Cells were then blocked in 10% normal donkey serum for 1 hour and 15 minutes at RT. After a quick wash, the primary antibody was diluted in .05% Triton-X/1% normal donkey serum/1% normal mouse serum (Jackson ImmunoResearch Laboratories) in TBS for 1 hour at RT. Cells were then washed 4 times with TBS and incubated with AlexaFluor 594 donkey anti-rabbit IgG (1:100, Invitrogen) diluted in .05% Triton-X in TBS for 45 minutes at RT. After secondary incubation, cells were washed 4 times with TBS. Stained cells were then mounted with Vectashield mounting media with DAPI for fluorescence (Vector) and imaged using a Retiga 1300i camera (QImaging) connected to a Nikon Eclipse 80i microscope. The percent of positive cells in each condition was determined. A "no primary

antibody" control was utilized to determine specificity. Three biological samples were evaluated.

RT^2 Profiler PCR Arrays

Directly following FACS, RNA was isolated from freshly isolated c-kit$^+$ cells and control cardiomyocytes using an optimized version of the TRIzol (Invitrogen) protocol to increase precipitation time in isopropanol. RNA was pooled from 2 independent cell sorts to accumulate 1000 ng total RNA and assigned RIN values by an Agilent 2100 bioanalyzer. cDNA first was synthesized using the RT^2 First Strand Kit and then added to the RT^2qPCR Master Mix according to manufacturer's instructions (Qiagen-SABiosciences). The mixture was aliquoted across the PCR Array plates and thermal cycling was performed (see qPCR Section). Data was analyzed using the RT^2 Profiler PCR Array Data Analysis Template available on the manufacturer's website.

Statistical Analysis

Results are expressed as mean ± SEM. Data were analyzed by Student's *t* test for comparisons between two groups, or ANOVA followed by the Tukey post-test for multiple comparisons. Statistical analyses were performed using Prism (GraphPad Software, Inc.).

RESULTS

C-kit$^+$ CPCs Exhibit Reduced ROS Levels In Vitro and In Vivo

Emerging data indicate that some precursor cell types reside in relatively low ROS niches to maintain their stemness [34-36]. To determine the intracellular ROS profile of c-kit$^+$ CPCs *in vitro* and *in vivo*, I utilized DHE microfluorography. As shown in representative images (Figures 3.2A-B) and in summary (Figure 3.2C), there was a significant decrease in DHE fluorescence intensity in early postnatal c-kit$^+$ CPCs compared to c-kit$^-$ cells (2.15-fold, $p<0.05$). To rule out the possibility that cell isolation and culturing conditions altered the physiological redox state of c-kit$^+$ CPCs, I also utilized *in vivo* DHE microfluorography to measure ROS levels of c-kit$^+$ CPCs within the intact left ventricular myocardium of c-kit^{BAC}-EGFP neonates. Similar to my observations from the *in vitro* study, representative DHE microfluorography confocal images (Figures 3.2D-E) and summary data (Figure 3.2F) revealed a significant decrease in ROS levels in ventricular c-kit$^+$ CPCs compared to neighboring c-kit$^-$ cells (1.84-fold, $p<0.05$). Taken together, these results demonstrate reduced ROS formation within c-kit$^+$ CPCs.

Nox2 is Selectively Downregulated in Freshly Isolated C-kit$^+$ CPCs and is Upregulated Along with Nox4 Over the Course of Differentiation

Given the importance of Nox enzymes in cardiac ROS generation and signaling [10, 11], I utilized qPCR to profile basal transcript levels of Nox1, 2, and 4, along with a subset of their subunits, in freshly isolated early postnatal c-kit$^+$ and control cells. As shown in Figure 3.3A, Nox1 and Nox4 were expressed at low but detectable levels, but showed no difference in expression between control cardiomyocytes and freshly isolated c-kit$^+$ CPCs (1.45-fold and 1.52-fold,

Figure 3.2. C-kit^{+} CPCs Exhibit Reduced ROS Levels *In vitro* and *In vivo*. (A) Representative green fluorescent image of a c-kit^{+} cell (white arrow) and three c-kit^{-} cells (white inverted triangles) isolated from PN0-4 heterozygote c-kit^{BAC}-EGFP pup hearts and cultured for 48 hours; scale bar = 20μm. (B) Red fluorescent image from same field demonstrating that the c-kit^{+} cell (white arrow) shows lower DHE fluorescence intensity than the c-kit^{-} cells (white inverted triangles); scale bar = 20μm. (C) Summary of *in vitro* DHE fluorescence intensity in c-kit^{-} and c-kit^{+} cells (3 separate experiments). (D) Green fluorescent image of c-kit^{+} cells (white arrows) residing in the left ventricular myocardium of PN0 homozygote c-kit^{BAC}-EGFP pup hearts. (E) Corresponding red fluorescent image from same field demonstrating that the c-kit^{+} cells (white arrows) show lower DHE fluorescence intensity than neighboring c-kit^{-} cells. (H) Summary of *in vivo* DHE fluorescence intensity in neighboring c-kit^{-} cells and c-kit^{+} cells (n=5 neonates). Numbers of cells analyzed in each experiment are depicted on the bars; *$p<0.05$ vs. c-kit^{+} cells.

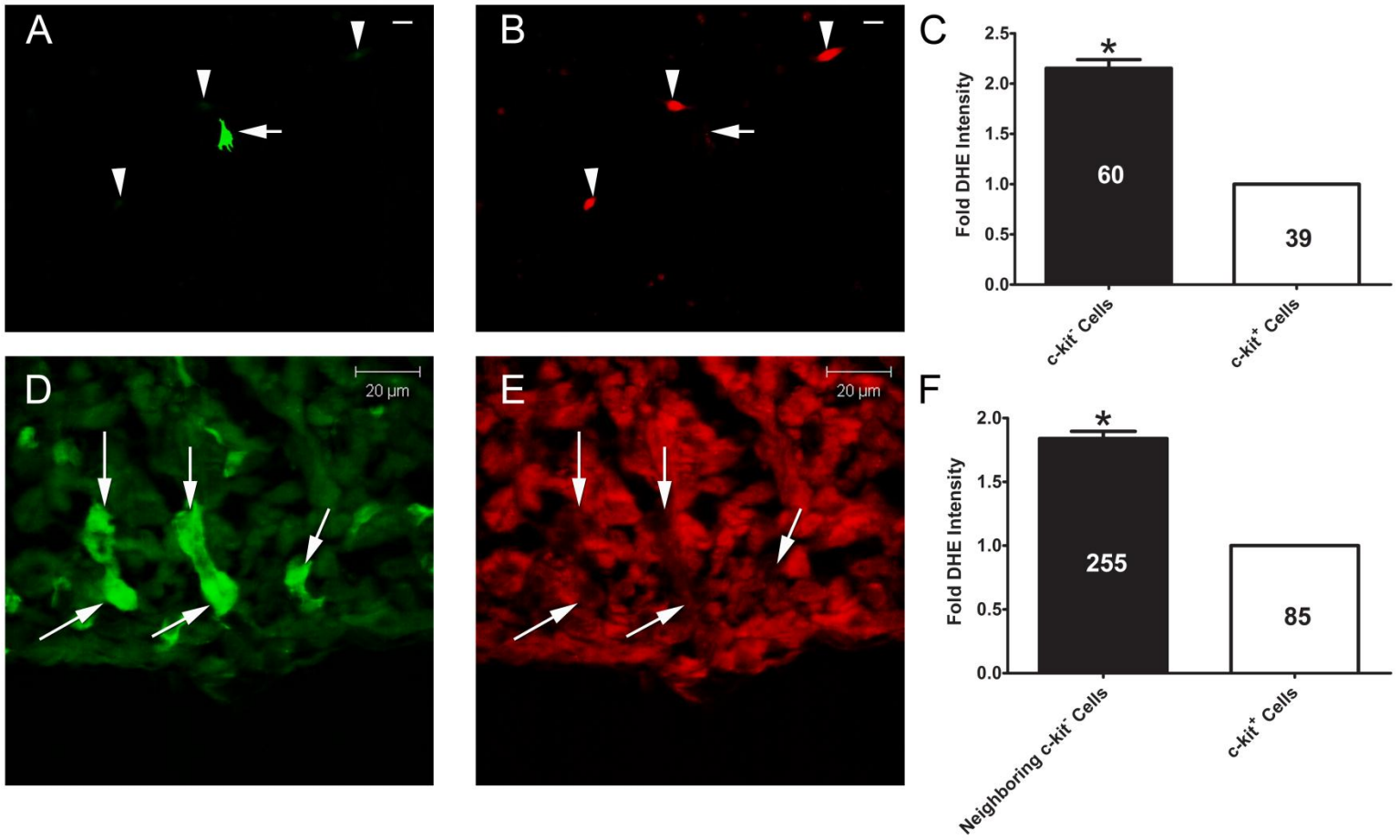
A
B
C
D
E
F
20 µm
20 µm
Fold DHE Intensity
2.5
2.0
1.5
1.0
0.5
0.0
*
60
39
c-kit⁻ Cells
c-kit⁺ Cells
Fold DHE Intensity
2.0
1.5
1.0
0.5
0.0
*
255
85
Neighboring c-kit⁻ Cells
c-kit⁺ Cells

respectively, $p>0.05$). Moreover, two subunits required for Nox1 activity, NoxA1 and NoxO1, displayed no difference in expression between the groups (1.26-fold and 1.33-fold, respectively, $p>0.05$; Figure 3.3B). Similarly, $p22^{phox}$, a subunit utilized by all three of the cardiac Nox enzymes and the only subunit necessary for Nox4 activity [11], was unchanged between c-kit$^+$ and control cells (1.06-fold, $p>0.05$; Figure 3.3B). Interestingly, Nox2 was expressed at markedly higher levels than Nox1 and Nox4 in control cardiomyocytes, consistent with previous reports for primary rat neonatal cardiomyocytes [32], however freshly isolated c-kit$^+$ CPCs showed a dramatic reduction in basal Nox2 expression compared to control cardiomyocytes (12.0-fold, $p<0.05$; Figure 3.3A). Expression of $p67^{phox}$, a critical player in Nox2 activity [11], also was reduced significantly in freshly isolated c-kit$^+$ CPCs compared to controls (2.71-fold, $p<0.05$; Figure 3.3B). Together, these data reveal marked downregulation of the potent ROS generator Nox2 and its critical subunit $p67^{phox}$ in freshly isolated c-kit$^+$ CPCs, which may contribute to the low ROS levels observed in these cells (see Figure 3.2).

Having identified a unique basal Nox expression profile in freshly isolated c-kit$^+$ CPCs, next I examined whether Nox enzyme expression was induced upon differentiation as has been reported for ESCs [20, 21, 37] and adult cardiac stem cells [22]. C-kit$^+$ CPCs were cultured for 3, 9, or 14 days and Nox enzyme expression was profiled by qPCR as above. As seen in Figure 3.3C, Nox1 transcript levels remained low, but detectable, and did not change significantly throughout the differentiation time-course. Similar to basal expression data, Nox2 transcript levels were low and remained so at Days 3 and 9, however by Day 14 there was a marked upregulation of this Nox homologue (8.96-fold vs. Day 3 and 12.18-fold vs. Day 9, $p<0.05$). Nox4 exhibited a gradual increase in expression over time, and by Day 14 (5.21-fold vs. Day 3, $p<0.05$) was

Figure 3.3. Nox2 is Selectively Downregulated in Freshly Isolated C-kit$^+$ CPCs and is Upregulated Along with Nox4 Over the Course of Differentiation. (A) Summary of basal Nox homologue and (B) a subgroup of Nox subunit mRNA levels analyzed by qPCR in control cardiomyocytes and freshly isolated c-kit$^+$ cells. n=6/group for Nox homologues, n=3/group for Nox subunits; *$p<0.05$ vs. control cardiomyocytes; †$p<0.05$ vs. Nox1 and Nox4. (C) Transcript levels of Nox1, 2, and 4 in c-kit$^+$ cells cultured for 3, 9, and 14 days. n=4/group; * $p<0.05$ vs. Day 3, † $p<0.05$ vs. Day 9. Gene expression was normalized to β-actin.

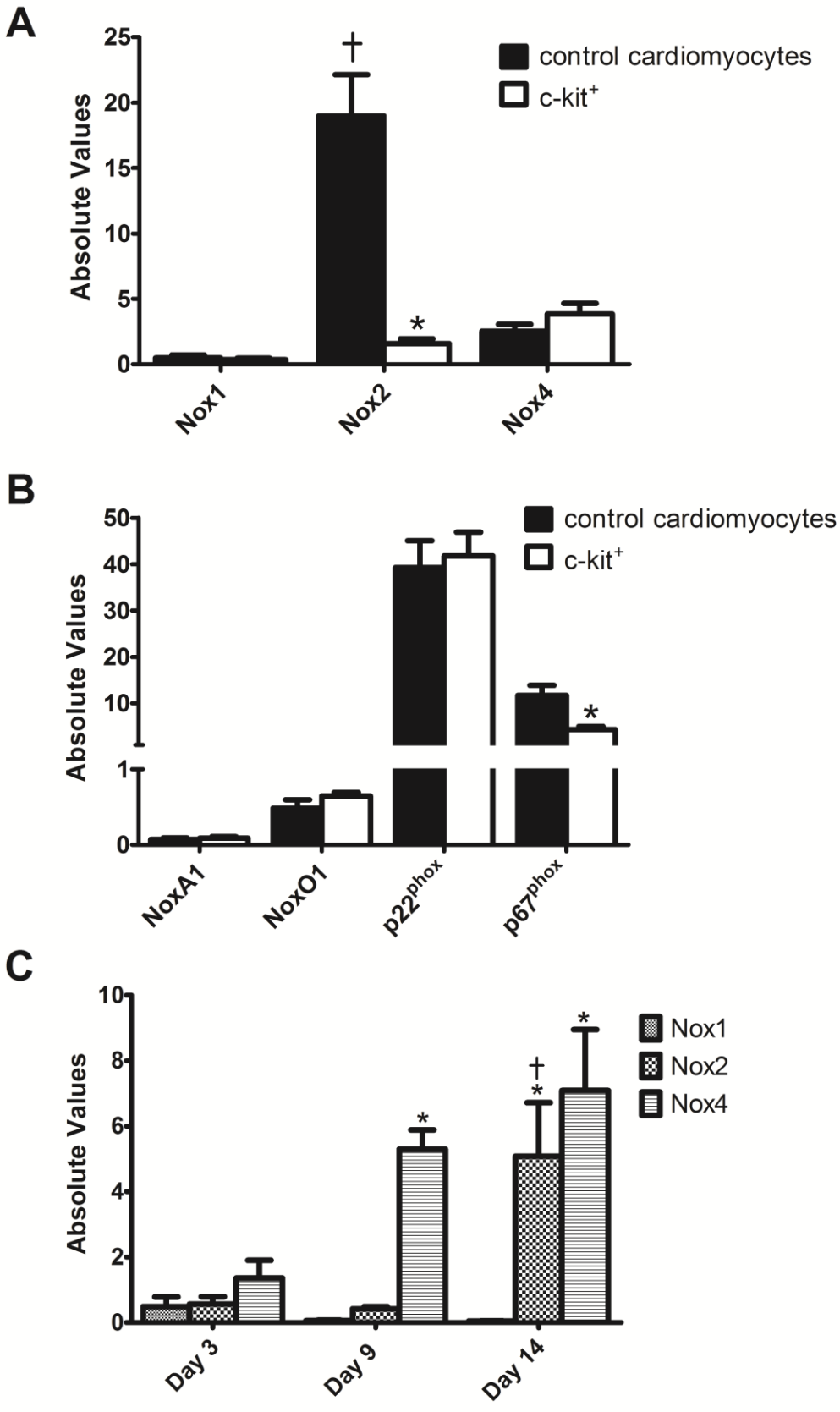
A
Absolute Values
25
20
15
10
5
0
†
*
control cardiomyocytes
c-kit+
Nox1
Nox2
Nox4
B
Absolute Values
50
40
30
20
10
1
0
*
control cardiomyocytes
c-kit+
NoxA1
NoxO1
p22phox
p67phox
C
Absolute Values
10
8
6
4
2
0
*
†
*
Nox1
Nox2
Nox4
Day 3
Day 9
Day 14

similar to Nox2 expression. Together, these findings demonstrate that Nox2 and Nox4 are upregulated in a time-specific manner over the course of c-kit^{+} CPC differentiation, suggesting they may be involved in ROS-mediated cardiac lineage commitment.

Targeted Silencing of Nox2 and Nox4 Alters C-kit^{+} Precursor and Lineage Commitment Status

To determine if Nox2 and Nox4 are functionally linked to c-kit^{+} precursor cell status and/or cardiac cell differentiation *in vitro*, I utilized adenoviruses encoding U6 promoter-driven siRNAs targeted to Nox2 (AdsiNox2) or Nox4 (AdsiNox4) previously established in our laboratory [30, 32, 33]. Importantly, our laboratory has demonstrated that these viruses efficiently and selectively silence Nox2 and Nox4, respectively, in cultured cardiomyocytes and *in vivo* [30, 32, 33] as well as in neonatal c-kit^{+} CPCs (Figures 3.1A-B). C-kit^{+} CPCs isolated from early postnatal c-kit^{BAC}-EGFP hearts were infected with one or both of these adenoviruses or a control virus (AdsiCON) and expression of several cardiac precursor (c-kit and Flk-1) [5-7] and differentiation genes (α-Smooth Muscle Actin, α-SMA; cardiac Troponin T, cTnT; endothelial Von Willebrand Factor, vWF) [6, 7] were analyzed by qPCR.

As shown in Figure 3.4A, c-kit^{+} CPCs infected with AdsiNox2 exhibited a significant increase in precursor genes c-kit and Flk-1 (10.27-fold and 14.27-fold, respectively, $p<0.05$) compared to cells infected with a control siRNA (AdsiCON). This was accompanied by a marked downregulation of α-SMA (4.02-fold, $p<0.05$), but no effect on cTnT or vWF transcript levels (Figure 3.4D). Interestingly, cells infected with AdsiNox4 also demonstrated a significant increase in one of the stemness markers (Flk-1, 12.12-fold, $p<0.05$), and in these cells there was

Figure 3.4. Targeted Silencing of Nox2 and Nox4 Increases Expression of Cardiac Precursor Genes and Decreases Expression of Specific Differentiation Genes. (A-C) Transcript levels for stemness genes c-kit and Flk-1 and (D-F) differentiation genes α-SMA, cTnT, and vWF analyzed by qPCR in c-kit^{+} cells isolated from PN0-4 heterozygote c-kit^{BAC}-EGFP pup hearts and infected with AdsiCON, AdsiNox2, AdsiNox4, or AdsiNox2/4. qPCR was performed 7 days post-infection. n=4-5/group; *$p<0.05$ vs. AdsiCON. Gene expression was normalized to β-actin.

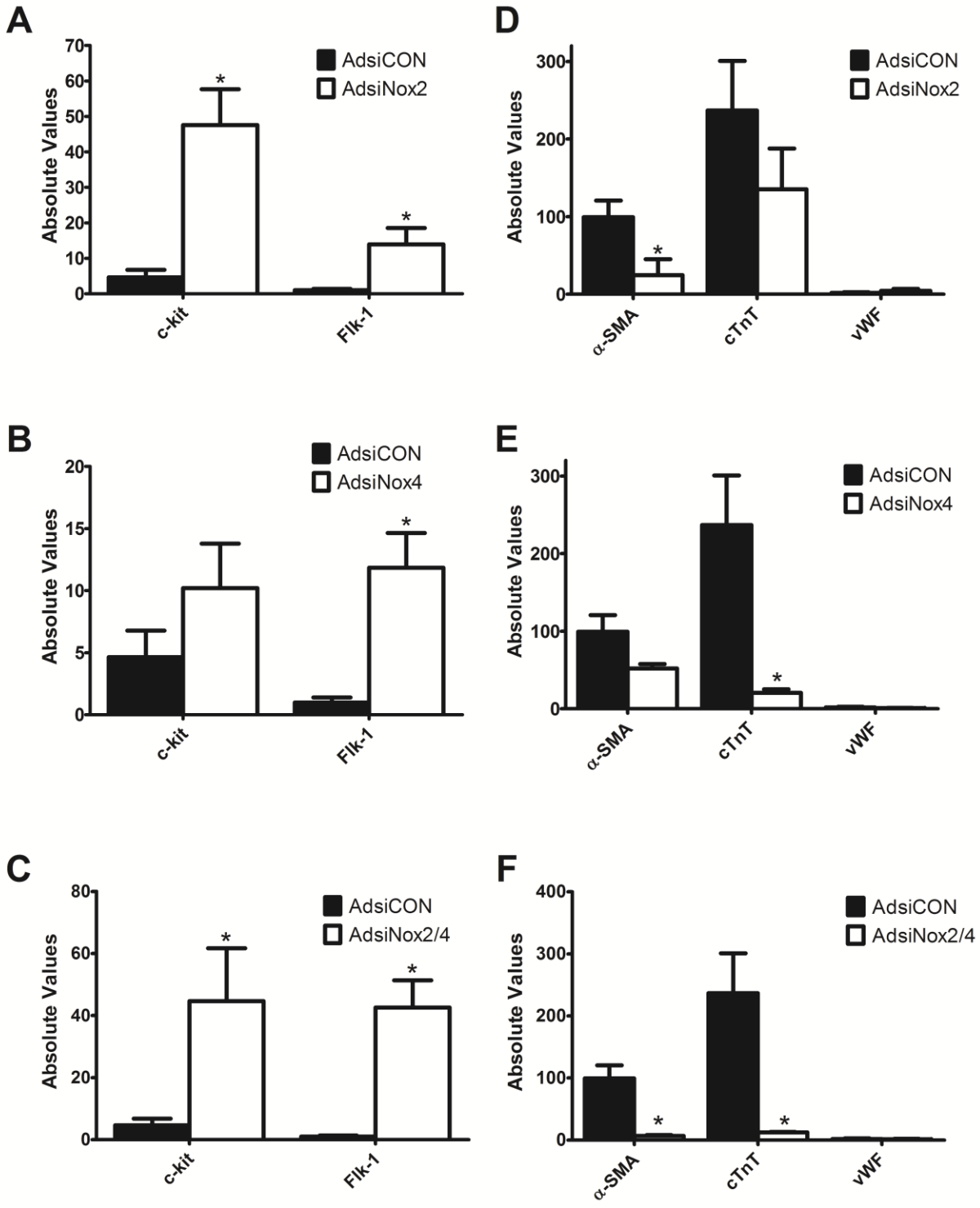
A
Absolute Values
70
60
50
40
30
20
10
0
AdsiCON
AdsiNox2
*
*
c-kit
Flk-1
D
Absolute Values
300
200
100
0
AdsiCON
AdsiNox2
*
α-SMA
cTnT
vWF
B
Absolute Values
20
15
10
5
0
AdsiCON
AdsiNox4
*
c-kit
Flk-1
E
Absolute Values
300
200
100
0
AdsiCON
AdsiNox4
*
α-SMA
cTnT
vWF
C
Absolute Values
80
60
40
20
0
AdsiCON
AdsiNox2/4
*
*
c-kit
Flk-1
F
Absolute Values
400
300
200
100
0
AdsiCON
AdsiNox2/4
*
*
α-SMA
cTnT
vWF

a corresponding and selective decrease in cTnT (11.48-fold, $p<0.05$) with no changes observed in the other differentiation markers compared to control treatment (Figures 3.4B and 3.4E). Finally, co-infection of c-kit$^+$ CPCs with AdsiNox2 and AdsiNox4 triggered a marked increase in both of the precursor genes c-kit and Flk-1 (9.65-fold and 43.63-fold, respectively, $p<0.05$) compared to AdsiCON (Figure 3.4C). This was accompanied by marked decreases in both α-SMA (14.20-fold, $p<0.05$) and cTnT (18.79-fold, $p<0.05$) transcript levels, but still no effect on the endothelial marker vWF (Figure 3.4F). Interestingly, another gene utilized for the induction of pluripotent stem cells, Klf4 [38], was found to be expressed at detectable levels in c-kit$^+$ cells treated with control virus (AdsiCON), but was unaltered upon knockdown of Nox2 and/or Nox4 (data not shown).

Because mRNA levels of vWF were low and unaltered in each of the experiments, I also investigated expression of VEGF-A, a growth factor critical for endothelial cell differentiation and proliferation [39, 40]. I found that VEGF-A was expressed at detectable levels in c-kit$^+$ CPCs, however, no changes in transcript levels were observed upon silencing of Nox2 and/or Nox4 (Figure 3.5A). In addition, I sought to verify that viral silencing of the Nox enzymes, either separately or in combination, did not alter cell proliferation when compared to cells transduced with the control vector. As seen in Figures 3.6A-C, there were no differences in expression of the cell proliferation marker Ki67 in any of the virus treatment groups compared to AdsiCON-treated c-kit$^+$ CPCs.

To further verify these findings and validate the mRNA data observed with Nox isozyme silencing, I next performed a series of western immunoblot and immunocytochemistry

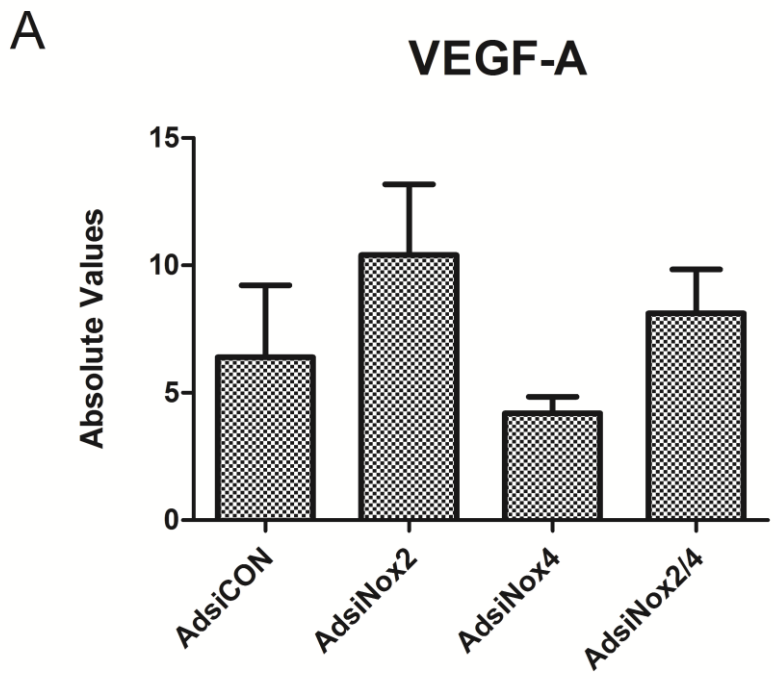

Figure 3.5. Targeted Silencing of Nox2 and Nox4 does not Alter VEGF-A Expression. (A) VEGF-A transcript levels analyzed by qPCR in c-kit^{+} cells isolated from PN0-4 heterozygote c-kit^{BAC}-EGFP pup hearts and infected with AdsiCON, AdsiNox2, AdsiNox4, or AdsiNox2/4 for 7 days. n=3-5/group. No significant differences were observed between the groups; $p>0.05$ vs. AdsiCON. Gene expression was normalized to β-actin.

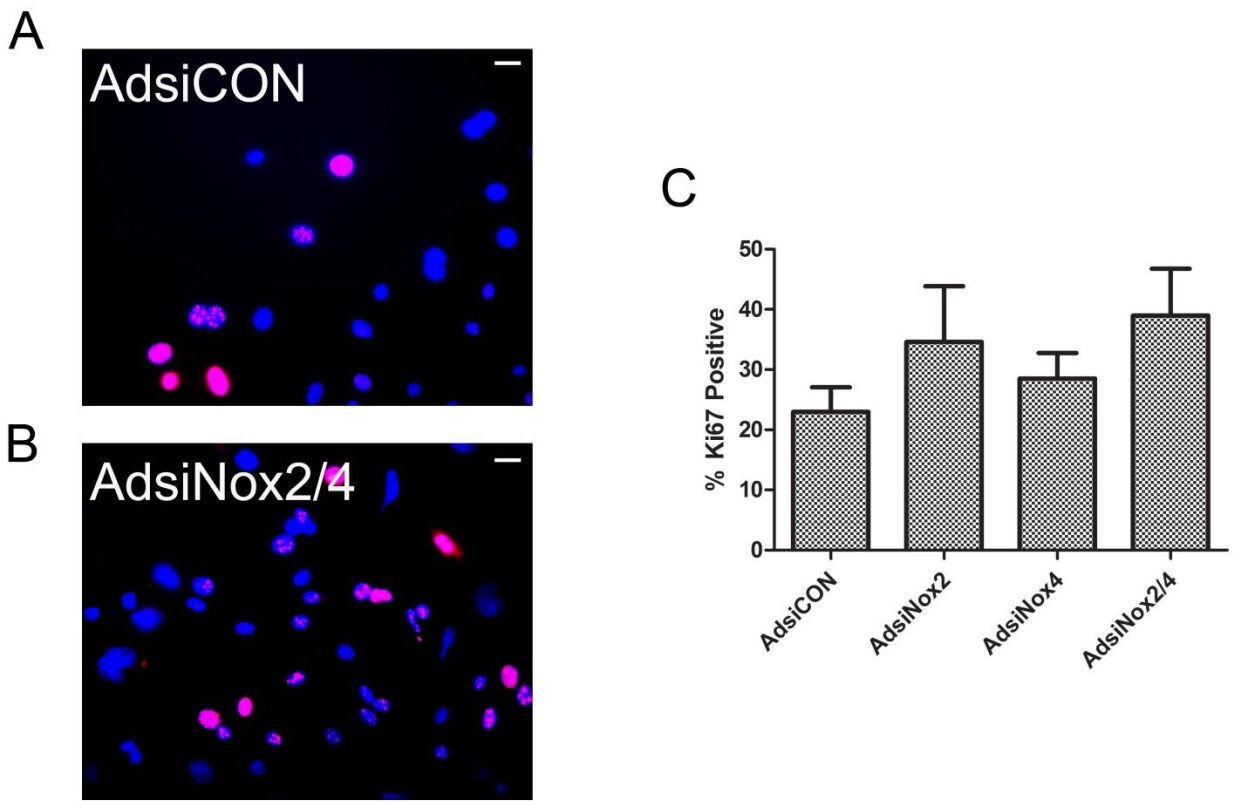

Figure 3.6. Targeted Silencing of Nox2 and Nox4 does not Alter Cell Proliferation. Representative images of Ki67 immunocytochemistry in DAPI-stained c-kit^{+} cells isolated from PN0-4 heterozygote c-kit^{BAC}-EGFP pup hearts and treated with (A) AdsiCON and (B) AdsiNox2/4 for 7 days; scale bar = 10µm. (C) Summary of percent of total cells positive for Ki67 at Day 7 following viral transduction. No significant differences were observed between the groups. 3 independent experiments were analyzed comprising ≥200 cells/condition; $p>0.05$ vs. AdsiCON.

experiments. As shown in Figure 3.7A, I observed significant increases in total c-kit protein after either AdsiNox2 (2.54-fold, $p=0.05$) and AdsiNox4 (2.48-fold, $p<0.05$) alone or in combination (4.31-fold, $p=0.05$) compared to AdsiCON. I also examined the percent of cells expressing either α-SMA or cTnT using immunocytochemistry. Importantly, the proportions of control cells expressing differentiation markers α-SMA and cTnT (Figures 3.7D-3.7E) were similar to our laboratory's previous report [6]. As shown in representative images (Figures 3.7B-C) and summary graphs (Figures 3.7D-E), and in line with my mRNA data, significant reductions in the percent of α-SMA-expressing cells after treatment with AdsiNox2 (6.64-fold, $p<0.05$) or AdsiNox2/4 (6.37-fold, $p<0.05$) and cTnT-expressing cells after treatment with AdsiNox4 (4.02-fold, $p<0.05$) or AdsiNox2/4 (104.96-fold, $p<0.05$) were observed. Knockdown of Nox2 also led to a reduction in the percent of cTnT-positive cells (7.95-fold, $p<0.05$), even though the decrease in cTnT transcript level was not different from control (Figure 3.4D). Collectively, these results demonstrate that low levels of Nox2 and Nox4 are critical for the maintenance of precursor status in these c-kit$^+$ CPCs, and that increasing levels of Nox2 and Nox4 are important for expression of smooth muscle and cardiac cell markers.

Targeted Silencing of Nox2 and Nox4 Alters Expression of Transcription Factors and Cytokines

In order to begin to tease apart the mechanisms by which Nox isoforms act during c-kit$^+$ CPC specification, I utilized qPCR to measure the expression levels of two transcription factors, Gata6 and Gata4, and the cytokine, TGF-β1, each known to play important roles in cardiac lineage commitment [41]. As shown in Figure 3.8A, viral silencing of Nox2 reduced the expression of the smooth muscle-specific transcription factor Gata6 (2.51-fold, $p<0.05$) and

Figure 3.7. Targeted Silencing of Nox2 and Nox4 Alters Population of Lineage Committed Cells. (A) Representative immunoblot (left) and summary (right) of quantification of c-kit protein in cell lysates from c-kit^{+} cells isolated from PN0-4 heterozygote c-kit^{BAC}-EGFP pup hearts and infected with AdsiCON, AdsiNox2, AdsiNox4, or AdsiNox2/4 for 7 days. n=3; *$p<0.05$ vs. AdsiCON, †$p=.05$ vs. AdsiCON. Immunocytochemistry for (B) α-SMA and (C) cTnT in virally transduced c-kit^{+} cells; scale bar = 10μm. Summary of percent of total cells positive for (D) α-SMA and (E) cTnT 7 days following viral transduction. 4 independent experiments were analyzed comprising ≥550 cells/condition; *$p<0.05$ vs. AdsiCON.

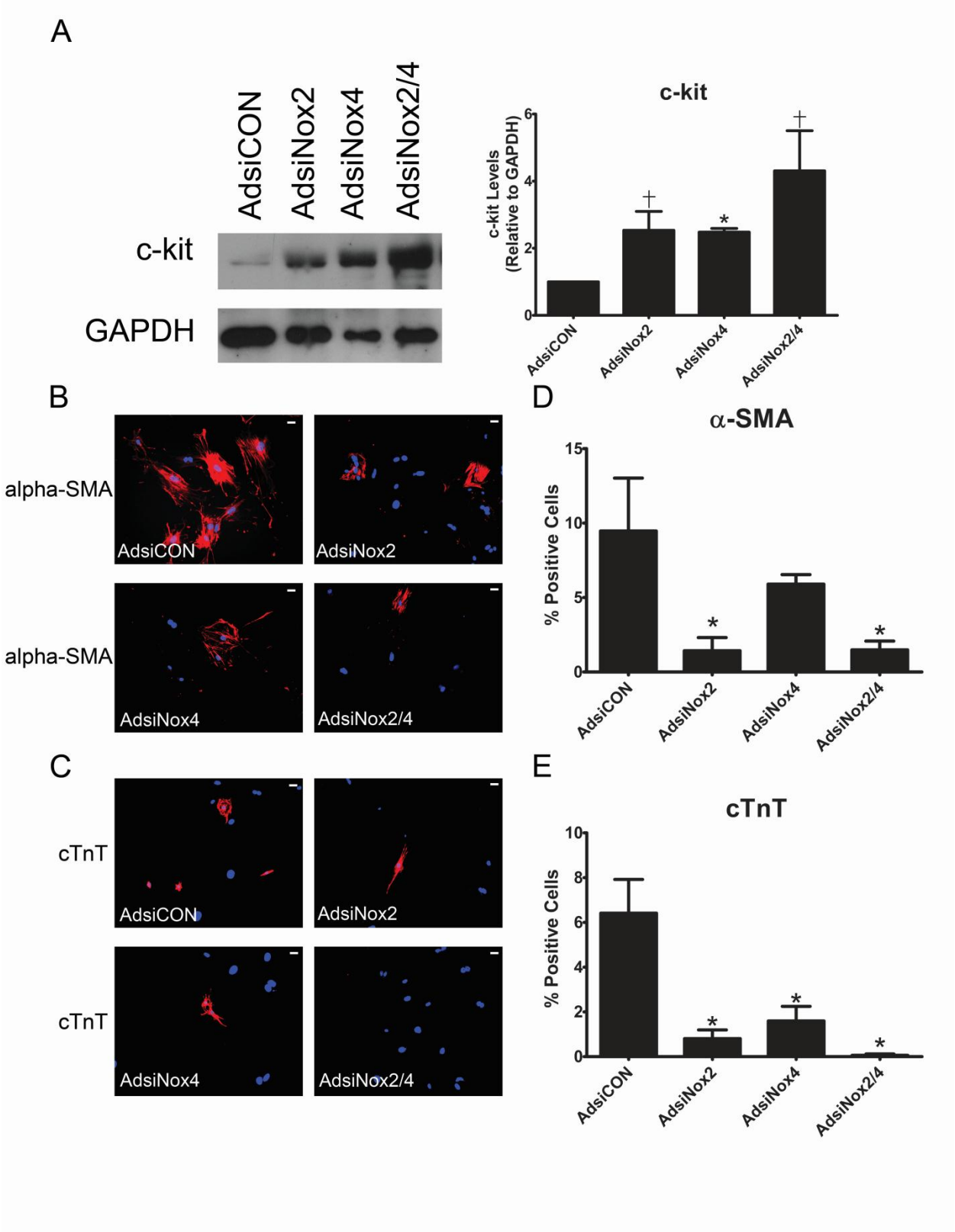
A
AdsiCON
AdsiNox2
AdsiNox4
AdsiNox2/4
c-kit
GAPDH
c-kit
c-kit Levels (Relative to GAPDH)
AdsiCON
AdsiNox2
AdsiNox4
AdsiNox2/4
B
alpha-SMA
AdsiCON
AdsiNox2
alpha-SMA
AdsiNox4
AdsiNox2/4
D
α-SMA
% Positive Cells
AdsiCON
AdsiNox2
AdsiNox4
AdsiNox2/4
C
cTnT
AdsiCON
AdsiNox2
cTnT
AdsiNox4
AdsiNox2/4
E
cTnT
% Positive Cells
AdsiCON
AdsiNox2
AdsiNox4
AdsiNox2/4

Figure 3.8. Targeted Silencing of Nox2 and Nox4 Alters Expression of Transcription Factors and Cytokines. (A-C) Gata6, Gata4, and TGF-β transcript levels analyzed by qPCR in c-kit^{+} cells isolated from PN0-4 heterozygote c-kit^{BAC}-EGFP pup hearts and infected with AdsiCON, AdsiNox2, AdsiNox4, or AdsiNox2/4 for 7 days. n=3-6/group; *$p<0.05$ vs. AdsiCON. Gene expression was normalized to β-actin.

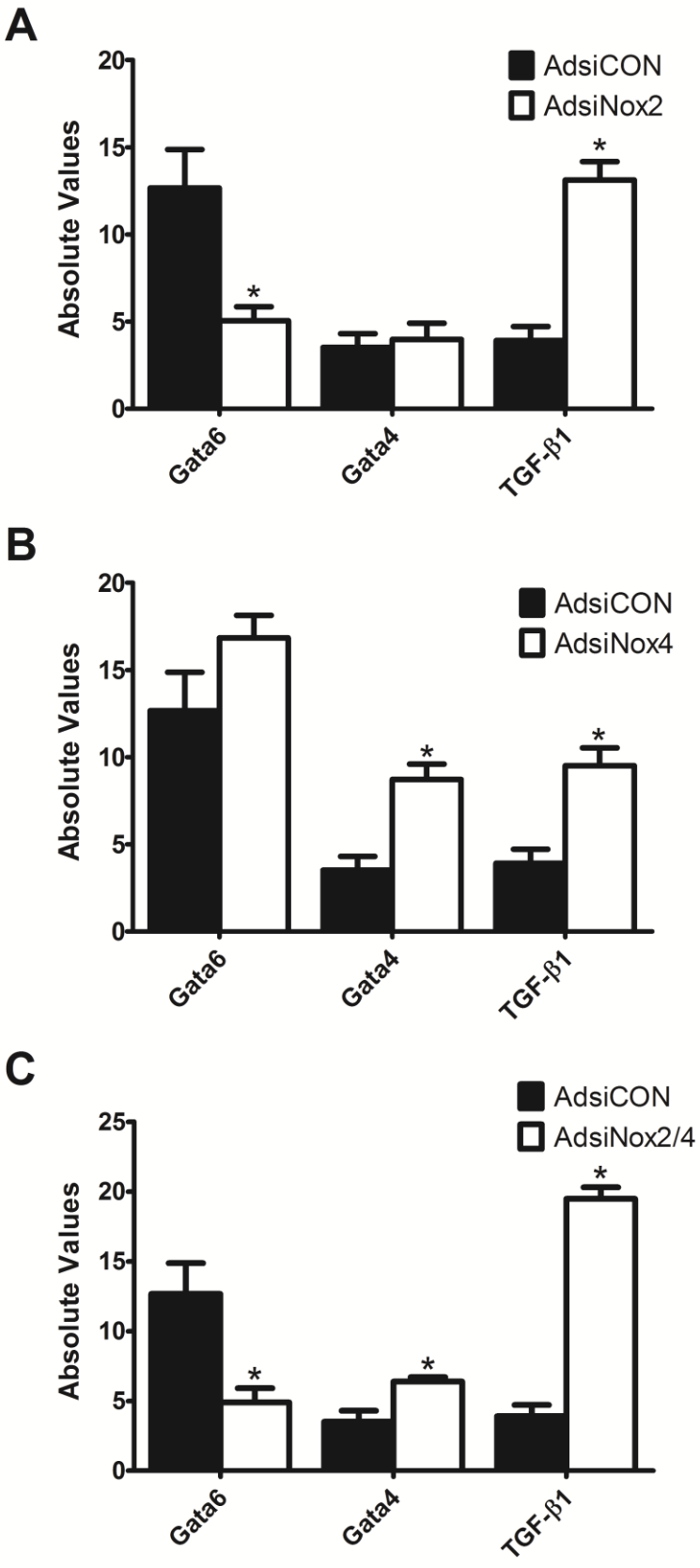
A
AdsiCON
AdsiNox2
Absolute Values
20
15
10
5
0
*
*
Gata6
Gata4
TGF-β1
B
AdsiCON
AdsiNox4
Absolute Values
20
15
10
5
0
*
*
Gata6
Gata4
TGF-β1
C
AdsiCON
AdsiNox2/4
Absolute Values
25
20
15
10
5
0
*
*
*
Gata6
Gata4
TGF-β1

significantly increased expression of TGF-β1 (3.35-fold, $p<0.05$), which is a critical modulator of ESC-mediated smooth muscle generation [42]. AdsiNox4 significantly increased expression of the early cardiac transcription factor Gata4 (2.48-fold, $p<0.05$) and TGF-β1 (2.43-fold, $p<0.05$), but had no effect on Gata6 expression (Figure 3.8B). In combination, knockdown of Nox2 and Nox4 led to a significant reduction in Gata6 mRNA expression (2.58-fold, $p<0.05$) along with a significant increase in both Gata4 (1.82-fold, $p<0.05$) and TGF-β1 (4.98-fold, $p<0.05$) mRNA levels (Figure 3.8C). Thus, it appears that Nox2- and Nox4-derived ROS may target the early transcription pathways necessary for mesodermal differentiation.

C-kit$^+$ CPCs Exhibit Enhanced Antioxidant Capacity at the mRNA Level

Thus far, I have focused on pro-oxidant generators and their influence over c-kit$^+$ CPC function; however, I speculate that overall redox balance is an important modulator of c-kit$^+$ CPC state and I recognize that a variety of antioxidants likely are involved in the pathways mediating CPC self-renewal and differentiation. Therefore, I turned to the RT^2 Profiler PCR Array system to simultaneously monitor the mRNA expression levels of 84 different genes involved in *Mouse Oxidative Stress and Antioxidant Defense* systems in a population of freshly isolated c-kit$^+$ CPCs. Utilizing qPCR, I found that 23 redox genes were upregulated and 4 genes were downregulated in freshly isolated c-kit$^+$ cells compared to control cardiomyocytes (Figure 3.9A and Tables 3.2 and 3.3). Fold changes were considered significant at a ≥2-fold change in either direction ($p<0.05$). Of these 23 genes, many represented entire families of redox-related molecules. For example, upregulated genes included two of the three superoxide dismutase isoforms (Sod1, Sod2) and four members of the peroxiredoxin family (Prdx2, Prdx3, Prdx5, Prdx6), all of which are involved in ROS scavenging. The four downregulated genes included the third member of the Sod family (Sod3), apolipoprotein E, cytoglobin, as well as previously

Figure 3.9. C-kit^{+} CPCs Exhibit Enhanced Antioxidant Capacity at the mRNA Level.

(A) Summary of transcript levels of 84 redox genes analyzed by RT^{2}Profiler PCR Array in c-kit^{+} cells and control cardiomyocytes isolated from PN0-4 heterozygote c-kit^{BAC}-EGFP and wildtype littermate pup hearts, respectively. Fold changes were considered significant at ≥2-fold change in either direction (solid lines). n=3; $p<0.05$. (B) Summary of a subset of upregulated and downregulated genes analyzed by qPCR in c-kit^{+} cells and control cardiomyocytes expressed fold control cardiomyocytes and compared to the Array data-set. n=3; $p>0.05$. Gene expression was normalized to β-actin.

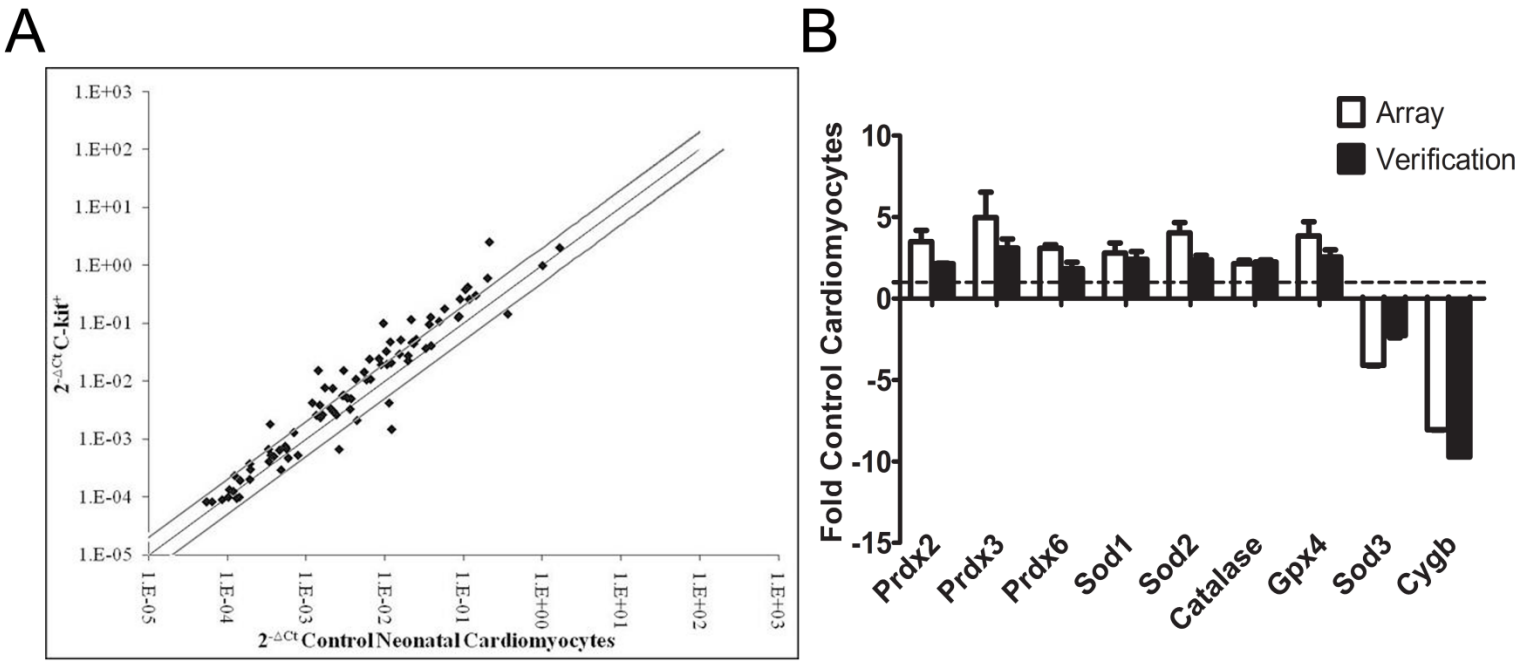
A
1.E+03
1.E+02
1.E+01
1.E+00
1.E-01
1.E-02
1.E-03
1.E-04
1.E-05
2-ΔCt C-kit+
1.E-05
1.E-04
1.E-03
1.E-02
1.E-01
1.E+00
1.E+01
1.E+02
1.E+03
2-ΔCt Control Neonatal Cardiomyocytes
B
Array
Verification
Fold Control Cardiomyocytes
10
5
0
-5
-10
-15
Prdx2
Prdx3
Prdx6
Sod1
Sod2
Catalase
Gpx4
Sod3
Cygb

Table 3.2. 23 Upregulated Redox Genes and their Functions.

Upregulated			
Gene	**Fold Change (≥2)**	**P value (<.05)**	**Gene Function**
Mb	12.09	0.0188	Globin, storage/movement of O_2 in muscle
Xirp1	10.8	0.0028	Stabilizes actin filaments
Tmod1	10.56	0.0029	Blocks depolarization of actin filaments
Prdx3	5.42	0.041	Reduces H_2O_2 and alkyl hydroperoxides in mitochondria
Nqo1	5.13	0.0215	Quinone reductase, cellular detoxification
Slc41a3	4.45	0.0108	Magnesium transporter
Sod2	4.11	0.0077	Dismutates superoxide in mitochondria
Gstk1	3.8	0.0211	Glutathione transferase, cellular detoxification
Gpx4	3.78	0.0153	Catalyzes reduction of H_2O_2
Prdx2	3.67	0.0215	Reduces H_2O_2 and alkyl hydroperoxides in cytosol
Txnrd2	3.53	0.0115	Reduces thioredoxin
Slc38a1	3.47	0.0007	Amino acid transporter
Prdx5	3.38	0.0028	Reduces H_2O_2 and alkyl hydroperoxides in mitochondria/peroxisomes
Prdx6-rs1	3.27	0.0014	Peroxiredoxin 6 related sequence-1
Prdx6	3.17	0.0042	Reduces H_2O_2 and alkyl hydroperoxides in cytosol
Psmb5	3.14	0.0163	Proteasome subunit
Txnip	3.02	0.0488	Inhibits thioredoxin activity
Sod1	2.94	0.0486	Dismutates superoxide in cytoplasmic compartment
Park7	2.63	0.0043	Member of peptidase C56 family, sensor of oxidative stress
Nudt15	2.6	0.0205	Helps prevent incorporation of 8-oxo-dGTP into DNA
Catalase	2.22	0.0312	Decomposes H_2O_2
Dnm2	2.17	0.015	GTP-binding protein, endocytosis
Ptgs1	2.13	0.0154	Prostaglandin synthesis, cell proliferation

Table 3.3. 4 Downregulated Redox Genes and their Functions.

Downregulated			
Gene	**Fold Change (≥2)**	**P value (<.05)**	**Gene Function**
Cygb	0.12	0.0002	O_2 storage/transfer
Sod3	0.25	0.0188	Dismutates superoxide in extracellular compartment
Ncf2 (p67phox)	0.37	0.0196	Subunit of NADPH oxidase complex in neutrophils
Apoe	0.4	0.0062	Lipoprotein metabolism

identified pro-oxidant, $p67^{phox}$. RT^2Profiler PCR Array results were confirmed using independently designed qPCR primers for select target genes run on 3 distinct samples, and close alignment was found (Figure 3.9B). These data reveal an interesting genetic redox profile in freshly isolated c-kit^+ CPCs which introduces new molecules that likely contribute to maintenance of a low ROS state and preservation of a stemness phenotype.

DISCUSSION

With cell-based therapies emerging as potential strategies for a variety of disease states including heart failure [41], it is increasingly important to understand the mechanisms underlying precursor cell self-renewal and differentiation. Redox signaling is recognized to play key roles both in maintaining stemness and in mediating lineage commitment in multiple precursor cell types [8, 9]. However, currently little is known about the redox status of c-kit$^+$ CPCs and the interplay between ROS and CPC differentiation. Here I report that early postnatal c-kit$^+$ CPCs exhibit reduced ROS levels under basal conditions, and that Nox2 and Nox4 modulate the balance between c-kit$^+$ cell precursor and differentiation status in part by altering the expression of transcription factors Gata6 and Gata4 and the cytokine TGF-β1.

Several precursor cell types, including endothelial progenitor cells (EPCs) and hematopoietic stem cells have now been shown to exist in a ROS-protected state [34-36]. It is postulated that this may be necessary for progenitor cell survival by shielding them from DNA damage, and also to promote progenitor status by limiting their exposure to molecules that trigger differentiation [34-36, 43, 44]. Using DHE as a ROS indicator in freshly isolated c-kit$^+$ CPCs *in vitro* and in the intact myocardium of early postnatal c-kit^{BAC}-EGFP mice, this is the first report to demonstrate that early postnatal c-kit$^+$ CPCs also exhibit reduced ROS levels. While I am aware that DHE fluorescence intensity is a semi-quantitative measurement of ROS, I believe that, similar to these other cell types, my findings reflect the fact that c-kit$^+$ CPCs reside within well-protected niche environments [35, 36].

After demonstrating a decrease in ROS production in c-kit$^+$ CPCs, next I turned to analyzing Nox1, Nox2, and Nox4 since they are the main ROS generators in cardiovascular tissues and are known to be involved in cardiac signaling and differentiation [10, 11]. Nox1, which has limited expression in the mature heart [10, 11], was expressed at low basal levels both in early postnatal c-kit$^+$ CPCs and control cardiomyocytes, and, unlike the other two homologues, showed no induction upon c-kit$^+$ CPC differentiation. In addition, the two required subunits for Nox1 activity, NoxA1 and NoxO1, also were not differentially expressed in c-kit$^+$ CPCs. Therefore, Nox1 likely plays a very limited role in c-kit$^+$ cell precursor status or lineage commitment. On the other hand, Nox2 and its critical functional subunit, p67^{phox}, were significantly downregulated in early postnatal c-kit$^+$ CPCs compared to control cells. Interestingly, this was not the case for Nox4, which leads me to speculate that the low ROS state of early postnatal c-kit$^+$ CPCs is due at least in part to selective downregulation of Nox2 expression and function in these cells. However, like in other precursor cell populations [34], the results of the RT^{2}Profiler PCR arrays suggest that increased expression of antioxidant enzymes such as Sod, Prdx, Gpx, and catalase also contribute to the low ROS state of c-kit$^+$ CPCs and I am currently investigating the influence of these additional redox targets on c-kit$^+$ cell precursor status and differentiation.

Both Nox2 and Nox4 exhibited increased expression over the course of c-kit$^+$ cell differentiation, with Nox4 showing upregulation somewhat earlier than Nox2. This is consistent with evidence that both of these homologues are expressed in multiple developing and mature cardiac cell types [10, 11, 17, 20, 21, 37]. Previously, our laboratory reported that c-kit$^+$ cells differentiate into all three lineages of the heart *in vitro* [6], so to determine if Nox2 and/or Nox4 are functionally linked to c-kit$^+$ CPC differentiation, I went on to utilize gene silencing viruses targeted selectively to each of these two homologues [30, 32, 33]. Upon knockdown of Nox2, there was a significant increase in

both the CPC marker c-kit and the early mesodermal cell marker Flk-1, concomitant with a decrease in expression of α-SMA at the mRNA and protein levels. Although it has been reported previously that Nox2 plays a key role in skeletal muscle differentiation [45] and in remodeling/revascularization after ischemic injury in other systems [14, 15], this is the first report that Nox2 is critical for the differentiation of CPCs along the smooth muscle lineage. In line with previous reports that Gata6 expression follows that of α-SMA [46], I also observed a significant downregulation of Gata6 mRNA in AdsiNox2-transduced c-kit$^+$ CPCs, and this was not further altered by the addition of AdsiNox4. This was accompanied by significant upregulation of TGF-β1, which is consistent with reports that Gata6 is critical for the maintenance of a differentiated phenotype in VSMCs and is a known to be a suppressor of TGF-β1[47, 48]. Because these transcription factors and this cytokine have broad cellular implications, it is not surprising that downregulation of Nox2 also led to a significant reduction in the number of cTnT-expressing cells, even though this was not significant at the transcript level. Together with a recent report that Nox2 contributes to cardiomyogenesis by ESCs [21], these data suggest that Nox2- derived ROS plays a critical role in the smooth muscle and perhaps cardiac commitment of c-kit$^+$ CPCs.

A role for Nox4 in ESC-mediated cardiomyogenesis recently has emerged [20, 37], and my studies suggest a similar mechanism at play in the differentiation of c-kit$^+$ CPCs along the cardiomyocyte lineage. Selective knockdown of Nox4 with AdsiNox4 reduced expression of cTnT mRNA as well as the percent of cells expressing cTnT protein. As with AdsiNox2 treatment, this was accompanied by increased expression of stemness markers c-kit and Flk-1. Interestingly, although previous reports also link Nox4 to smooth muscle cell differentiation [17],

my data do not support a similar role for Nox4 since AdsiNox4 did not significantly alter α-SMA transcript levels or the percent of α-SMA-positive cells. Furthermore, AdsiNox4 did not alter Gata6 expression, whereas it did alter expression of early cardiac transcription factor Gata4. As Gata4 is regulated through both ROS-dependent and ROS-independent pathways, I hypothesize that the increase in Gata4 observed after silencing Nox4 is a result of a ROS-independent and antioxidant-sensitive mechanism [49]. This is further supported by the fact that Gata4 is a retinoic-acid inducible transcription factor in the heart [50]. In addition, treatment with AdsiNox4 significantly increased transcript expression of TGF-β1, a finding consistent with evidence that signaling through TGF-β1 is critical for cardiomyogenesis [51]. Further studies will be required to elucidate these mechanisms.

In line with our laboratory's earlier report that approximately 39% of c-kit$^+$ CPCs analyzed 24 hours post-FACS express α-SMA, 30% express cTnT, and a negligible number express endothelial markers PECAM1 or vWF [6], I noted very low but detectable levels of vWF in all conditions, and failed to observe differential effects of AdsiNox2 and/or AdsiNox4 on endothelial cell differentiation. This was verified further using VEGF-A, a growth factor critical for endothelial cell differentiation and proliferation [39, 40]. It should be noted, however, that I cannot rule out the possibility that specific media conditions and growth factors vital for endothelial cells to differentiate from c-kit$^+$ CPCs were lacking in my protocol and this may have contributed to my findings [6]. While I believe it is unlikely that Nox2 or Nox4 play a prominent role in the differentiation of c-kit$^+$ CPCs into mature endothelial cells, it remains to be elucidated whether overall redox state and/or Nox signaling via other Nox homologues are critical for the differentiation of c-kit$^+$ CPCs along the endothelial cell lineage in optimized media conditions.

Although it is clear that ROS derived from the different Nox isoforms feed into divergent signaling cascades and lead to specific cellular outcomes [11], my data suggest that there also may be convergent signaling pathways for Nox-derived ROS in c-kit$^+$ CPCs. For example, when AdsiNox2 and AdsiNox4 were used concomitantly, I observed a significant and even more robust upregulation of cardiovascular precursor marker Flk-1 than that observed after the downregulation of either Nox isoform alone. Interestingly, Flk-1 also has been reported as a marker of EPCs [52] and vascular stem cells [53]. Because I did not observe an increase in endothelial cell markers after downregulation of Nox2 and Nox4, I do not believe that this increase in Flk-1 is indicative of a shift to an endothelial cell fate, but instead I hypothesize that it is a reversal to either a multipotent cardiovascular or a more restricted vascular precursor cell state. The idea of convergent signaling pathways for Nox-derived ROS also was observed for TGF-β1 mRNA, where a more robust increase was seen after concurrent treatment with AdsiNox2 and AdsiNox4. The augmentation in induction observed here may reflect an attempt to overcompensate for the drastic loss of Nox signaling as TGF-β1 is a known agonist of Nox activity.

In conclusion, my study reveals two novel redox targets, Nox2 and Nox4, which are involved in the balance between neonatal c-kit$^+$ cell precursor and differentiation status. Utilizing microfluorography to measure ROS, along with genetic tools to profile and manipulate the redox status of early postnatal c-kit$^+$ CPCs, my results demonstrate that c-kit$^+$ CPCs exist in a low ROS state and that Nox2 and Nox4 are functionally linked to their differentiation into smooth muscle and cardiac cell lineages. The downstream pathways modulated by Nox-derived ROS

production in CPCs also will require further study, but likely involve redox sensitive signaling pathways such as RAS, JNK, ERK1/2, p38MAPK, and PI3K [11]. Here I focused on pro-oxidant Nox isozymes, however, through the RT^2Profiler PCR Arrays, I am cognizant that additional sources of ROS, most notably the mitochondria, as well as overall redox balance are likely important and that a variety of additional pro-oxidant and/or antioxidant molecules may be involved in the pathways mediating c-kit^+ CPC self-renewal and differentiation. Although uncovering the specific redox pathways and mechanisms that drive these outcomes will require additional investigation, I believe that this study highlights several target genes which may be utilized in directed differentiation for cell-based therapies of the heart.

REFERENCES

1. Bergmann O, Bhardwaj RD, Bernard S, Zdunek S, Barnabe-Heider F, Walsh S, Zupicich J, Alkass K, Buchholz BA, Druid H, Jovinge S, Frisen J. Evidence for cardiomyocyte renewal in humans. *Science*. 2009;324:98-102.

2. Lloyd-Jones D, Adams RJ, Brown TM, Carnethon M, Dai S, De Simone G, Ferguson TB, Ford E, Furie K, Gillespie C, Go A, Greenlund K, Haase N, Hailpern S, Ho PM, Howard V, Kissela B, Kittner S, Lackland D, Lisabeth L, Marelli A, McDermott MM, Meigs J, Mozaffarian D, Mussolino M, Nichol G, Roger VL, Rosamond W, Sacco R, Sorlie P, Stafford R, Thom T, Wasserthiel-Smoller S, Wong ND, Wylie-Rosett J, American Heart Association Statistics Committee and Stroke Statistics Subcommittee. Executive summary: Heart disease and stroke statistics--2010 update: A report from the american heart association. *Circulation*. 2010;121:948-954.

3. Moretti A, Caron L, Nakano A, Lam JT, Bernshausen A, Chen Y, Qyang Y, Bu L, Sasaki M, Martin-Puig S, Sun Y, Evans SM, Laugwitz KL, Chien KR. Multipotent embryonic isl1+ progenitor cells lead to cardiac, smooth muscle, and endothelial cell diversification. *Cell*. 2006;127:1151-1165.

4. Wu SM, Fujiwara Y, Cibulsky SM, Clapham DE, Lien C, Schultheiss TM, Orkin SH. Developmental origin of a bipotential myocardial and smooth muscle cell precursor in the mammalian heart. *Cell,*. 2006;127:1137-1150.

5. Kattman SJ, Huber TL, Keller GM. Multipotent flk-1+ cardiovascular progenitor cells give rise to the cardiomyocyte, endothelial, and vascular smooth muscle lineages. *Dev Cell*. 2006;11:723-732.

6. Tallini YN, Greene KS, Craven M, Spealman A, Breitbach M, Smith J, Fisher PJ, Steffey M, Hesse M, Doran RM, Woods A, Singh B, Yen A, Fleischmann BK, Kotlikoff MI. C-kit expression identifies cardiovascular precursors in the neonatal heart. *Proc Natl Acad Sci U S A*. 2009;106:1808-1813.

7. Beltrami AP, Barlucchi L, Torella D, Baker M, Limana F, Chimenti S, Kasahara H, Rota M, Musso E, Urbanek K, Leri A, Kajstura J, Nadal-Ginard B, Anversa P. Adult cardiac stem cells are multipotent and support myocardial regeneration. *Cell*,. 2003;114:763-776.

8. Noble M, Mayer-Proschel M, Proschel C. Redox regulation of precursor cell function: Insights and paradoxes. *Antioxid Redox Signal*. 2005;7:1456-1467.

9. Pervaiz S, Taneja R, Ghaffari S. Oxidative stress regulation of stem and progenitor cells. *Antioxid Redox Signal*. 2009.

10. Griendling KK. Novel NAD(P)H oxidases in the cardiovascular system. *Heart*. 2004;90:491-493.

11. Cave AC, Brewer AC, Narayanapanicker A, Ray R, Grieve DJ, Walker S, Shah AM. NADPH oxidases in cardiovascular health and disease. *Antioxid Redox Signal*. 2006;8:691-728.

12. Zhang M, Brewer AC, Schroder K, Santos CX, Grieve DJ, Wang M, Anilkumar N, Yu B, Dong X, Walker SJ, Brandes RP, Shah AM. NADPH oxidase-4 mediates protection against

chronic load-induced stress in mouse hearts by enhancing angiogenesis. *Proc Natl Acad Sci U S A.* 2010;107:18121-18126.

13. Pollock JD, Williams DA, Gifford MA, Li LL, Du X, Fisherman J, Orkin SH, Doerschuk CM, Dinauer MC. Mouse model of X-linked chronic granulomatous disease, an inherited defect in phagocyte superoxide production. *Nat Genet*. 1995;9:202-209.

14. Chen Z, Keaney JF,Jr, Schulz E, Levison B, Shan L, Sakuma M, Zhang X, Shi C, Hazen SL, Simon DI. Decreased neointimal formation in Nox2-deficient mice reveals a direct role for NADPH oxidase in the response to arterial injury. *Proc Natl Acad Sci U S A*. 2004;101:13014-13019.

15. Urao N, Inomata H, Razvi M, Kim HW, Wary K, McKinney R, Fukai T, Ushio-Fukai M. Role of nox2-based NADPH oxidase in bone marrow and progenitor cell function involved in neovascularization induced by hindlimb ischemia. *Circ Res*. 2008;103:212-220.

16. Looi YH, Grieve DJ, Siva A, Walker SJ, Anilkumar N, Cave AC, Marber M, Monaghan MJ, Shah AM. Involvement of Nox2 NADPH oxidase in adverse cardiac remodeling after myocardial infarction. *Hypertension*. 2008;51:319-325.

17. Xiao Q, Luo Z, Pepe AE, Margariti A, Zeng L, Xu Q. Embryonic stem cell differentiation into smooth muscle cells is mediated by Nox4-produced H2O2. *Am J Physiol Cell Physiol*. 2009;296:C711-23.

18. Puceat M, Travo P, Quinn MT, Fort P. A dual role of the GTPase rac in cardiac differentiation of stem cells. *Mol Biol Cell*. 2003;14:2781-2792.

19. Sharifpanah F, Wartenberg M, Hannig M, Piper HM, Sauer H. Peroxisome proliferator-activated receptor alpha agonists enhance cardiomyogenesis of mouse ES cells by utilization of a reactive oxygen species-dependent mechanism. *Stem Cells*. 2008;26:64-71.

20. Buggisch M, Ateghang B, Ruhe C, Strobel C, Lange S, Wartenberg M, Sauer H. Stimulation of ES-cell-derived cardiomyogenesis and neonatal cardiac cell proliferation by reactive oxygen species and NADPH oxidase. *J Cell Sci*. 2007;120:885-894.

21. Bartsch C, Bekhite MM, Wolheim A, Richter M, Ruhe C, Wissuwa B, Marciniak A, Muller J, Heller R, Figulla HR, Sauer H, Wartenberg M. NADPH oxidase and eNOS control cardiomyogenesis in mouse embryonic stem cells on ascorbic acid treatment. *Free Radic Biol Med*. 2011.

22. Gurusamy N, Mukherjee S, Lekli I, Bearzi C, Bardelli S, Das DK. Inhibition of ref-1 stimulates the production of reactive oxygen species and induces differentiation in adult cardiac stem cells. *Antioxid Redox Signal*. 2009;11:589-600.

23. Oh H, Bradfute SB, Gallardo TD, Nakamura T, Gaussin V, Mishina Y, Pocius J, Michael LH, Behringer RR, Garry DJ, Entman ML, Schneider MD. Cardiac progenitor cells from adult myocardium: Homing, differentiation, and fusion after infarction. *Proc Natl Acad Sci U S A*. 2003;100:12313-12318.

24. Craven M, Kotlikoff MI, Nadworny AS. C-kit expression identifies cardiac precursor cells in neonatal mice. *Methods Mol Biol*. 2012;843:177-189.

25. Zimmerman MC, Dunlay RP, Lazartigues E, Zhang Y, Sharma RV, Engelhardt JF, Davisson RL. Requirement for Rac1-dependent NADPH oxidase in the cardiovascular and dipsogenic actions of angiotensin II in the brain. *Circ Res*. 2004;95:532-539.

26. Kuhn LT, Liu Y, Advincula M, Wang YH, Maye P, Goldberg AJ. A nondestructive method for evaluating in vitro osteoblast differentiation on biomaterials using osteoblast-specific fluorescence. *Tissue Eng Part C Methods*. 2010;16:1357-1366.

27. Wakselman S, Bechade C, Roumier A, Bernard D, Triller A, Bessis A. Developmental neuronal death in hippocampus requires the microglial CD11b integrin and DAP12 immunoreceptor. *J Neurosci*. 2008;28:8138-8143.

28. Douglas RM, Ryu J, Kanaan A, Del Carmen Rivero M, Dugan LL, Haddad GG, Ali SS. Neuronal death during combined intermittent hypoxia/hypercapnia is due to mitochondrial dysfunction. *Am J Physiol Cell Physiol*. 2010;298:C1594-602.

29. Phifer CB, Terry LM. Use of hypothermia for general anesthesia in preweanling rodents. *Physiol Behav*. 1986;38:887-890.

30. Peterson JR, Burmeister MA, Tian X, Zhou Y, Guruju MR, Stupinski JA, Sharma RV, Davisson RL. Genetic silencing of Nox2 and Nox4 reveals differential roles of these NADPH oxidase homologues in the vasopressor and dipsogenic effects of brain angiotensin II. *Hypertension*. 2009;54:1106-1114.

31. Xia H, Mao Q, Paulson HL, Davidson BL. siRNA-mediated gene silencing in vitro and in vivo. *Nat Biotechnol*. 2002;20:1006-1010.

32. Hingtgen SD, Tian X, Yang J, Dunlay SM, Peek AS, Wu Y, Sharma RV, Engelhardt JF, Davisson RL. Nox2-containing NADPH oxidase and akt activation play a key role in angiotensin II-induced cardiomyocyte hypertrophy. *Physiol Genomics*. 2006;26:180-191.

33. Infanger DW, Cao X, Butler SD, Burmeister MA, Zhou Y, Stupinski JA, Sharma RV, Davisson RL. Silencing nox4 in the paraventricular nucleus improves myocardial infarction-induced cardiac dysfunction by attenuating sympathoexcitation and periinfarct apoptosis. *Circ Res*. 2010;106:1763-1774.

34. Dernbach E, Urbich C, Brandes RP, Hofmann WK, Zeiher AM, Dimmeler S. Antioxidative stress-associated genes in circulating progenitor cells: Evidence for enhanced resistance against oxidative stress. *Blood*. 2004;104:3591-3597.

35. Jang YY, Sharkis SJ. A low level of reactive oxygen species selects for primitive hematopoietic stem cells that may reside in the low-oxygenic niche. *Blood*. 2007;110:3056-3063.

36. Owusu-Ansah E, Banerjee U. Reactive oxygen species prime drosophila haematopoietic progenitors for differentiation. *Nature*. 2009;461:537-541.

37. Li J, Stouffs M, Serrander L, Banfi B, Bettiol E, Charnay Y, Steger K, Krause KH, Jaconi ME. The NADPH oxidase NOX4 drives cardiac differentiation: Role in regulating cardiac transcription factors and MAP kinase activation. *Mol Biol Cell*. 2006;17:3978-3988.

38. Armstrong L, Tilgner K, Saretzki G, Atkinson SP, Stojkovic M, Moreno R, Przyborski S, Lako M. Human induced pluripotent stem cell lines show stress defense mechanisms and

mitochondrial regulation similar to those of human embryonic stem cells. *Stem Cells*. 2010;28:661-673.

39. Tammela T, Enholm B, Alitalo K, Paavonen K. The biology of vascular endothelial growth factors. *Cardiovasc Res*. 2005;65:550-563.

40. Nourse MB, Halpin DE, Scatena M, Mortisen DJ, Tulloch NL, Hauch KD, Torok-Storb B, Ratner BD, Pabon L, Murry CE. VEGF induces differentiation of functional endothelium from human embryonic stem cells: Implications for tissue engineering. *Arterioscler Thromb Vasc Biol*. 2010;30:80-89.

41. Anversa P, Kajstura J, Leri A, Bolli R. Life and death of cardiac stem cells: A paradigm shift in cardiac biology. *Circulation*. 2006;113:1451-1463.

42. Sinha S, Hoofnagle MH, Kingston PA, McCanna ME, Owens GK. Transforming growth factor-beta1 signaling contributes to development of smooth muscle cells from embryonic stem cells. *Am J Physiol Cell Physiol*. 2004;287:C1560-8.

43. Steinbeck MJ, Kim JK, Trudeau MJ, Hauschka PV, Karnovsky MJ. Involvement of hydrogen peroxide in the differentiation of clonal HD-11EM cells into osteoclast-like cells. *J Cell Physiol*. 1998;176:574-587.

44. Smith J, Ladi E, Mayer-Proschel M, Noble M. Redox state is a central modulator of the balance between self-renewal and differentiation in a dividing glial precursor cell. *Proc Natl Acad Sci U S A*. 2000;97:10032-10037.

45. Piao YJ, Seo YH, Hong F, Kim JH, Kim YJ, Kang MH, Kim BS, Jo SA, Jo I, Jue DM, Kang I, Ha J, Kim SS. Nox 2 stimulates muscle differentiation via NF-kappaB/iNOS pathway. *Free Radic Biol Med*. 2005;38:989-1001.

46. Lepparanta O, Pulkkinen V, Koli K, Vahatalo R, Salmenkivi K, Kinnula VL, Heikinheimo M, Myllarniemi M. Transcription factor GATA-6 is expressed in quiescent myofibroblasts in idiopathic pulmonary fibrosis. *Am J Respir Cell Mol Biol*. 2010;42:626-632.

47. Abe M, Hasegawa K, Wada H, Morimoto T, Yanazume T, Kawamura T, Hirai M, Furukawa Y, Kita T. GATA-6 is involved in PPARgamma-mediated activation of differentiated phenotype in human vascular smooth muscle cells. *Arterioscler Thromb Vasc Biol*. 2003;23:404-410.

48. Froese N, Kattih B, Breitbart A, Grund A, Geffers R, Molkentin JD, Kispert A, Wollert KC, Drexler H, Heineke J. GATA6 promotes angiogenic function and survival in endothelial cells by suppression of autocrine transforming growth factor {beta}/Activin receptor-like kinase 5 signaling. *J Biol Chem*. 2011;286:5680-5690.

49. Suzuki YJ. Cell signaling pathways for the regulation of GATA4 transcription factor: Implications for cell growth and apoptosis. *Cell Signal*. 2011;23:1094-1099.

50. Arceci RJ, King AA, Simon MC, Orkin SH, Wilson DB. Mouse GATA-4: A retinoic acid-inducible GATA-binding transcription factor expressed in endodermally derived tissues and heart. *Mol Cell Biol*. 1993;13:2235-2246.

51. Behfar A, Zingman LV, Hodgson DM, Rauzier JM, Kane GC, Terzic A, Puceat M. Stem cell differentiation requires a paracrine pathway in the heart. *FASEB J*. 2002;16:1558-1566.

52. Thomas RA, Pietrzak DC, Scicchitano MS, Thomas HC, McFarland DC, Frazier KS. Detection and characterization of circulating endothelial progenitor cells in normal rat blood. *J Pharmacol Toxicol Methods*. 2009;60:263-274.

53. Leri A, Hosoda T, Kajstura J, Anversa P, Rota M. Identification of a coronary stem cell in the human heart. *J Mol Med*. 2011.

CHAPTER FOUR: DISCUSSION

4.1 Summary of Findings

CHD is one of the leading causes of morbidity and mortality in the developed world, producing an enormous economic burden on society [1]. To date, this cost to society has been unmet by scientific discovery of a true cure. Heart disease is quickly becoming an epidemic problem made worse by an aging population and the retirement of individuals from the "baby boomer" generation. Due to a severe lack of hearts available for organ transplantation, the field of regenerative cardiology has emerged as a way to couple advances from multiple disciplines to promote the creation of functional replacement myocardium. While the fundamental view of the heart as a post-mitotic organ has been at the crux of basic research and clinical practice for a majority of the last century, the past few decades have witnessed a paradigm shift to the belief that the heart has some regenerative capability.

In addition to the very recent proof of myocyte turnover by two independent groups [2, 3], the work presented in this thesis, along with the work of others [4, 5], provides strong experimental evidence indicating the presence of resident CPCs in the myocardium. As described in the introduction and subsequent chapters, CPCs are identified by several markers including c-kit, which marks a CPC population exhibiting the three qualities of stemness [4-6]. This population shows great promise for cell-based therapy as its counterpart population also has been identified in humans and shown to possess similar cardiogenic properties [7, 8].

Despite the presence of resident CPCs in the heart, the response of the heart to ischemic injury is principally one of fibrosis and non-contractile scar formation [9]. Several reasons for this

phenomenon exist, including the belief that stem cell niches in the heart play an important role in maintaining homeostasis, but do not respond well to injury or aging [10, 11]. Therefore, evidence presented in this thesis suggests that exogenous expansion and genetic manipulation of CPCs is necessary to achieve substantial cardiac regeneration following infarct.

With the field of regenerative cardiology in its infancy and the discovery of CPCs less than a decade old, I sought a better understanding of the neonatal c-kit$^+$ CPC population. I hypothesized that the study of c-kit$^+$ CPCs would provide important information regarding their genetic status, mechanisms of differentiation and commitment, as well as their biological and therapeutic potential. Disheartened by the marginal improvements observed in cardiac function following cell therapy in conjunction with several strategies to precondition or genetically modify cells, I recognized the serious dearth of information regarding the basic mechanisms that regulate CPC stemness and differentiation. Therefore, the work presented in this thesis provides the following information to the scientific community: (1) A reproducible and reliable method to identify, isolate, and culture neonatal c-kit$^+$ CPCs, (2) The characterization of neonatal c-kit$^+$ CPCs *in vitro* and an analysis of their lineage plasticity and capacity for differentiation, and (3) An understanding of the redox biology of neonatal c-kit$^+$ CPCs, with an eye toward better stem cell-based therapies in the future. A detailed summary of findings from each chapter is presented below.

4.1.1 Chapter 2

Prior to these studies of c-kit expression in the murine heart, minimal promoter and enhancer elements as well as knock-in strategies were used to mark c-kit expression in the hematopoietic system, germ cells, gut, and brain [12, 13]. While the results of these

studies showed partial concordance between reporter and endogenous c-kit expression, an incomplete understanding of the regulatory elements necessary for normal c-kit expression coupled with the dominant nature of the c-kit gene complicated downstream analyses. In order to circumvent these problems, our laboratory chose to generate a BAC transgenic mouse in which EGFP expression was placed under control of the c-kit promoter. BAC recombineering has many benefits over traditional transgenesis, including a large insert size which contains most, if not all, of the cis-regulatory elements necessary for gene expression as well as some resistance against positional effects which may cause ectopic or weak transgene expression [14]. In addition, BAC constructs typically integrate at low copy number, less than five copies, as opposed to concatemer repeats of up to several hundred copies [14, 15].

For our studies, we utilized standard PCR to identify a founder line and critically compared reporter gene EGFP expression with endogenous c-kit expression using a CD117 antibody (Chapter 2: Figures 2.1-2.2). In order to accurately determine transgene copy number, the number of integration sites, and whether or not the BAC integrated as an intact construct, however, we recognize that we would need to perform additional experiments including Southern blot assays. As expected from a genetic strategy in which the endogenous locus is not altered, the c-kit^{BAC}-EGFP line displays no apparent phenotype and transmits the transgene in a Mendelian ratio. The generation of this transgenic line not only allowed us to identify our target neonatal c-kit^{+} CPC population for the studies presented in this thesis, but also serves as a tool for the scientific community in the study of a variety of cells and tissues in which c-kit is a valid marker.

After verifying co-localization of expression between EGFP and c-kit in several tissues known to express c-kit, we went on to determine c-kit expression in early embryonic and postnatal hearts. We identified clusters of c-kit$^+$ cells in several areas of the heart including the atrial and ventricular walls (Chapter 2: Figure 2.2). These precursor cell niches have been observed previously and suggest that specific locations within the heart that are protected from hemodynamic load and wall stress are critical for maintaining stemness [11, 16]. Not surprisingly, it has been reported that electrical impulse and mechanical strain contribute to ESC-mediated cardiomyogenesis [17-19]. In addition, the location of CPC clusters within the left ventricle is thought to strategically position primitive cells in close proximity to the site of ischemic injury, allowing for a shorter migratory path to the border zone [11]. Similar to the findings of Gude, et al. [20], we noted a small population of c-kit$^+$ cells within the neonatal myocardium that accounted for less than 1% of the total heart population and declined significantly by adulthood. Therefore, we decided to focus our studies on the early neonatal heart.

To isolate c-kit$^+$ cells and determine their potential to differentiate into multiple cell lineages, we designed and optimized a dissociation protocol adapted from Worthington's Neonatal Cardiomyocyte Isolation System and utilized FACS to capture cells based on their EGFP fluorescence [21]. This sorting method avoided problems associated with possible epitope destruction by enzymatic digestion which might limit the pool of cells recognized by the c-kit antibody. At 24 hours post-FACS, we confirmed previous reports of the progressive nature of the c-kit$^+$ CPC population [22], demonstrating a mixed

population of cells with a majority co-expressing precursor cell marker nestin [23, 24] and approximately one-third expressing either smooth or cardiac muscle specific markers (Chapter 2: Figure 2.3). In addition to expression of nestin, co-expression of Flk-1 also was observed in the PN2 heart, further supporting a precursor cell state (Chapter 2: Figure 2.2) [25, 26]. Interestingly, we saw no evidence of Sca-1 expression in our population, indicating partial digestion of the Sca-1 epitope during enzymatic cell dissociation, a completely distinct precursor cell population, or, more likely, precise temporal and spatial regulation over precursor antigen expression. Not surprisingly, we observed no overlap in our CPC population with Isl-1, a precursor cell marker which is thought to be restricted to embryonic development [27] although its stemness has been called into question in recent years [10, 28].

Because there are few c-kit$^+$ cells in the neonatal heart, and an even smaller population in the adult myocardium, next we attempted to expand the c-kit$^+$ population *in vitro* as a way to assess its therapeutic potential. In culture, we observed evidence of cell proliferation by PCNA staining as well as the presence of all three cardiac lineages (smooth muscle, cardiac, and endothelial) (Chapter 2: Figure 2.3). In addition, we confirmed the stemness of a sub-population of our c-kit$^+$ cells through single cell dilutions in clonal assays (Chapter 2: Figure 2.5). With directed differentiation becoming a critical modulator of cardiac repair, we investigated the lineage plasticity of our c-kit$^+$ population by varying media conditions to include growth factors and cytokines which are known to be involved in mesodermal differentiation (Chapter 2: Figure 2.5). The number of cells expressing cardiac marker, cTnT, was increased

markedly by inclusion of bFGF and these conditions produced a population of spontaneously beating cells. The functional relevance of these rhythmic action potentials was analyzed by standard patch clamp methods and revealed characteristics similar to those reported previously for ESC-derived cardiomyocytes [29-31], suggestive of an immature cardiac phenotype (Chapter 2: Figure 2.4). Beltrami, et al. [4] observed a similar phenotype noting that *in vitro* differentiated c-kit$^+$ cells were morphologically underdeveloped and lacked mature sarcomeric structures.

Following myocardial injury, our studies demonstrate that endogenous c-kit$^+$ cells contribute to revascularization and fibrosis within the border zone of the infarcted heart, but their presence declines drastically within a few weeks (Chapter 2: Figure 2.6). As mentioned previously, it is not surprising that endogenous stem cell niches are not capable of widespread cardiac repair, especially since many of these precursor cells succumb to apoptosis and necrosis alongside their mature counterparts [10]. Therefore, we believe that exogenous expansion of the CPC pool followed by cell therapy is necessary to achieve significant cardiac regeneration and functional restoration after injury. While it is still unclear whether or not a subset of the c-kit$^+$ population retains its multipotency after long-term expansion and passage in culture, some studies suggest the use of mixed populations in cell therapy, such as those derived from cardiospheres, to generate better cardiac outcomes, as these populations contain precursor cells capable of differentiation in addition to the supporting cells necessary for their survival [32]. However, before we can truly understand the therapeutic potential of c-kit$^+$ CPCs in myocardial repair, the mechanisms driving c-kit$^+$ CPC self-renewal and differentiation need to be elucidated.

4.1.2 Chapter 3

In order to begin tease apart the signaling pathways mediating c-kit$^+$ CPC self-renewal and differentiation, I turned my attention to the influence of redox biology over precursor cell state. In 2002, two independent laboratories reported a molecular profile of stem cells using microarray to compare gene expression among HSCs, NSCs, and ESCs [33, 34]. In total, approximately 200 genes were shared among the three cell types including a vast array of genes involved in resistance to stress. These genes included up-regulated DNA repair mechanisms, protein folding chaperones, ubiquitin pathways, and toxic stress response systems [34]. Several years later, it was reported that EPCs and HSCs exhibit increased antioxidant capacity and reduced ROS formation [35, 36]. These characteristics were predicted to confer progenitor status and self-renewal capacity with increases in ROS driving differentiation [37]. Therefore, my initial goal for these studies was to determine whether or not c-kit$^+$ CPCs also exhibit a protected redox profile in their basal state.

I began my studies by utilizing DHE microfluorography to measure intracellular ROS levels in cultured c-kit$^+$ CPCs as well as c-kit$^+$ CPCs within the intact left ventricular niche. Through these studies, I confirmed a low ROS state for c-kit$^+$ CPCs (Chapter 3: Figure 3.2). Overall, it is believed that a more reduced state favors self-renewal, while a more oxidized state promotes differentiation [38-42]. Therefore, my next step was to investigate which genes might be responsible for the initial low ROS state of c-kit$^+$ CPCs and the subsequent increase in ROS necessary for cardiogenic differentiation. Here, I turned to the cardiac Nox enzymes (Nox1, 2, and 4) which are essential components of

cardiac redox biology and generate ROS in a highly regulated manner [43-45]. Through qPCR, I found that Nox2 and its critical subunit, $p67^{phox}$, were downregulated in c-kit$^+$ CPCs (Chapter 3: Figure 3.3). This finding highlighted a potential mechanism by which c-kit$^+$ CPCs maintain a low ROS state. Next, I examined whether or not Nox homologue expression increases over the course of c-kit$^+$ CPC differentiation. Utilizing the same media conditions optimized in the studies presented in Chapter 2, I demonstrated a significant upregulation of both Nox2 and Nox4 by Day 14 in culture (Chapter 3: Figure 3.3). Together, these studies suggest a role for Nox2 and Nox4 in ROS-mediated cardiac lineage commitment of c-kit$^+$ CPCs.

To further confirm a functional role for Nox2 and Nox4 in c-kit$^+$ CPC differentiation, I utilized an adenovirus mediated knockdown strategy to silence the Nox isoforms at Day 7 in culture. This timepoint was chosen to effectively blunt the significant increase in Nox isoform expression observed by Day 14. Through qPCR, I measured transcript levels for two stemness genes, c-kit and Flk-1, as well as the three cardiac lineage commitment genes, α-SMA, cTnT, and vWF, at Day 7 post-transduction. I noticed significant upregulation of stemness genes, c-kit and Flk-1, following knockdown of Nox2, but only a significant increase in Flk-1 after silencing Nox4 (Chapter 3: Figure3.4). Not surprisingly, I observed a significant upregulation of both c-kit and Flk-1 after concomitant application of AdsiNox2 and AdsiNox4 (Chapter 3: Figure 3.4). These findings verified a critical role for Nox signaling in c-kit$^+$ CPC differentiation. The fact that I observed such a robust change in stemness transcript following knockdown of Nox2 and Nox4 despite the fact that I started with a very mixed population, as

highlighted in Chapter 2, suggests some level of plasticity within the population as well as a high sensitivity to redox state. The induction of c-kit transcript after application of AdsiNox2 and AdsiNox2/4 viruses was confirmed at the protein level using western immunoblot (Chapter 3: Figure 3.7). Interestingly, I also observed a significant increase in c-kit protein after knockdown of Nox4, even though the increase in transcript level did not reach statistical significance.

In addition to changes in stemness genes, I observed a decrease in commitment to the smooth muscle and cardiac lineages in a Nox2- and Nox4-dependent manner, respectively (Chapter 3: Figure 3.4), with little change seen in the generation of mature endothelial cells (Chapter 3: Figures 3.4 and 3.5). Although previous reports indicate a role for Nox2 in skeletal muscle differentiation [46] and in vascular recovery after arterial injury and hindlimb ischemia [47, 48], this is the first report that Nox2 enzymatic activity is critical for the differentiation of CPCs along the smooth muscle lineage. A role for Nox4 in ESC-mediated cardiomyogenesis [49-51], however, is well established, and my studies suggest a similar mechanism is at work in the cardiac differentiation of c-kit$^+$ CPCs. Changes observed in lineage commitment were verified at the protein level using immunocytochemistry with similar results (Chapter 3: Figure 3.7). Interestingly, I observed a greater change in the number of cells expressing cTnT protein after treatment with AdsiNox2 than the change observed at the transcript level, suggesting that Nox2 signaling also might be important for cardiac differentiation. A similar contribution of Nox2 during cardiomyogenesis by ESCs was reported recently [50].

In order to understand the mechanisms by which Nox-derived ROS act, next I examined the expression of several transcription factors and cytokines known to play a role in CPC lineage specification (Chapter 3: Figure 3.8). My results indicate an increased presence of a population of cells in a pre-committed state. For example, following knockdown of Nox2 and Nox4, I noted significant upregulation of TGF-β1 which is a known mediator of smooth muscle and cardiac differentiation [52-55]. In addition, I noted dysregulation of Gata6 and Gata4 after knockdown of Nox2 and Nox4, respectively, both of which are transcription factors involved in mesodermal differentiation and expressed at various time-points over the course of CPC lineage determination [22]. The molecular pathways by which these transcription factors and cytokines act during CPC commitment, however, remain to be seen.

Because I am aware that other redox molecules likely are involved in the pathways mediating c-kit$^+$ CPC self-renewal and differentiation, I utilized RT^{2}Profiler PCR Arrays to measure the mRNA expression levels of 84 different genes involved in *Mouse Oxidative Stress and Antioxidant Defense* systems (Chapter 3: Figure 3.9 and Tables 3.2 and 3.3). To this end, a wide-array of ROS scavengers were found to be upregulated in c-kit$^+$ CPCs including catalase, glutathione peroxidase 4 (Gpx4), several members of the peroxiredoxin (Prdx) family, and two Sod isoforms. Upregulated genes also included Park7, a sensor of oxidative stress, and Nqo1, a molecule involved in the detoxification of quinones. Downregulated genes included the potent pro-oxidant p67^{phox}, as described above, along with the third Sod isoform, Sod3. I speculate that these additional targets

play important roles in the redox biology of c-kit$^+$ CPCs and will provide novel targets for understanding the pathways mediating their directed differentiation.

4.2 Significance of Research and Proposed Model

Because the field of regenerative cardiology proved too eager to progress from the bench to the bedside in its support of clinical trials utilizing skeletal myoblasts as a therapeutic population [56], I took a step back and evaluated the fundamental properties and basic mechanisms underlying the CPC phenotype. Building from the discovery of resident CPCs in the early 2000's, I chose to study a sub-population of CPCs which are marked by c-kit and known to exhibit the three qualities of stemness [4]. I hypothesized that the isolation and characterization of this population not only would contribute to the basic understanding of c-kit$^+$ CPC biology, but also prove therapeutically meaningful in the treatment of myocardial infarction. While my experiments were in progress, c-kit$^+$ CPCs also were identified in the human myocardium and shown to have cardiogenic potential [8, 57, 58]. With clinical biopsies and *ex vivo* CPC expansion foreseeable events in patient care, I believed that studying the intricate pathways mediating c-kit$^+$ CPC survival, proliferation, and differentiation was critical for the future success of the field.

In contribution to the field, my studies in collaboration with my co-authors generated a BAC transgenic mouse in which c-kit expression can be identified easily by EGFP fluorescence. This mouse is listed with Mouse Genome Informatics (MGI) under reference number 3760303 and is a useful tool for the study of a variety of developmental pathways and other pathologies in which c-kit is a target. In addition, my studies were the first to evaluate the redox status of neonatal c-

kit$^+$ CPCs and, in doing so; I identified a number of dysregulated redox targets that influence the capacity of c-kit$^+$ CPCs to differentiate. I also provide a novel method for maintaining the stemness of the c-kit$^+$ CPC population *in vitro* by silencing Nox2- and Nox4-mediated signaling. I hypothesize that this genetically altered population will be more resilient when transplanted into the infarcted heart. Overall, the work presented in this thesis provides value to the field of regenerative cardiology as well as to those researchers interested in the intersection between stem cell and redox biology.

From the data generated in this thesis, I have developed a two part model. Each part is discussed below in detail.

4.2.1 Part I

Here, I describe the identification of a CPC population in the early neonatal heart that co-expresses c-kit and Flk-1 (Figure 4.1). While this is a very heterogeneous population, I have shown in clonal single cell expansions that a single c-kit$^+$ CPC is capable of generating the three lineages that specify the heart: smooth muscle, cardiac, and endothelial, as depicted by left to right progression of a c-kit$^+$Flk-1$^+$ CPC transitioning to the three mature cell types (smooth muscle cells [SMCs], cardiomyocytes [CMs], and endothelial cells [ECs]). To identify committed cells, I utilized α-SMA as a marker of smooth muscle cells, cTnT as a marker of cardiac cells, and PECAM/vWF as markers of endothelial cells all of which are indicated in the figure within each cell type. Emerging evidence suggests that redox mechanisms play important roles in maintaining stemness and in mediating the survival, proliferation, and differentiation of some precursor cell

Figure 4.1. Redox Control over C-kit$^+$ CPC Status and Differentiation (Part I).

C-kit$^+$Flk-1$^+$ CPCs exhibit an increased antioxidant capacity and a decreased pro-oxidant capacity. This protected redox state is thought to contribute to stemness. Over the course of differentiation, a tip in redox balance occurs and results in increased ROS production. This phenomenon is mediated, in part, by the upregulation of Nox2 and Nox4. Downregulated antioxidants have yet to be established. The increase in ROS generation is necessary for the differentiation of c-kit$^+$Flk-1$^+$ CPCs into smooth and cardiac muscle, and, likely, endothelial cells. Legend: ?? = unknown genes; Thin black arrow = progression to mature cell types; Dotted black arrow = possible contribution to mature cell type. Abbreviations: CPC- Cardiac Precursor Cell, ROS- Reactive Oxygen Species, SMC- Smooth Muscle Cell, CM- Cardiomyocyte, EC- Endothelial Cell

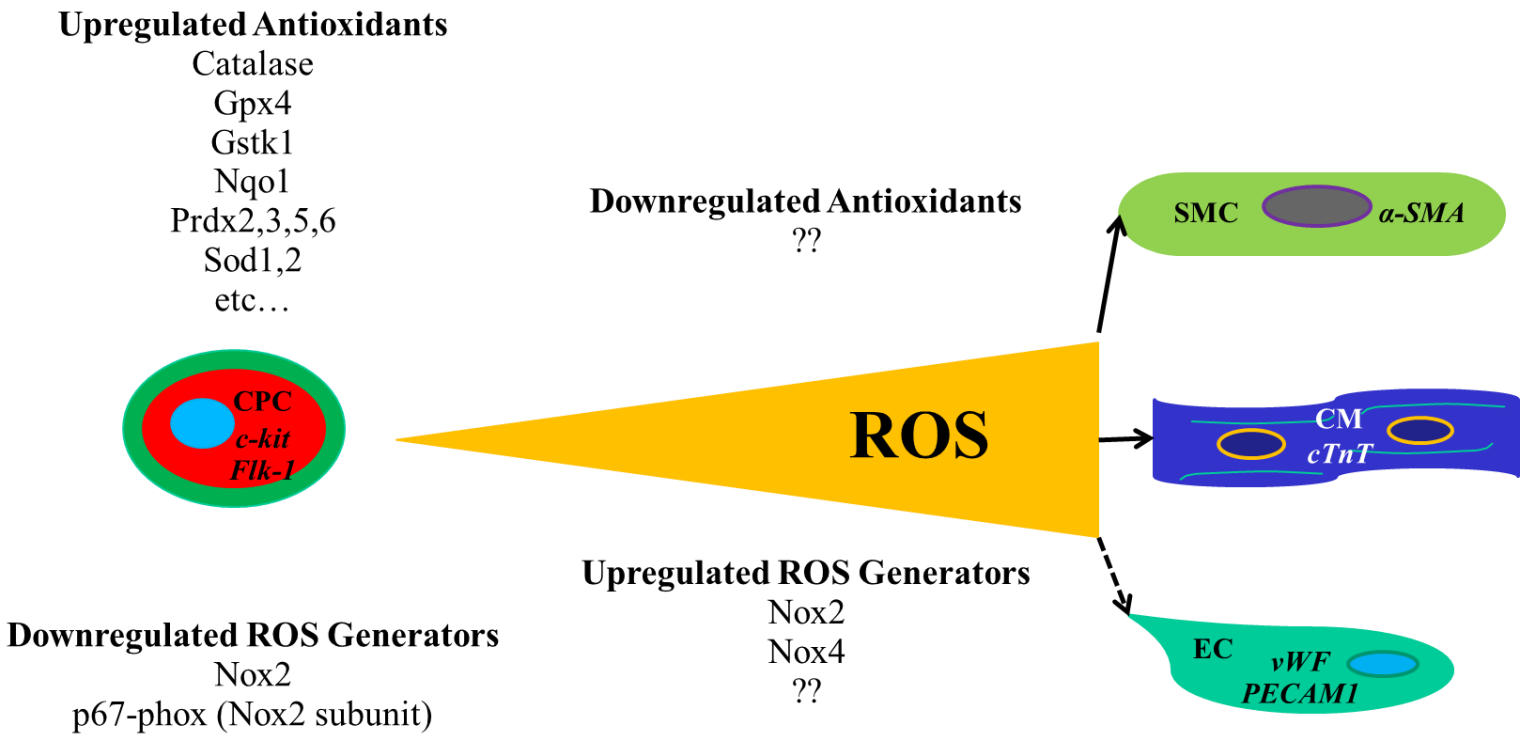
Upregulated Antioxidants
Catalase
Gpx4
Gstk1
Nqo1
Prdx2,3,5,6
Sod1,2
etc…
CPC
c-kit
Flk-1
Downregulated ROS Generators
Nox2
p67-phox (Nox2 subunit)
Downregulated Antioxidants
??
ROS
Upregulated ROS Generators
Nox2
Nox4
??
SMC
α-SMA
CM
cTnT
EC
vWF
PECAM1

types [38-42]. To this end, I found that our c-kit$^+$Flk-1$^+$ CPC population resides in a low ROS niche *in vivo* and, shortly following isolation, *in vitro*. I identified a number of targets through qPCR and RT^{2}Profiler PCR Arrays which contribute to this protected redox state including the upregulation of several antioxidants, a number of which are identified in the diagram (Figure 4.1), and the downregulation of a potent superoxide generator, Nox2, and its critical subunit, p67^{phox}. Increasing levels of ROS, shown in the figure by a swelling of the orange ROS banner, and subsequent redox signaling are thought to drive precursor cell differentiation. Here, I illustrate the upregulation of two pro-oxidants, Nox2 and Nox4, over the course of c-kit$^+$ CPC differentiation. However, I am aware that a tip in redox balance also might include a decrease in the presence of antioxidants and/or dysregulation of additional pro-oxidants not examined in my assays, the determination of which will require further investigation. These unknown targets are represented by question marks within the figure.

4.2.2 Part II

A model of the functional roles for Nox2 and Nox4 in c-kit$^+$ CPC differentiation and alteration of cardiac gene transcript is depicted in Figure 4.2. Following viral knockdown of Nox2 (Figure 4.2A), I noted a significant increase in the expression of precursor cell markers c-kit and in Flk-1. I also noticed a decrease in expression of α-SMA, indicating a reduction in the existence of mature smooth muscle cells. This occurred in a Nox isoform specific manner. In trying to tease apart the mechanisms by which silencing Nox2 altered the differentiation status of c-kit$^+$ CPCs, I investigated the expression levels of several transcriptions factors and cytokines involved in mesodermal development. As

Figure 4.2. Functional Roles for Nox2 and Nox4 in C-kit$^+$ CPC Differentiation (Part II). (A) In AdsiNox2 treated CPCs, there was a significant increase in transcript level for CPC markers, c-kit and Flk-1, and cytokine, TGF-β1, along with a decrease in mRNA level for transcription factor, Gata6, and mature smooth muscle marker, α-SMA. (B) In AdsiNox4 treated CPCs, there was a significant increase in transcript level for Flk-1, transcription factor, Gata4, and TGF-β1, along with a decrease in mRNA level for mature cardiac marker, cTnT. (C) In AdsiNox2/4 treated CPCs, there was a significant increase in transcript level for c-kit, Flk-1, Gata4, and TGF-β1, along with a decrease in mRNA level for Gata 6 and mature markers, α-SMA and cTnT. Legend: Thin black arrow = direction of differentiation; Dotted black arrow = possible contribution to mature cell type; Strike-through = silenced gene; Thick upward black arrow = increase in transcript; Thick downward black arrow = decrease in transcript; n.c. = no change in transcript. Abbreviations: E-PC- Endothelial Precursor Cell, SM-PC- Smooth Muscle Precursor Cell, CM-PC- Cardiomyocyte Precursor Cell, EC- Endothelial Cell, SMC- Smooth Muscle Cell, CM- Cardiomyocyte

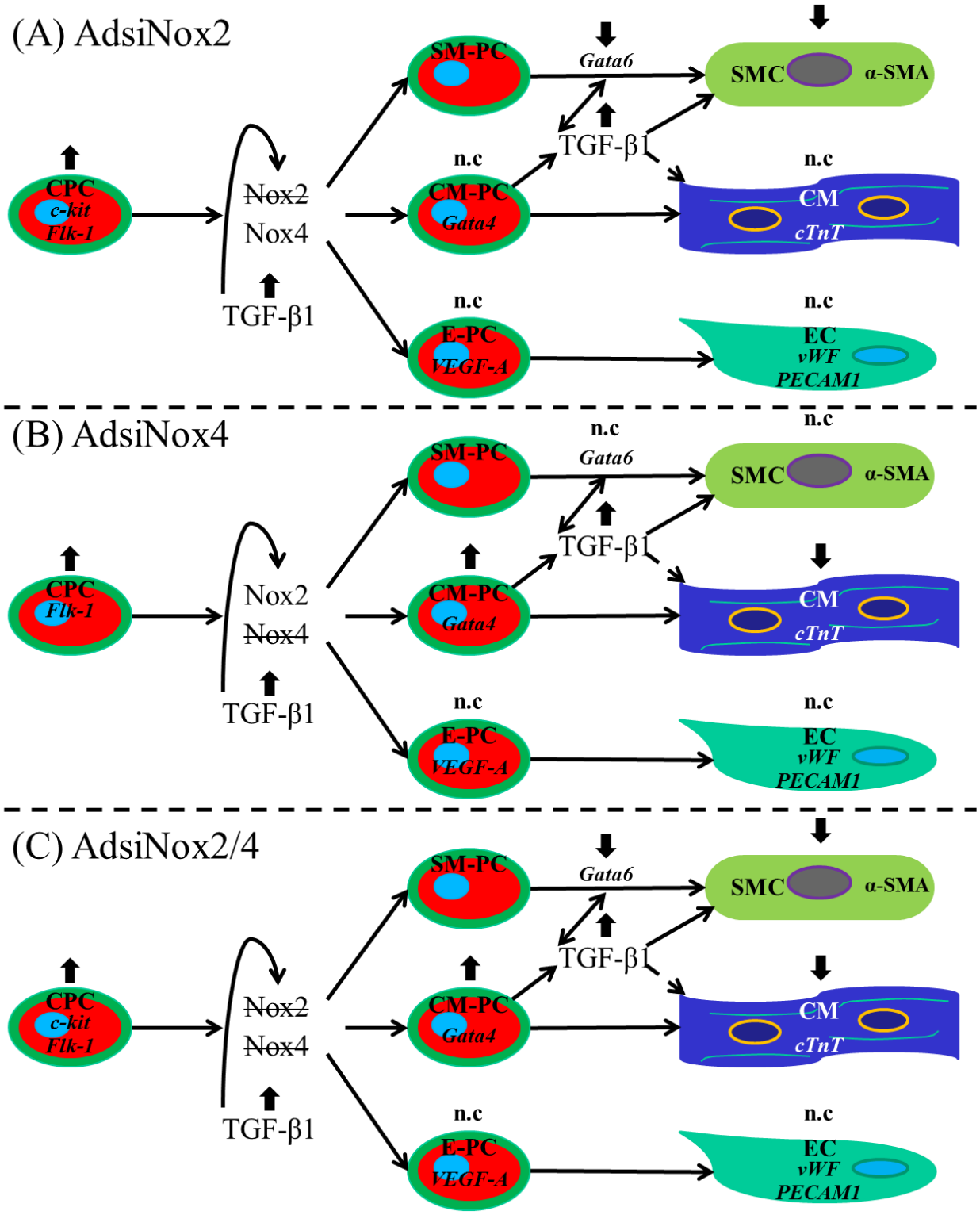
(A) AdsiNox2
CPC
c-kit
Flk-1
Nox2
Nox4
TGF-β1
SM-PC
Gata6
SMC
α-SMA
TGF-β1
n.c
CM-PC
Gata4
n.c
CM
cTnT
n.c
E-PC
VEGF-A
n.c
EC
vWF
PECAM1
(B) AdsiNox4
CPC
Flk-1
Nox2
Nox4
TGF-β1
n.c
SM-PC
Gata6
n.c
SMC
α-SMA
TGF-β1
CM-PC
Gata4
CM
cTnT
n.c
E-PC
VEGF-A
n.c
EC
vWF
PECAM1
(C) AdsiNox2/4
CPC
c-kit
Flk-1
Nox2
Nox4
TGF-β1
SM-PC
Gata6
SMC
α-SMA
TGF-β1
CM-PC
Gata4
CM
cTnT
n.c
E-PC
VEGF-A
n.c
EC
vWF
PECAM1

depicted in the model (Figure 4.2A), I saw a significant reduction in Gata6 expression as well as a rise in TGF-β1. This is not surprising given the literature which suggests negative regulation of TGF-β1 by Gata6 [59] and the necessity of Gata6 for the maintenance of a mature phenotype in VSMCs [60]. As such, I believe that an intricate feedback loop, shown by the bi-directional black arrow linking TGF-β1 and Gata6, may be at work between these two molecules and, ultimately, there is a need for sufficient Gata6 expression to maintain mature smooth muscle cells. Interestingly, knockdown of Nox2 led to a statistically significant decrease in the percent of cells positive for cTnT (not depicted), even though the level of cTnT transcript was unchanged from control, suggesting critical roles for additional transcription factors, cytokines, and signaling pathways that are yet to be uncovered. In this condition, I saw no change in either VEGF-A, a growth factor necessary for endothelial cell differentiation, or vWF expression, suggesting little effect on the endothelial cell fate.

After silencing Nox4 (Figure 4.2B), I saw a significant upregulation of Flk-1 expression as well as no change in smooth muscle cell commitment, even though an upregulation of TGF-β1 was observed. This further verifies a crucial role for adequate Gata6 levels in the progression of c-kit$^+$ CPCs to the mature smooth muscle cell phenotype. This finding also leaves open the possibility of alternative regulators of Gata6 that were not examined in my studies. The fact that I did not observe any change in α-SMA at the transcript or protein level (not depicted) in this condition suggests that Nox4 does not play an important role in smooth muscle cell generation in our system even though it does in ESCs [54]. Knockdown of Nox4 did, however, exhibit a cardiac specific phenotype,

resulting in increased expression of Gata4 which marks the early cardiac fate and decreased expression of the more mature cardiac cell marker cTnT. As Gata4 is regulated through both ROS-dependent and ROS-independent pathways, I hypothesize that the increase in Gata4 observed after silencing Nox4 is a result of a ROS-independent and antioxidant-sensitive mechanism [61]. This is further supported by the fact that Gata4 is a retinoic-acid inducible transcription factor in the heart [62]. Additional studies are required to elucidate these pathways and determine which is at work in this system. As seen in the AdsiNox2 condition (Figure 4.2A), I saw no changes in expression of VEGF-A or vWF.

Finally, the concomitant suppression of Nox2 and Nox4 (Figure 4.2C) led to a significant increase in both c-kit and Flk-1 expression, suggesting the strongest commitment to the precursor cell state. Interestingly, the rise in Flk-1 was even more robust than the increases observed with either virus alone (not depicted), signifying some convergence of Nox-mediated signaling. TGF-β1 also demonstrated a strong upregulation in this condition, along with further suppression of smooth muscle cell commitment. This finding is at odds with a recent report that TGF-β1 and notch signaling mediate stem cell differentiation into smooth muscle cells [55], and I speculate that the notch pathway might be compromised by Nox deficiency. Additional experiments are required to address this hypothesis. While the expression of Gata4 remained the same as that observed with the knockdown of Nox4 alone, I observed an even more substantial downregulation of cTnT (not depicted). I hypothesize that the robust increase in TGF-β1 might be playing a role here, as our studies from Chapter 2 revealed that addition of TGF-β1 to the culture

medium led to a significant decrease in cardiac commitment. More experimentation is necessary to determine if TGF-β1 is acting agonist or antagonist to cardiac commitment in this system, this uncertainty is depicted by the dotted black arrow (Figure 4.2). The considerable increase in TGF-β1 might also reflect an even broader feedback loop in cells faced with a drastic loss of Nox signaling, as TGF-β1 is a known activator of Nox enzymes. This feedback looks is shown by an arrow linking TGF-β1 to Nox2 and Nox4 transcript expression (Figure 4.2). In the combined viral condition (Figure 4.2C), there was no effect on VEGF-A or vWF expression, suggesting a minimal roles for Nox2- and Nox4-mediated signaling in endothelial cell commitment. It remains to be seen how well this genetically altered population fairs when transplanted into the infarcted heart. Although, I suspect that increased expression of stemness genes and an overall lower ROS state will give these cells a survival advantage and allow them to engraft in the hostile environment of the ischemic myocardium.

4.3 Future Directions

While I feel that these studies have provided insight into the molecular foundations of c-kit$^+$ CPC function, the findings introduce new questions that need to be addressed to fully understand the mechanisms controlling c-kit$^+$ CPC stemness and differentiation. Several of these questions are discussed in detail below.

1) In addition to changes observed in transcription factor and cytokine expression following transduction with AdsiNox2 and AdsiNox4, what signaling pathways are involved in Nox2- and Nox4-mediated c-kit$^+$ CPC specification?

Based on studies in ESCs, it is known that Nox-derived ROS act through signaling pathways such as Jak/STAT and ERK1/2 as well as redox sensitive transcriptions factors like NF- κβ to exert their effects on cardiac differentiation [17, 63, 64]. In addition, there is very clear evidence implicating Nox4-derived ROS in p38MAPK activity and the translocation of cardiac transcription factor, Mef2c, to the nucleus [51]. Additional studies suggest a critical relationship between Nox-derived ROS and eNOS phosphorylation which modulates ESC-mediated cardiomyogenesis [50, 65]. Therefore, I propose to carry out a series of Western immunoblots to detect phosphorylation of some of these key molecules including p-JAK, p-STAT, p-ERK1/2, p-p38MAPK, and p-eNOS following treatment of c-kit$^+$ CPCS with AdsiNox2, AdsiNox4, AdsiNox2/4, or AdsiCON. As described by Shah, et al. [66], it is well-established that the Nox isoforms mediate distinct cell signaling for a variety of reasons including divergent subcellular localization. Therefore, I predict that these studies will elucidate the mechanisms by which Nox2- and Nox4-derived ROS facilitate c-kit$^+$ CPC differentiation along the smooth muscle and cardiac lineages, respectively, as well as shed light upon their convergent signaling pathways. Further teasing apart these signaling pathways will also help me understand the alterations that I observed in Gata6, Gata4, and TGF-β1 expression following viral knockdown of Nox2 and Nox4 (Chapter 3: Figure 3.8) and will lead to a more accurate model of c-kit$^+$ CPC specification.

2) In addition to an increase in stemness gene expression and a decrease in cardiac cell lineage commitment, do c-kit$^+$ CPCs transduced with AdsiNox2 and AdsiNox4 also regain a protected low ROS profile?

In order to address this question, first I propose to perform DHE microfluorography as in Chapter 3: Figure 3.2, except here I will measure ROS levels 7 days following infection with

AdsiNox2, AdsiNox4, AdsiNox2/4, or AdsiCON. While our laboratory has performed similar studies both in cultured cells as well as *in vivo* [67, 68], I understand the importance of this verification in my system. Following confirmation of a functional decrease in ROS production after knockdown of Nox2 and Nox4, next, I will perform RT^{2}Profiler PCR Arrays as in Chapter 3: Figure 3.9 and Tables 3.2 and 3.3 to measure the mRNA expression levels of 84 different genes involved in *Mouse Oxidative Stress and Antioxidant Defense* 7 days following viral transduction. This will allow me to compare the expression levels of each of the redox genes following knockdown of Nox2 and Nox4 to those already established for freshly isolated c-kit$^+$ CPCs. I suspect that the more differentiated AdsiCON cells will show a tip in redox balance to a more oxidized state compared to freshly isolated c-kit$^+$ CPCs as I already know that Nox2 and Nox4 are unregulated by Day 14 of differentiation. In addition, I expect that each of the Nox knockdown conditions will demonstrate a more reduced phenotype, a profile similar to that observed in freshly isolated c-kit$^+$ CPCs. This reversal to a more protected redox state also has been observed in iPSCs [69]. I speculate that these studies will provide additional redox targets that will be useful in genetic strategies for cardiac repair.

3) What is the regenerative potential of our c-kit$^+$ CPC population genetically modified to silence expression of Nox2 and Nox4 *in vivo*? How can we trace these cells after transplantation into the infarcted myocardium?

Up to this point, I have focused mainly on determining how altered expression of Nox isoforms in c-kit$^+$ CPCs through viral manipulation can impact their precursor status and differentiation *in vitro*. Here, I will investigate the regenerative capacity of genetically altered c-kit$^+$ CPCs in the infarct region as it is well-established that free radicals are a major underlying mechanism of

graft cell death [70]. In order to determine the survival rate and proliferative capacity of c-kit$^+$ CPCs genetically engineered for Nox isoforms (Nox2 and Nox4) and a luciferase reporter, I propose to use *in vivo* bioluminescence following transplantation which is a monitoring tool widely used in small animal studies. I anticipate that c-kit$^+$ CPCs transduced with AdsiNox2 and AdsiNox4 will demonstrate increased survival and proliferation in and around the infarct region compared to AdsiCON treated cells as indicated by increased photon emission over longer periods of time.

To determine the potential of genetically engineered c-kit$^+$ CPCs to differentiate into cardiomyocytes *in vivo*, mice will be sacrificed for immunohistochemistry at several time-points post-MI and quantification of differentiation into the three cardiac lineages will be established. Because both c-kit$^+$ CPCs isolated from c-kit^{BAC}-EGFP mice and the Ad-vectors carry EGFP reporters, AdLuciferase immunostaining will be utilized to distinguish between transplanted and endogenous cells. I hypothesize that knockdown of the Noxes will give survival advantage to transplanted cells during the first week post-MI, a period known to be hostile to therapeutic populations, and, thereafter, either exogenous ROS or Nox-mediated ROS production after transient transgene expression diminishes, will allow these cells to differentiate effectively. Although I am most interested in an increase in cardiomyocyte generation as indicated by the presence of cTnT, I will also analyze cardiac sections for early cardiac marker Gata4 as well as markers for smooth muscle cells (Gata6 and α-SMA) and endothelial cells (PECAM1 and vWF) to determine the fate of injected c-kit$^+$ CPCs.

If I observe significant cardiac regeneration, I am prepared to perform functional studies utilizing the Vevo 770 high-resolution imaging system (VisualSonics) in a subset of mice as described by

our laboratory [71]. In addition, I am cognizant of the limitations of adenoviral gene transfer to mediate long-term transduction of cardiac tissue [72], however our laboratory's studies suggest that gene expression peaks and remains viable through at least Day 14 [73]. I am prepared in future studies to employ other viral vectors such as lentiviruses and adeno-associated viruses to study longer time-points if warranted. The use of lentiviruses for genetic modification of therapeutic cell populations provides a unique advantage in that self-renewal, clonogenicity, and multipotentiality can be analyzed *in vivo* by detecting viral integration sites through PCR [74]. Utilizing a fluorescent reporter, CPCs transduced with virus can be isolated by FACS and separated by lineage using commercially available antibodies to identify smooth muscle, cardiac, and endothelial cells. Clones and their progeny then can be identified as those having identical molecular weight bands corresponding to the viral site of integration into the host genome. While this method would provide critical information regarding the stemness and differentiation capacity of genetically altered cells, I am unsure of the biological impact that long-term silencing of Nox2 and Nox4 will have on c-kit$^+$ CPCs, as it is clear that these two Nox isoforms are critical for their final differentiation into smooth and cardiac muscle.

4) What other modifications might improve the survival, engraftment, and regenerative ability of our genetically altered c-kit$^+$ CPC population?

It is well-known that extracellular matrices play an essential role in myocardial function and provide critical signaling for precursor cell recruitment, activation, and maturation. Therefore, researchers in the field of regenerative cardiology have begun to investigate biomaterials as a way to enhance CPC engraftment and function in the damaged myocardium. In animal models, it has been demonstrated that biomaterials such as collagen and fibrin increase retention of

exogenously delivered precursor cells in the ischemic region and limit redistribution to other organs in the body [75, 76]. In addition, delivery of proteins such as IGF-1, a growth factor known to play an important role in cardiomyogenesis, can be achieved through the use of biotinylated self-assembling peptides. When introduced alongside cardiac stem cells, addition of IGF-1 enhanced myocardial function and increased the generation of mature cardiomyocytes [77]. Tissue engineering also can alter the physical microenvironment of therapeutic cell populations by accounting for important characteristics such as matrix stiffness, nanotopography, and mechanosensory stimuli [78]. Therefore, collaboration with tissue bioengineers is not only advised, but likely will prove necessary for cell-based therapy to reach its full potential in clinical trials.

More long-term goals will be to analyze the c-kit$^+$ CPC population at the level of the proteome and epigenome. While microarrays and microRNA microarrays are invaluable tools that have led to critical discoveries in the field of regenerative cardiology, it is well known that the transcriptome is not linearly proportional to the proteome and, often, the quantification of mRNA levels is not sufficient to fully understand intricate signaling pathways such as those directing CPC differentiation [79]. Utilizing modern tools available in proteomics research, it is possible to compare protein profiles of CPCs to those of CPC-derived smooth, cardiac, and endothelial cells as well as CPC-derived committed cells to their mature counterparts within the heart. This type of analysis not only will reveal the pathways involved in CPC differentiation, but also the validity of utilizing CPC-derived mature cells in cardiac repair [80]. In addition, it is clear that epigenetic modifications such as methylation, post-translational histone modification, and chromatin remodeling are critically involved in stemness and lineage specification [81, 82]. Therefore, understanding the epigenetic modifications involved in c-kit$^+$ CPC stemness and

differentiation as well as the stimuli that trigger these events will provide additional avenues for enhancing the regenerative capacity of c-kit$^+$ CPCs *in vivo*.

4.4 Concluding Remarks

In this thesis, I have provided clear evidence regarding the stemness of early neonatal c-kit$^+$ CPCs and data to suggest strong redox influence over c-kit$^+$ CPC status and differentiation. I have also highlighted several target molecules, transcription factors, and a cytokine that are involved in c-kit$^+$ CPC stemness and differentiation as well as proposed additional experiments to further unravel the molecular complexities of c-kit$^+$ CPC function along with strategies to enhance their therapeutic potential *in vivo*. While my studies provide some of the earliest attempts to understand the roles for ROS in CPC biology, I recognize that there is still a lot to learn before clinical application is warranted. As such, the interplay between redox biology and c-kit$^+$ CPC state is still a very active area of research and discovery, which likely will lead to a more precise understanding of the pathways and molecules involved in c-kit$^+$ CPC lineage commitment.

4.5 References

1. Lloyd-Jones D, Adams RJ, Brown TM, Carnethon M, Dai S, De Simone G, Ferguson TB, Ford E, Furie K, Gillespie C, Go A, Greenlund K, Haase N, Hailpern S, Ho PM, Howard V, Kissela B, Kittner S, Lackland D, Lisabeth L, Marelli A, McDermott MM, Meigs J, Mozaffarian D, Mussolino M, Nichol G, Roger VL, Rosamond W, Sacco R, Sorlie P, Stafford R, Thom T, Wasserthiel-Smoller S, Wong ND, Wylie-Rosett J, American Heart Association Statistics Committee and Stroke Statistics Subcommittee. Executive summary: Heart disease and stroke statistics--2010 update: A report from the american heart association. *Circulation*. 2010;121:948-954.

2. Bergmann O, Bhardwaj RD, Bernard S, Zdunek S, Barnabe-Heider F, Walsh S, Zupicich J, Alkass K, Buchholz BA, Druid H, Jovinge S, Frisen J. Evidence for cardiomyocyte renewal in humans. *Science*. 2009;324:98-102.

3. Kajstura J, Gurusamy N, Ogorek B, Goichberg P, Clavo-Rondon C, Hosoda T, D'Amario D, Bardelli S, Beltrami AP, Cesselli D, Bussani R, del Monte F, Quaini F, Rota M, Beltrami CA, Buchholz BA, Leri A, Anversa P. Myocyte turnover in the aging human heart. *Circ Res*. 2010;107:1374-1386.

4. Beltrami AP, Barlucchi L, Torella D, Baker M, Limana F, Chimenti S, Kasahara H, Rota M, Musso E, Urbanek K, Leri A, Kajstura J, Nadal-Ginard B, Anversa P. Adult cardiac stem cells are multipotent and support myocardial regeneration. *Cell,*. 2003;114:763-776.

5. Wu SM, Fujiwara Y, Cibulsky SM, Clapham DE, Lien C, Schultheiss TM, Orkin SH. Developmental origin of a bipotential myocardial and smooth muscle cell precursor in the mammalian heart. *Cell,*. 2006;127:1137-1150.

6. Tallini YN, Greene KS, Craven M, Spealman A, Breitbach M, Smith J, Fisher PJ, Steffey M, Hesse M, Doran RM, Woods A, Singh B, Yen A, Fleischmann BK, Kotlikoff MI. C-kit expression identifies cardiovascular precursors in the neonatal heart. *Proc Natl Acad Sci U S A*. 2009;106:1808-1813.

7. Messina E, De Angelis L, Frati G, Morrone S, Chimenti S, Fiordaliso F, Salio M, Battaglia M, Latronico MV, Coletta M, Vivarelli E, Frati L, Cossu G, Giacomello A. Isolation and expansion of adult cardiac stem cells from human and murine heart. *Circ Res*. 2004;95:911-921.

8. Bearzi C, Rota M, Hosoda T, Tillmanns J, Nascimbene A, De Angelis A, Yasuzawa-Amano S, Trofimova I, Siggins RW, Lecapitaine N, Cascapera S, Beltrami AP, D'Alessandro DA, Zias E, Quaini F, Urbanek K, Michler RE, Bolli R, Kajstura J, Leri A, Anversa P. Human cardiac stem cells. *Proc Natl Acad Sci U S A*. 2007;104:14068-14073.

9. Hori M, Nishida K. Oxidative stress and left ventricular remodelling after myocardial infarction. *Cardiovasc Res*. 2009;81:457-464.

10. Leri A, Kajstura J, Anversa P. Role of cardiac stem cells in cardiac pathophysiology: A paradigm shift in human myocardial biology. *Circ Res*. 2011;109:941-961.

11. Hosoda T, Rota M, Kajstura J, Leri A, Anversa P. Role of stem cells in cardiovascular biology. *J Thromb Haemost*. 2011;9 Suppl 1:151-161.

12. Cairns LA, Moroni E, Levantini E, Giorgetti A, Klinger FG, Ronzoni S, Tatangelo L, Tiveron C, De Felici M, Dolci S, Magli MC, Giglioni B, Ottolenghi S. Kit regulatory elements required for expression in developing hematopoietic and germ cell lineages. *Blood*. 2003;102:3954-3962.

13. Wouters M, Smans K, Vanderwinden JM. WZsGreen/+: A new green fluorescent protein knock-in mouse model for the study of KIT-expressing cells in gut and cerebellum. *Physiol Genomics*. 2005;22:412-421.

14. Giraldo P, Montoliu L. Size matters: Use of YACs, BACs and PACs in transgenic animals. *Transgenic Res*. 2001;10:83-103.

15. Yang XW, Gong S. An overview on the generation of BAC transgenic mice for neuroscience research. *Curr Protoc Neurosci*. 2005;Chapter 5:Unit 5.20.

16. Urbanek K, Cesselli D, Rota M, Nascimbene A, De Angelis A, Hosoda T, Bearzi C, Boni A, Bolli R, Kajstura J, Anversa P, Leri A. Stem cell niches in the adult mouse heart. *Proc Natl Acad Sci U S A*. 2006;103:9226-9231.

17. Sauer H, Rahimi G, Hescheler J, Wartenberg M. Effects of electrical fields on cardiomyocyte differentiation of embryonic stem cells. *J Cell Biochem*. 1999;75:710-723.

18. Serena E, Figallo E, Tandon N, Cannizzaro C, Gerecht S, Elvassore N, Vunjak-Novakovic G. Electrical stimulation of human embryonic stem cells: Cardiac differentiation and the generation of reactive oxygen species. *Exp Cell Res*. 2009.

19. Schmelter M, Ateghang B, Helmig S, Wartenberg M, Sauer H. Embryonic stem cells utilize reactive oxygen species as transducers of mechanical strain-induced cardiovascular differentiation. *FASEB J*. 2006;20:1182-1184.

20. Gude N, Muraski J, Rubio M, Kajstura J, Schaefer E, Anversa P, Sussman MA. Akt promotes increased cardiomyocyte cycling and expansion of the cardiac progenitor cell population. *Circ Res*. 2006;99:381-388.

21. Craven M, Kotlikoff MI, Nadworny AS. C-kit expression identifies cardiac precursor cells in neonatal mice. *Methods Mol Biol*. 2012;843:177-189.

22. Anversa P, Kajstura J, Leri A, Bolli R. Life and death of cardiac stem cells: A paradigm shift in cardiac biology. *Circulation*. 2006;113:1451-1463.

23. Drapeau J, El-Helou V, Clement R, Bel-Hadj S, Gosselin H, Trudeau LE, Villeneuve L, Calderone A. Nestin-expressing neural stem cells identified in the scar following myocardial infarction. *J Cell Physiol*. 2005;204:51-62.

24. Scobioala S, Klocke R, Kuhlmann M, Tian W, Hasib L, Milting H, Koenig S, Stelljes M, El-Banayosy A, Tenderich G, Michel G, Breithardt G, Nikol S. Up-regulation of nestin in the infarcted myocardium potentially indicates differentiation of resident cardiac stem cells into various lineages including cardiomyocytes. *FASEB J*. 2008;22:1021-1031.

25. Kattman SJ, Huber TL, Keller GM. Multipotent flk-1+ cardiovascular progenitor cells give rise to the cardiomyocyte, endothelial, and vascular smooth muscle lineages. *Dev Cell*. 2006;11:723-732.

26. Yang L, Soonpaa MH, Adler ED, Roepke TK, Kattman SJ, Kennedy M, Henckaerts E, Bonham K, Abbott GW, Linden RM, Field LJ, Keller GM. Human cardiovascular progenitor cells develop from a KDR+ embryonic-stem-cell-derived population. *Nature*. 2008;453:524-528.

27. Bu L, Jiang X, Martin-Puig S, Caron L, Zhu S, Shao Y, Roberts DJ, Huang PL, Domian IJ, Chien KR. Human ISL1 heart progenitors generate diverse multipotent cardiovascular cell lineages. *Nature*. 2009;460:113-117.

28. Dodou E, Verzi MP, Anderson JP, Xu SM, Black BL. Mef2c is a direct transcriptional target of ISL1 and GATA factors in the anterior heart field during mouse embryonic development. *Development*. 2004;131:3931-3942.

29. Kolossov E, Lu Z, Drobinskaya I, Gassanov N, Duan Y, Sauer H, Manzke O, Bloch W, Bohlen H, Hescheler J, Fleischmann BK. Identification and characterization of embryonic stem cell-derived pacemaker and atrial cardiomyocytes. *FASEB J*. 2005;19:577-579.

30. Gryshchenko O, Fischer IR, Dittrich M, Viatchenko-Karpinski S, Soest J, Bohm-Pinger MM, Igelmund P, Fleischmann BK, Hescheler J. Role of ATP-dependent K(+) channels in the electrical excitability of early embryonic stem cell-derived cardiomyocytes. *J Cell Sci*. 1999;112 (Pt 17):2903-2912.

31. Kuzmenkin A, Liang H, Xu G, Pfannkuche K, Eichhorn H, Fatima A, Luo H, Saric T, Wernig M, Jaenisch R, Hescheler J. Functional characterization of cardiomyocytes derived from murine induced pluripotent stem cells in vitro. *FASEB J*. 2009;23:4168-4180.

32. Lee ST, White AJ, Matsushita S, Malliaras K, Steenbergen C, Zhang Y, Li TS, Terrovitis J, Yee K, Simsir S, Makkar R, Marban E. Intramyocardial injection of autologous cardiospheres or cardiosphere-derived cells preserves function and minimizes adverse ventricular remodeling in pigs with heart failure post-myocardial infarction. *J Am Coll Cardiol*. 2011;57:455-465.

33. Ivanova NB, Dimos JT, Schaniel C, Hackney JA, Moore KA, Lemischka IR. A stem cell molecular signature. *Science*. 2002;298:601-604.

34. Ramalho-Santos M, Yoon S, Matsuzaki Y, Mulligan RC, Melton DA. "Stemness": Transcriptional profiling of embryonic and adult stem cells. *Science*. 2002;298:597-600.

35. Dernbach E, Urbich C, Brandes RP, Hofmann WK, Zeiher AM, Dimmeler S. Antioxidative stress-associated genes in circulating progenitor cells: Evidence for enhanced resistance against oxidative stress. *Blood*. 2004;104:3591-3597.

36. Jang YY, Sharkis SJ. A low level of reactive oxygen species selects for primitive hematopoietic stem cells that may reside in the low-oxygenic niche. *Blood*. 2007;110:3056-3063.

37. Owusu-Ansah E, Banerjee U. Reactive oxygen species prime drosophila haematopoietic progenitors for differentiation. *Nature*. 2009;461:537-541.

38. Noble M, Mayer-Proschel M, Proschel C. Redox regulation of precursor cell function: Insights and paradoxes. *Antioxid Redox Signal*. 2005;7:1456-1467.

39. Haneline LS. Redox regulation of stem and progenitor cells. *Antioxid Redox Signal*. 2008;10:1849-1852.

40. Ogasawara MA, Zhang H. Redox regulation and its emerging roles in stem cells and stem-like cancer cells. *Antioxid Redox Signal*. 2008.

41. Pervaiz S, Taneja R, Ghaffari S. Oxidative stress regulation of stem and progenitor cells. *Antioxid Redox Signal*. 2009.

42. Ushio-Fukai M, Urao N. Novel role of NADPH oxidase in angiogenesis and stem/progenitor cell function. *Antioxid Redox Signal*. 2009;11:2517-2533.

43. Griendling KK. Novel NAD(P)H oxidases in the cardiovascular system. *Heart*. 2004;90:491-493.

44. Cave AC, Brewer AC, Narayanapanicker A, Ray R, Grieve DJ, Walker S, Shah AM. NADPH oxidases in cardiovascular health and disease. *Antioxid Redox Signal*. 2006;8:691-728.

45. Akki A, Zhang M, Murdoch C, Brewer A, Shah AM. NADPH oxidase signaling and cardiac myocyte function. *J Mol Cell Cardiol*. 2009;47:15-22.

46. Piao YJ, Seo YH, Hong F, Kim JH, Kim YJ, Kang MH, Kim BS, Jo SA, Jo I, Jue DM, Kang I, Ha J, Kim SS. Nox 2 stimulates muscle differentiation via NF-kappaB/iNOS pathway. *Free Radic Biol Med*. 2005;38:989-1001.

47. Chen Z, Keaney JF,Jr, Schulz E, Levison B, Shan L, Sakuma M, Zhang X, Shi C, Hazen SL, Simon DI. Decreased neointimal formation in Nox2-deficient mice reveals a direct role for NADPH oxidase in the response to arterial injury. *Proc Natl Acad Sci U S A*. 2004;101:13014-13019.

48. Urao N, Inomata H, Razvi M, Kim HW, Wary K, McKinney R, Fukai T, Ushio-Fukai M. Role of nox2-based NADPH oxidase in bone marrow and progenitor cell function involved in neovascularization induced by hindlimb ischemia. *Circ Res*. 2008;103:212-220.

49. Buggisch M, Ateghang B, Ruhe C, Strobel C, Lange S, Wartenberg M, Sauer H. Stimulation of ES-cell-derived cardiomyogenesis and neonatal cardiac cell proliferation by reactive oxygen species and NADPH oxidase. *J Cell Sci*. 2007;120:885-894.

50. Bartsch C, Bekhite MM, Wolheim A, Richter M, Ruhe C, Wissuwa B, Marciniak A, Muller J, Heller R, Figulla HR, Sauer H, Wartenberg M. NADPH oxidase and eNOS control cardiomyogenesis in mouse embryonic stem cells on ascorbic acid treatment. *Free Radic Biol Med*. 2011.

51. Li J, Stouffs M, Serrander L, Banfi B, Bettiol E, Charnay Y, Steger K, Krause KH, Jaconi ME. The NADPH oxidase NOX4 drives cardiac differentiation: Role in regulating cardiac transcription factors and MAP kinase activation. *Mol Biol Cell*. 2006;17:3978-3988.

52. Behfar A, Zingman LV, Hodgson DM, Rauzier JM, Kane GC, Terzic A, Puceat M. Stem cell differentiation requires a paracrine pathway in the heart. *FASEB J*. 2002;16:1558-1566.

53. Sinha S, Hoofnagle MH, Kingston PA, McCanna ME, Owens GK. Transforming growth factor-beta1 signaling contributes to development of smooth muscle cells from embryonic stem cells. *Am J Physiol Cell Physiol*. 2004;287:C1560-8.

54. Xiao Q, Luo Z, Pepe AE, Margariti A, Zeng L, Xu Q. Embryonic stem cell differentiation into smooth muscle cells is mediated by Nox4-produced H2O2. *Am J Physiol Cell Physiol*. 2009;296:C711-23.

55. Kurpinski K, Lam H, Chu J, Wang A, Kim A, Tsay E, Agrawal S, Schaffer DV, Li S. Transforming growth factor-beta and notch signaling mediate stem cell differentiation into smooth muscle cells. *Stem Cells*. 2010;28:734-742.

56. Menasche P, Alfieri O, Janssens S, McKenna W, Reichenspurner H, Trinquart L, Vilquin JT, Marolleau JP, Seymour B, Larghero J, Lake S, Chatellier G, Solomon S, Desnos M, Hagege AA. The myoblast autologous grafting in ischemic cardiomyopathy (MAGIC) trial: First randomized placebo-controlled study of myoblast transplantation. *Circulation*. 2008;117:1189-1200.

57. Smith RR, Barile L, Cho HC, Leppo MK, Hare JM, Messina E, Giacomello A, Abraham MR, Marban E. Regenerative potential of cardiosphere-derived cells expanded from percutaneous endomyocardial biopsy specimens. *Circulation*. 2007;115:896-908.

58. Itzhaki-Alfia A, Leor J, Raanani E, Sternik L, Spiegelstein D, Netser S, Holbova R, Pevsner-Fischer M, Lavee J, Barbash IM. Patient characteristics and cell source determine the number of isolated human cardiac progenitor cells. *Circulation*. 2009;120:2559-2566.

59. Froese N, Kattih B, Breitbart A, Grund A, Geffers R, Molkentin JD, Kispert A, Wollert KC, Drexler H, Heineke J. GATA6 promotes angiogenic function and survival in endothelial cells by suppression of autocrine transforming growth factor {beta}/Activin receptor-like kinase 5 signaling. *J Biol Chem*. 2011;286:5680-5690.

60. Abe M, Hasegawa K, Wada H, Morimoto T, Yanazume T, Kawamura T, Hirai M, Furukawa Y, Kita T. GATA-6 is involved in PPARgamma-mediated activation of differentiated phenotype in human vascular smooth muscle cells. *Arterioscler Thromb Vasc Biol*. 2003;23:404-410.

61. Suzuki YJ. Cell signaling pathways for the regulation of GATA4 transcription factor: Implications for cell growth and apoptosis. *Cell Signal*. 2011;23:1094-1099.

62. Arceci RJ, King AA, Simon MC, Orkin SH, Wilson DB. Mouse GATA-4: A retinoic acid-inducible GATA-binding transcription factor expressed in endodermally derived tissues and heart. *Mol Cell Biol*. 1993;13:2235-2246.

63. Sauer H, Rahimi G, Hescheler J, Wartenberg M. Role of reactive oxygen species and phosphatidylinositol 3-kinase in cardiomyocyte differentiation of embryonic stem cells. *FEBS Lett*. 2000;476:218-223.

64. Sauer H, Neukirchen W, Rahimi G, Grunheck F, Hescheler J, Wartenberg M. Involvement of reactive oxygen species in cardiotrophin-1-induced proliferation of cardiomyocytes differentiated from murine embryonic stem cells. *Exp Cell Res*. 2004;294:313-324.

65. Milosevic N, Bekhite MM, Sharifpanah F, Ruhe C, Wartenberg M, Sauer H. Redox stimulation of cardiomyogenesis versus inhibition of vasculogenesis upon treatment of mouse embryonic stem cells with thalidomide. *Antioxid Redox Signal*. 2010;13:1813-1827.

66. Anilkumar N, Weber R, Zhang M, Brewer A, Shah AM. Nox4 and nox2 NADPH oxidases mediate distinct cellular redox signaling responses to agonist stimulation. *Arterioscler Thromb Vasc Biol*. 2008;28:1347-1354.

67. Hingtgen SD, Tian X, Yang J, Dunlay SM, Peek AS, Wu Y, Sharma RV, Engelhardt JF, Davisson RL. Nox2-containing NADPH oxidase and akt activation play a key role in angiotensin II-induced cardiomyocyte hypertrophy. *Physiol Genomics*. 2006;26:180-191.

68. Peterson JR, Burmeister MA, Tian X, Zhou Y, Guruju MR, Stupinski JA, Sharma RV, Davisson RL. Genetic silencing of Nox2 and Nox4 reveals differential roles of these NADPH oxidase homologues in the vasopressor and dipsogenic effects of brain angiotensin II. *Hypertension*. 2009;54:1106-1114.

69. Armstrong L, Tilgner K, Saretzki G, Atkinson SP, Stojkovic M, Moreno R, Przyborski S, Lako M. Human induced pluripotent stem cell lines show stress defense mechanisms and mitochondrial regulation similar to those of human embryonic stem cells. *Stem Cells*. 2010;28:661-673.

70. Zhang M, Methot D, Poppa V, Fujio Y, Walsh K, Murry CE. Cardiomyocyte grafting for cardiac repair: Graft cell death and anti-death strategies. *J Mol Cell Cardiol*. 2001;33:907-921.

71. Lindley TE, Infanger DW, Rishniw M, Zhou Y, Doobay MF, Sharma RV, Davisson RL. Scavenging superoxide selectively in mouse forebrain is associated with improved cardiac function and survival following myocardial infarction. *Am J Physiol Regul Integr Comp Physiol*. 2009;296:R1-8.

72. Lyon AR, Sato M, Hajjar RJ, Samulski RJ, Harding SE. Gene therapy: Targeting the myocardium. *Heart*. 2008;94:89-99.

73. Hingtgen SD, Li Z, Kutschke W, Tian X, Sharma RV, Davisson RL. Superoxide scavenging and AKT inhibition in the myocardium ameliorate pressure overload-induced NFkB activation and cardiac hypertrophy. *In Press. Physiological Genomics.* 2009.

74. Hosoda T, D'Amario D, Cabral-Da-Silva MC, Zheng H, Padin-Iruegas ME, Ogorek B, Ferreira-Martins J, Yasuzawa-Amano S, Amano K, Ide-Iwata N, Cheng W, Rota M, Urbanek K, Kajstura J, Anversa P, Leri A. Clonality of mouse and human cardiomyogenesis in vivo. *Proc Natl Acad Sci U S A.* 2009;106:17169-17174.

75. Frederick JR, Fitzpatrick JR,3rd, McCormick RC, Harris DA, Kim AY, Muenzer JR, Marotta N, Smith MJ, Cohen JE, Hiesinger W, Atluri P, Woo YJ. Stromal cell-derived factor-1alpha activation of tissue-engineered endothelial progenitor cell matrix enhances ventricular function after myocardial infarction by inducing neovasculogenesis. *Circulation*. 2010;122:S107-17.

76. Danoviz ME, Nakamuta JS, Marques FL, dos Santos L, Alvarenga EC, dos Santos AA, Antonio EL, Schettert IT, Tucci PJ, Krieger JE. Rat adipose tissue-derived stem cells transplantation attenuates cardiac dysfunction post infarction and biopolymers enhance cell retention. *PLoS One*. 2010;5:e12077.

77. Padin-Iruegas ME, Misao Y, Davis ME, Segers VF, Esposito G, Tokunou T, Urbanek K, Hosoda T, Rota M, Anversa P, Leri A, Lee RT, Kajstura J. Cardiac progenitor cells and biotinylated insulin-like growth factor-1 nanofibers improve endogenous and exogenous myocardial regeneration after infarction. *Circulation*. 2009;120:876-887.

78. Segers VF, Lee RT. Biomaterials to enhance stem cell function in the heart. *Circ Res.* 2011;109:910-922.

79. Gygi SP, Rochon Y, Franza BR, Aebersold R. Correlation between protein and mRNA abundance in yeast. *Mol Cell Biol*. 1999;19:1720-1730.

80. Prokopi M, Mayr M. Proteomics: A reality-check for putative stem cells. *Circ Res*. 2011;108:499-511.

81. Surani MA, Hayashi K, Hajkova P. Genetic and epigenetic regulators of pluripotency. *Cell*. 2007;128:747-762.

82. Orkin SH, Hochedlinger K. Chromatin connections to pluripotency and cellular reprogramming. *Cell*. 2011;145:835-850.